Institute for Molecular Medicine Finland, FIMM
University of Helsinki
Helsinki, Finland

EPIGENETIC PROFILING OF OBESITY AND SMOKING

Sailalitha Bollepalli

ACADEMIC DISSERTATION

To be presented for public examination with the permission of the Faculty of Medicine of the University of Helsinki, in Lecture Hall 2, Biomedicum 1, Haartmaninkatu 8, on 27 March 2020 at noon.

Helsinki, Finland 2020

Cover layout by Anita Tienhaara

Cover picture by Nikita Mathur

ISBN 978-951-51-5806-2 (paperback)
ISBN 978-951-51-5807-9 (PDF)
ISSN 2342-3161 (PRINT)
ISSN 2342-317X (ONLINE)

Unigrafia
Helsinki 2020

The Faculty of Medicine uses the Urkund system (plagiarism recognition) to examine all doctoral dissertations.

Supervisors

Adjunct Professor Miina Ollikainen, PhD
Institute for Molecular Medicine Finland (FIMM),
University of Helsinki, Helsinki, Finland

Professor Jaakko Kaprio, MD, PhD
Institute for Molecular Medicine Finland (FIMM),
Department of Public Health,
University of Helsinki, Helsinki, Finland

Thesis Advisory Committee

Professor Sampsa Hautaniemi, DTech
Research Program in Systems Oncology,
University of Helsinki, Helsinki, Finland

Dr Panu Somervuo, D.Sc. (Tech.)
Organismal and Evolutionary Biology Research Programme,
University of Helsinki, Helsinki, Finland

Reviewers

Dr Christopher G. Bell, MBChB, PhD, FRCPA
William Harvey Research Institute,
John Vane Science Centre,
Barts & The London School of Medicine and Dentistry,
Queen Mary University of London, London,
United Kingdom

Assistant Professor Juulia Jylhävä, PhD
Department of Medical Epidemiology and Biostatistics,
Karolinska Institutet, Stockholm, Sweden

Opponent

Assistant Professor Tuuli Lappalainen, PhD
Department of Systems Biology, Columbia University, New York, USA,
Core Faculty Member, New York Genome Center, New York, USA

Faculty Representative

Adjunct Professor Nina Kaminen-Ahola, PhD
Department of Medical Genetics,
University of Helsinki, Helsinki, Finland

“In God we trust. All others must bring data.”
- William E. Deming

“All models are wrong, but some are useful.”
- George E. P. Box

To my family

Abstract

Obesity and smoking are the two major preventable causes of global mortality associated with a multitude of comorbidities, inflicting greater public health and economic burden. Complex interactions between genetic and environmental factors influence susceptibility to obesity and smoking. Epigenetic modifications provide a mechanistic link between genetic and non-genetic factors causing complex diseases or traits. Epigenetic modifications also function as an additional layer of gene regulation by modifying the structure and accessibility of DNA and chromatin. The fundamental objective of this thesis is to elucidate the role of epigenetic and transcriptomic markers in obesity and smoking. Hence, this thesis focuses on identifying epigenetic and transcriptomic markers associated with weight loss and smoking behavior using different study designs and by applying computational and statistical approaches. Genome-wide transcriptome and methylome were assessed in an unbiased, hypothesis-free setting to identify weight-loss and smoking-associated signals in Study I and II, respectively. Validation of the main findings from the discovery analyses and integration of transcriptomic and methylation data were performed to assess the validity and biological significance of the identified markers. A machine learning approach was employed in Study III to develop a robust smoking status classifier based on DNA methylation profiles. The performance of the classifier was tested in three different test datasets and also in comparison with two other existing approaches. Therefore, this thesis encompasses both application and method development aspects to achieve the corresponding aims of the studies.

In Study I, clinical parameters, genome-wide transcriptome, and methylome analyses were assessed longitudinally at three time points during a one-year weight loss intervention study, to understand the temporal changes in transcriptome and methylome of subcutaneous adipose tissue (SAT) in response to weight-loss. Results from the discovery analyses were validated using monozygotic (MZ) twin pairs discordant for acquired obesity, to examine whether weight loss and acquired obesity exhibit reciprocal transcriptome and methylome profiles. Gene expression and methylation profiles of the SAT at the three time points were also integrated to enhance our understanding of their interaction and thereby their contribution in weight loss. Based on the weight loss trajectory of the participants, three comparisons were performed: short-term (baseline to the fifth month), continuous (fifth to twelfth month), and long-term weight loss (baseline to twelfth month). Clinical parameters were improved with the weight loss (e.g. from baseline to fifth month, total and low-density lipoprotein cholesterol; triglycerides; and systolic blood pressure decreased and insulin sensitivity increased) and several significant transcriptome profiles were identified in response to weight loss at the three comparisons. No genome-wide significant methylation profiles were identified for the three comparisons. However, several significant correlations were observed between expression and methylation, indicating a potential regulatory role of DNA methylation in weight loss -

associated transcriptome profiles. At the pathway level, short-term weight loss was implicated in lipoprotein metabolism and long-term weight loss associated with various pathways associated with multiple functions of the SAT. Furthermore, several weight loss -associated genes exhibited opposite direction of expression in acquired obesity in the validation cohort of MZ twins, validating the robustness of identified associations.

In Study II, discovery analyses focused on understanding the widespread effects of smoking on SAT by simultaneous assessment of genome-wide transcriptome and methylome of SAT. Discovery analyses performed on the current (n=54) and never (n=291) smokers in the TwinsUK cohort identified 42 significantly differentially methylated signals and 42 significant differentially expressed genes (DEGs) indicating a substantial impact of smoking on metabolically important SAT. Integration of these results revealed an overlap at five genes (*AHRR*, *CYP1A1*, *CYP1B1*, *CYTL1*, and *F2RL3)* comprising 14 CpG sites. To further characterize the widespread effects of smoking on metabolic disease risk three adiposity phenotypes (total fat mass [TFM], android-to-gynoid fat ratio [AGR] and visceral fat mass [VFM]) were assessed with regards to the identified smoking-associated methylation and expression signals. Three CpG sites in *CYP1A1* showed significant associations with VFM and AGR, and an inverse association was identified between methylation levels of cg14120703 (*NOTCH1*) and AGR. To validate these associations, a subset of younger Finnish twins (n=69, 21 current smokers) was used as a replication cohort. The overall inverse association between cg10009577 (*CYP1A1*) and AGR was replicated and exhibited a similar direction for interaction effects between smoking status and AGR. However, this association did not reach the genome-wide significance level. Expression levels of *F2RL3* showed a significant association with all three adiposity phenotypes. While *OR51E1* expression levels were significantly associated with AGR and VFM. Our results show that smoking affects both the methylome and transcriptome of the SAT with overlapping signals. Furthermore, smoking-associated methylation and transcriptome profiles are also associated with adiposity phenotypes indicating a broader impact of smoking on human metabolic health.

In Study III, I developed a methylation-based smoking status classifier using a machine learning approach to overcome the limitations of cotinine and carbon monoxide biomarkers (i.e. limited to measuring recent exposure to smoking due to their short half-lives in body fluids) and the existing DNA methylation score-based approaches and to advance the practical applicability of smoking-associated methylation signals. I considered three smoking status categories (current, former and never) and used multinomial LASSO regression coupled with internal cross-validation to build the classifier. I demonstrated the global applicability and robustness of our classifier by evaluation of its performance in three independent test datasets from different populations and also compared the performance with two existing approaches. Our classifier differs from the existing approaches by curtailing the need to compute a threshold value specific to each dataset to predict smoking status. Our classifier showed good discriminative ability in identifying current and never smokers compared to other approaches. I also performed an extensive phenotypic evaluation to understand the results of our classifier. Accurate classification of former smokers is challenging

as their classification is affected by cessation time and smoking intensity prior to quitting. I provide the functionalities of our classifier including other the two methods as an R package *EpiSmokEr* (Epigenetic Smoking status Estimator), facilitating prediction of smoking status in future studies.

In conclusion, this doctoral thesis (1) enhances our understanding of obesity and smoking by integrating methylation and transcriptome data and identifying several weight-loss and smoking-associated signals, (2) shows wide-spread impact of smoking on metabolic health risk by evaluating the associations between smoking-associated signals and adiposity measures, and (3) demonstrates the role of DNA methylation profiles as a robust biomarker to predict smoking status by developing a smoking-status classifier.

Table of Contents

List of original publications

This thesis is based on the following original publications and are referred in the text by their Roman numerals:

I. **Bollepalli S**, Kaye S, Heinonen S, Kaprio J, Rissanen A, Virtanen KA, Pietiläinen KH, Ollikainen M. *Subcutaneous adipose tissue gene expression and DNA methylation respond to both short- and long-term weight loss.* International Journal of Obesity, 2018. 42: p. 412. PMID: 28978976

II. Tsai P-C, Glastonbury CA, Eliot MN, **Bollepalli S**, Yet I, Castillo-Fernandez JE, Carnero-Montoro E, Hardiman T, Martin TC, Vickers A, Mangino M, Ward K, Pietiläinen KH, Deloukas P, Spector TD, Viñuela A, Loucks EB, Ollikainen M, Kelsey KT, Small KS, Bell JT. *Smoking induces coordinated DNA methylation and gene expression changes in adipose tissue with consequences for metabolic health.* Clinical Epigenetics, 2018. 10(1): p. 126. PMID: 30342560.

III. **Bollepalli S**, Korhonen T, Kaprio J, Anders S*, Ollikainen M*. *EpiSmokEr: A robust classifier to determine smoking status from DNA methylation data.* Epigenomics, 2019. 11(13): p. 1469. PMID:31466478.

*These authors equally contributed to this research.

All publications are reprinted at the end of this book with permissions from the publishers.

Abbreviations

5caC	5-carboxylcytosine
5fC	5-formylcytosine
5hmC	5-hydroxymethylcytosine
5mC	5-methylcytosine
AGR	Android-to-gynoid fat ratio
AT	Adipose Tissue
ATAC-seq	Assay for Transposase-Accessible Chromatin using sequencing
BMI	Body Mass Index
CpG	Cytosine-phosphate-guanine dinucleotide
DEG	differentially expressed gene
DEXA	Dual energy X-ray absorptiometry
DILGOM	DIetary, Lifestyle and Genetic determinants of Obesity and Metabolic syndrome
DNAm	DNA methylation
DNMT	DNA Methyltransferase
DZ	Dizygotic
EIRA	Epidemiological Investigation of Rheumatoid Arthritis
EpiSmokEr	Epigenetic Smoking status Estimator
EWAS	Epigenome-Wide Association Study
FTC	Finnish Twin cohort
GWAS	Genome-Wide Association Study
HDL-C	High Density Lipoprotein-cholesterol
HOMA-index	Homeostatic Model Assessment – *quantifies insulin resistance and beta-cell function*
IDAT	Intensity Data
ILN	Illumina normalization
LASSO	Least Absolute Shrinkage and Selection Operator
LD	Linkage Disequilibrium
LDL	Low Density Lipoprotein
mQTL	Methylation Quantitative Trait Loci
Matsuda-index	an insulin sensitivity index
MR	Mendelian Randomization
MRI	Magnetic Resonance Imaging
MRS	Magnetic Resonance Spectroscopy
MS	Methylation Score
MZ	Monozygotic
OGTT	Oral Glucose Tolerance Test
PC	Principal Component
PCA	Principal Component Analysis
QC	Quality Control

QN	Quantile normalization
RMA	Robust Multi-array Average
SAT	Subcutaneous Adipose Tissue
scRNA-seq	Single-cell RNA sequencing
SNP	Single Nucleotide Polymorphism
SQN	Subset Quantile Normalization
SSc	Smoking Score
SVD	Singular value decomposition
TET	Ten-eleven Translocation
TFM	Total fat mass
TWAS	Transcriptome-wide association study
VAT	Visceral Adipose Tissue
VFM	Visceral fat mass
WLS	Weight Loss Study

1 Introduction

The ultimate goal of modern genetics research is to develop effective drugs and design efficient prevention strategies to treat and prevent diseases. A key challenge associated with this goal is to identify causal genetic variants and molecular mechanisms contributing to diseases. The recent explosion of genomic data and genome-wide association studies (GWAS) have significantly enhanced our understanding of the genetic architecture of several complex diseases and traits. However, a majority of the genetic variants identified by GWAS have modest effect sizes explaining only a smaller proportion of genetic predisposition (heritability) and are confined to non-coding regions of the genome. In addition to the genetic factors, environmental and lifestyle factors also implicate the disease phenotype and etiology. Epigenetic mechanisms provide mechanistic links accounting for both missing heritability and non-genetic factors influencing the genome. These mechanisms act as an interface between a stably inherited genome and a dynamically changing environment by regulating gene expression.

The field of epigenetics is rapidly progressing with a plethora of studies aiming to understand different phenomena, specifically the development of complex diseases. DNA methylation is the most widely studied epigenetic mark which mediates environmental effects on gene-expression regulation by controlling transcriptional machinery. Genome-wide assessment of DNA methylation has become an affordable avenue to uncover biomarkers for complex diseases. Moreover, the transient and reversible nature of DNA methylation makes it an ideal predictor to estimate the effect of diseases and environmental exposures. Combined evaluation of genetics, transcriptomics and epigenetics data provides a greater opportunity to obtain a holistic understanding of the disease mechanism. This increased understanding facilitates the development of improved drugs and treatments.

The prevalence of obesity and smoking is governed by a combination of genetic, epigenetic and environmental factors. Both obesity and smoking inflict metabolic diseases, subsequently posing a major risk for mortality and imposing a heavy economic burden worldwide. Losing weight and quitting smoking have become high-priority global public health issues, holding a promise of improving the quality and duration of life.

The major objective of this thesis is to identify epigenetic and transcriptomic markers associated with weight loss/obesity and smoking by applying computational and statistical approaches. This thesis has two major parts: (1) application part outlines integrative analysis of DNA methylation and transcriptome data using most relevant analysis pipelines to understand the concurrently occurring changes in response to weight loss and smoking (2) methods development part presents the development and implementation of an epigenetic classifier using a machine learning approach to predict smoking status based on DNA methylation profiles.

Genome-wide transcriptome and methylome analyses of SAT were performed in Study I to identify and integrate gene expression and DNA methylation profiles reactive to short- and long-term weight-loss. Furthermore, weight-loss associated gene expression profiles were tested for reciprocal effects in acquired obesity. Study II focused on comprehensively investigating the impact of smoking on adipose tissue by performing transcriptome- and methylome-wide association studies. Identified smoking-associated methylation changes were used to characterize the broader impact of smoking on metabolic disease phenotypes. In Study III a machine learning methodology was used to train a robust DNA-methylation based classifier to predict smoking status. I demonstrated global applicability and higher accuracy of our classifier by testing its performance on multiple independent test datasets and by comparing it with two other existing methods. I provided the implementation of this classifier as an R package, *EpiSmokEr*, facilitating smoking status prediction in future studies.

Overall, this thesis contributes to enhancing our understanding of the role of DNA methylation in obesity and smoking by using several statistical and bioinformatics tools. We comprehensively analyzed transcriptome and methylome in Studies I and II to capture the simultaneously occurring changes in response to obesity and smoking. In Study III, I have overcome the limitations of existing methods by employing a penalized regression coupled with internal cross-validation to identify smoking-associated CpGs to build the smoking status classifier. The following chapter presents an overview of the current state of epigenetics of obesity and smoking by summarizing key concepts, technologies and analysis strategies, followed by aims of the three studies. The next chapter describes the materials and methods employed in this thesis along with a new methodology implemented to build the smoking status classifier, followed by the results and discussion from all the three studies. Final chapters present implications and future directions and conclusions.

2 Literature Review

This chapter provides an overview of the importance of epigenetic mechanisms in the broader context of obesity and smoking. It serves to introduce the key concepts in epigenetics and reviews the literature with a focus on the main research goals of this thesis. Table 1 provides a glossary of key terms used in this thesis.

Table 1: Glossary of key terms

BMI-Discordant MZ Twin Pairs	BMI-discordant monozygotic twin pairs are discordant for obesity despite the same genotype, with one twin being heavy and other being lean (here: a minimum of 3 units of BMI (kg/m2) difference).
CpG	A CpG site represents cytosine adjacent to a guanine on the same strand of DNA. DNA methylation usually occurs at the cytosine in the context of CpGs. CpG islands are long stretches of non-methylated CpGs with high GC content (>50%) and high frequency of CpGs compared to the rest of the genome. CpG islands usually occur at gene promoters and increased methylation at CpG islands is conventionally associated with gene repression.
DZ twins	Dizygotic (DZ) or fraternal twins are derived from two distinct zygotes and share on average 50% of their segregating genes. DZ twins are non-identical and can be of the same or opposite sex, sharing age and common early childhood environment.
Epigenome	Collection of chemical modifications overlaying the genome which can profoundly influence gene expression without changing the underlying DNA sequence. DNA methylation, histone modifications and non-coding RNAs are the most widely known epigenetic modifications.
EWAS	Epigenome-Wide Association Study; quantifies statistical association between epigenetic variation (DNA methylation in this thesis) and a phenotype (a trait or disease).
Genome	The complete set of genetic instructions of an organism inherited from parents, which remains (nearly) constant throughout the lifespan.
GWAS	Genome-Wide Association Study; quantifies statistical association between genetic variation (SNPs) and a phenotype (a trait or disease).
Heritability	Heritability measures the proportion of the phenotypic variance that can be explained by genotypic differences between individuals. Heritability is a population parameter which can differ based on age, sex, geographical regions and time period. Conventionally, twin and family studies have been used to yield heritability estimates for various traits [1].

Linkage Disequilibrium	Linkage disequilibrium (LD) refers to the non-random association of alleles at two or more loci in a general population. Under LD, alleles occur together on the same haplotype with either more frequency (positive LD) or less frequency (negative LD) than the expected frequency when the alleles are independent of each other. LD is influenced by the rate of genetic recombination, mutation rate, selection, genetic drift, the system of mating, population structure, and genetic linkage.
Methylome	Complete set of DNA methylation modifications in a particular cell or tissue.
mQTL	methylation Quantitative Trait Loci; Genotype (usually genetic variants like SNP) at a specific loci influencing methylation pattern. Based on the location of the genetic variant they are classified as *cis*- (≤ 250 kb) and *trans*- (> 250 kb) mQTLs [2].
MZ twins	Monozygotic (MZ) twins arise from a single fertilized egg (zygote) and are hence genetically identical. MZ co-twins are of same sex, age and also share early-life environment. MZ twins can be further divided into subtypes based on placentation and amniotic sacs: separate placentas and amniotic sacs (dichorionic diamniotic MZ twins), shared placenta with two amniotic sacs (monochorionic diamniotic MZ twins), and same placenta and amniotic sac (monochorionic monoamniotic MZ twins).
Omics	Collective technologies used to characterize and quantify different types of biological molecules that determine structure, function and dynamics of the cells of an organism.
Phenotype	Measured or observed set of characteristics of an individual caused by a complex interaction between genetic and environmental factors.
SNP	Single Nucleotide Polymorphism; Variation at a single position in a DNA sequence found in at least 1% of population.

2.1 Multi-ome

The genetic constitution of an individual can determine their susceptibility to disease. However, complex diseases arise from a combination of genetic and environmental factors. The effects of varying combinations of these two factors form the basis of inter-individual variability, making each of us unique to disease susceptibility and treatment. The central dogma of molecular biology describes transfer of genetic information starting from genes to proteins (Figure 1). This sequential transfer of information involves transcription of DNA into messenger ribonucleic acid (mRNA) and subsequent translation into proteins.

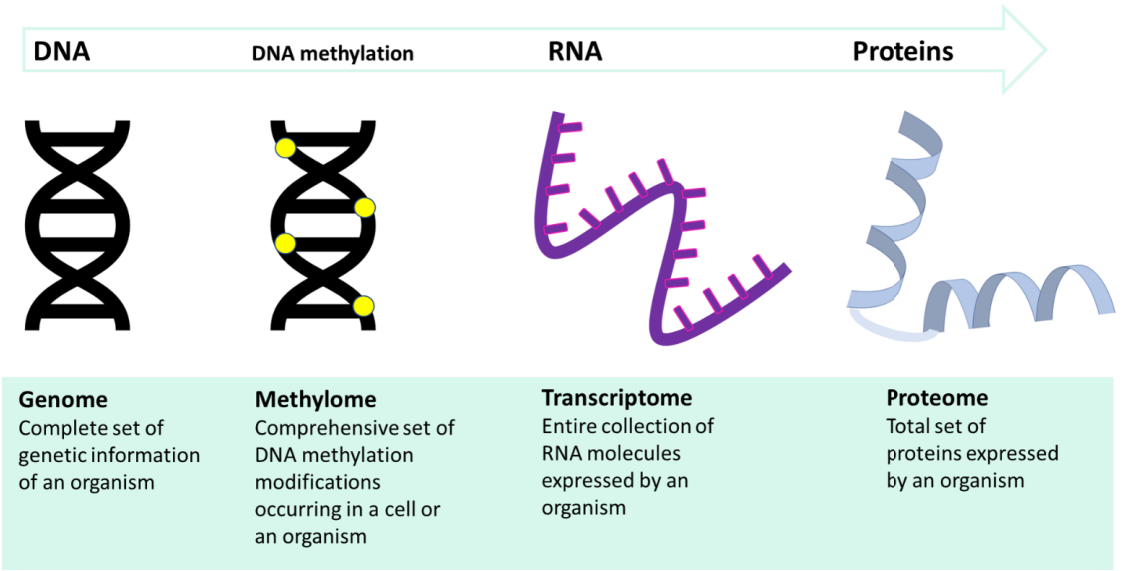

Figure 1: An illustration of the central dogma showing the transfer of information from DNA to proteins. Epigenetic mechanisms act as additional layer of control on this transfer of information. This schema shows the most widely studied epigenetic mechanism, DNA methylation.

Genomics is the study of the complete genome of an organism, specifically structure and function of genes. While transcriptomics deals with entire collection of RNA molecules expressed by an organism. Proteomics studies the total set of proteins expressed by an organism. However, the information transfer from DNA to proteins is not just linear. All these biological layers interact with one another giving rise to a complex and multi-dimensional interactome. In addition to these three layers, epigenetic mechanisms mediate developmental and environmental effects on expression and translation by changing the structure and conformation of DNA (Figure 1). Therefore, it is integral to comprehensively analyze interactions among genetic, epigenetic and transcriptomic mechanisms to understand and treat complex diseases effectively. Recent technological developments and collaborative research efforts have enabled us to integrate the interactions across these multiple layers revolutionizing biomedical research and medical practice. The next three subsections provide an overview of genome, epigenome and transcriptome.

2.1.1 Genome

Decoding the causal factors behind complex diseases has been a prime focus of human genetics and has been catapulted by the human genome project [3] which unveiled the complete human genome sequence. The human genome comprises over 3 billion base pairs of DNA and the genetic information encoded by these base pairs are unique for each individual except for monozygotic (identical) twins. This uniqueness

arises from less than 0.1% percent of our genome in the form of single-base pair substitutions termed as single nucleotide polymorphism (SNPs), insertions or deletions and structural variation. Human genome has around 10 million SNPs making it the most common form of genetic variants contributing to inter-individual variation. SNPs and their associated gene expression levels have been considered as the major causal factors for disease susceptibility. For instance, the comprehensive catalogue of genetic variants generated by the HapMap project allows for deeper interrogation of genomic variation in human health and disease [4].

Genome-wide association studies (GWAS) further enabled the identification of disease-associated genetic variants by scanning whole genome of cases and controls in an unbiased and hypothesis-free approach. GWASs revolutionized our understanding of complex diseases by identifying several associated and causal variants [5,6]. Furthermore, extensive resources and collaborative efforts have made GWAS a powerful genetic approach [5]. A recent systematic study performed on 4155 GWASs across 2965 unique traits demonstrated that ~61% of the genome is covered with trait-associated loci, with 93% loci being associated with more than one trait (pleiotropy) [7]. Such widespread pleiotropy can occur due to the same gene in a locus being associated with multiple traits or due to different genes or SNPs that are in linkage disequilibrium being associated with multiple traits [7]. Interestingly, almost 90% of the identified GWAS findings occur in non-coding regions with most of them located in intronic regions [7,8]. Moreover, the identified disease-associated SNPs explain lower proportion of genetic variance than twin or family studies giving rise to the “missing heritability” problem. Some of the prevailing explanations of the missing heritability are: common variants with small effects that are not reaching genome-wide significance level, rare variants with large effects that are not tagged by SNP arrays, and overestimation of heritability estimates in twin studies (due to shared environment) [9]. However, by using whole-genome sequencing, the proportion of variance accounted for by measured variants is close to that found in family studies for height and BMI [10]. Non-genetic or environmental influence on gene regulation through epigenetic mechanisms can also contribute to substantial proportion of missing heritability [11,12]. However, the extent of autonomy of epigenetic marks can range from obligatory to pure epigenetic variation, depending on the relationship between epigenetic states and their genotypic context [13]. Here obligatory epigenetic variation refers to the epigenetic variation that is completely dependent on the genetic variation, whereas pure epigenetic variation occurs when the epigenetic variation is largely independent of genetic variation.

2.1.2 Epigenome

The term “epigenetics” meaning “above genetics” was coined by Conrad Waddington [14]. His famous “epigenetic landscape” [15] illustrates that the destiny of a pluripotent cell to form a specialized cell is largely determined by the path it travels. Epigenetic mechanisms govern this cell specialization by controlling tissue and time specific expression [16,17] without modifying the underlying identical DNA sequence present in all

the cells of an individual. In addition to the cell development, epigenetic mechanisms have been predominantly associated with genomic imprinting [18] and X-inactivation [19–21]. Genomic imprinting leads to monoallelic expression of a small subset of genes in a parent-of-origin-specific manner while X-inactivation is a dosage compensation mechanism of sex chromosome genes occurring in females, where each cell randomly silences one of its X chromosomes. These two epigenetically regulated mechanisms are vital in ensuring normal mammalian development [18,20]. Since Waddington, epigenetics as a field has shown tremendous progress, which is evident from the series of definitions of epigenetics, that evolved with advancement in technology and accumulation of evidence [22–27]. Currently, epigenetic modifications are considered as stable and heritable changes without changing the underlying DNA sequence. Although epigenetic inheritance to daughter cells through mitosis is widely accepted, more conclusive evidence is needed to prove transgenerational inheritance via meiosis in humans [28–33].

DNA methylation (DNAm), histone modifications and non-coding RNAs (ncRNAs) are the main epigenetic mechanisms (Figure 2). Epigenetic marks are transient and reversible in nature and exhibit tissue and cell-type specific profiles. DNAm is the central focus of this thesis and is explained in detail in the following section 2.1.2.1.

Histone proteins are responsible for compaction and packaging of DNA inside the cell nucleus. DNA wrapped around the histone proteins forms chromatin, where each unit of the chromatin is called a nucleosome. This DNA-protein complex is tightly wound owing to the positive charge of histone proteins and negative charge of DNA (from phosphate groups in its phosphate-sugar backbone). Each nucleosome has a nucleosome core, composed of histone octamer (two copies of each: H2A, H2B, H3, and H4) serving as a spool to wrap ~147 bp of DNA [34,35]. Linker histone proteins (H1 or H5) connect adjacent nucleosomes. Histone modifications occurring at the N-terminal tails of histone proteins can alter the interactions between histone proteins, DNA and nuclear proteins. They affect DNA condensation and make DNA accessible (euchromatin) or inaccessible (heterochromatin) to transcriptional machinery [36]. Specific histone modifications are associated with transcriptional activation (e.g. H3 trimethylation at lysine 4 [H3K4me3]) and repression (e.g. H3 trimethylation at lysine 27 [H3K27me3]) [37]. Heterochromatin can be further classified into facultative and constitutive heterochromatin. Constitutive heterochromatin remains condensed and transcriptionally silent (e.g. H3 trimethylation at lysine 9 [H3K9me3]), whereas facultative heterochromatin (e.g. H3K27me3) has the potential to interconvert between hetero and euchromatin, with a possibility to decondense and allow transcription within temporal and spatial contexts [38]. NIH Roadmap Epigenomics project has comprehensively characterized various histone modifications across several human tissues [39].

RNAs that are transcribed but not translated to proteins in eukaryotes are termed as non-coding RNAs (ncRNAs). ncRNAs perform a wide range of functions, specifically regulation of transcription and translation [40,41], and are classified into two major classes based on their length short (e.g. microRNA [miRNA]), and long ncRNAs (e.g. Antisense ncRNA).

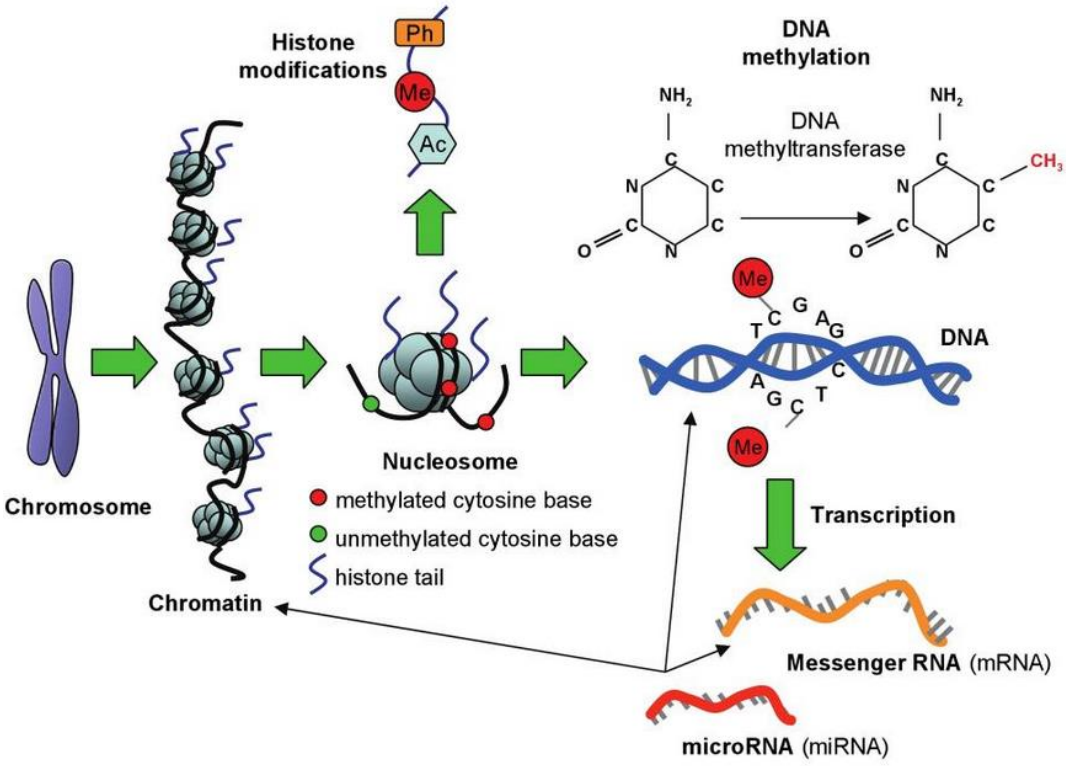

Figure 2: A schematic representation of genetic and epigenetic architecture. Chromosomes are composed of chromatin. DNA wrapped around histone proteins forms chromatin, each unit of chromatin is called a nucleosome. Histone modifications like phosphorylation (Ph), methylation (Me), and acetylation (Ac) occur on the tails of histone proteins. DNA is methylated by covalent attachment of a methyl group to the fifth carbon of a cytosine adjacent to a guanine. Transcription converts DNA to messenger RNA (mRNA) which can be repressed by epigenetic modifications. microRNA, a short ncRNA, can repress conversion of mRNA into proteins, establish DNA methylation, and may alter chromatin structure by regulating histone modifiers. All these three epigenetic marks control gene regulation by altering transcription and/or translation. *Figure reproduced from Relton, C. L., & Davey Smith, G. (2010)* [42].

2.1.2.1 DNA methylome

In the mammalian genome, DNA methylation (DNAm) usually occurs at the cytosine–phosphate–guanine dinucleotides (CpGs) by the covalent attachment of a methyl group to the fifth carbon of a cytosine forming 5-methylcytosine (5mC) (Figure 2). DNAm also occurs in a non-CG context (such as CpA, CpT and CpC), and has been observed in embryonic stem cells, neurons, and oocytes [43]. DNAm is catalyzed by a family of DNA methyltransferase (DNMT) enzymes using S-adenosylmethionine (SAM) as a methyl donor [44]. DNMT1 targets hemimethylated strands generated through DNA replication and methylates the CpGs on the newly synthesized strand [44]. This maintenance methylation by DNMT1 ensures the mitotic heritability of pre-existing methylation patterns. DNMT3a and DNMT3b perform genome-wide *de novo* methylation (both at hemi- and unmethylated DNA) after embryo implantation and are also essential for early development [45,46]. However, some evidence suggests that all these three DNMTs work in a coordinated fashion and are involved in both maintenance and *de novo* methylation [47].

There are about 28 million CpG sites distributed throughout the human genome, of which 60 to 90% are estimated to be methylated [48,49]. However, their occurrence is regarded as a “rarity” as they occur at about one-fifth of the expected frequency determined from base composition [48]. This rarity was attributed to the spontaneous mutation of 5mC to form thymine [50]. However, there are long stretches of CpGs occurring at higher frequency with elevated GC content compared to the rest of the genome defined as CpG islands (CGI). Unlike most CpGs in the entire genome, CGIs are typically unmethylated in healthy cells and around 56% of the human genes harbor CGIs in their promoter regions [48,51]. The conventional notion of DNAm as a gene silencing mark stems from the majority of the initial studies which have focused on the methylation of CGIs near transcription start sites (TSS). However, studies have revealed that the function of DNAm and its influence on transcription is context-dependent and is largely determined by its genomic position [52]. For instance, DNAm in the regions downstream of TSS (e.g. first intron) is also highly informative of transcription [53,54]. A clear and consistent inverse correlation between DNAm of the first intron and transcription has been demonstrated across tissues and species [54]. The regulatory role of this inverse relationship can be partially explained by the presence of intronic enhancers interacting with the promoters of their corresponding genes [54]. Furthermore, DNAm can have positive and negative effects on transcription factor binding, even within promoter loci [55].

In addition to its well-documented role in transcription, constantly increasing evidence from various scientific studies established DNAm as a prime epigenetic factor with diverse roles in development and disease [56].

DNAm is stable both chemically and genetically compared to other epigenetic marks. However, 5mC can be reversed by passive or active demethylation. Passive demethylation occurs in the absence of DNA methylation maintenance machinery, resulting in fully unmethylated strands during successive DNA

replication cycles. Active demethylation is catalyzed by ten-eleven translocation (TET) enzymes by iteratively oxidizing 5mC to 5-hydroxymethylcytosine (5hmC), 5-formylcytosine (5fC) and 5-carboxylcytosine (5caC). TET-thymine DNA glycosylase (TDG)-mediated pathway completes DNA demethylation by first excising 5hmC, 5fC and 5caC from the genome and then replacing them with unmethylated cytosines through base excision repair mechanism [57]. Global DNA demethylation of the human zygote is a crucial step of epigenetic reprogramming while aberrant DNA demethylation serves as a biomarker for several cancers [57]. DNAm profile can be altered due to genetic [58], disease [59], developmental (e.g. ageing, embryo development) [16], lifestyle (e.g. smoking, diet, exercise) [60–62], stochastic and environmental factors [25,42]. In recent years, epigenome-wide association studies (EWAS) have gained importance in unravelling the DNAm variants associated with several complex diseases and traits [59,63,64]. In addition to investigating effects of single epigenetic marks in isolation, their combined evaluation will yield a more comprehensive view of epigenome and disease mechanism [65].

2.1.3 Transcriptome

Transcription facilitates the transfer of genetic information in DNA by synthesizing a complementary strand of RNA (mRNA) which is later translated into proteins by ribosomes. Transcription occurs in three stages initiation, elongation and termination. Transcription factors (TFs) along with RNA polymerase enzymes initiate transcription. First, TFs bind to specific DNA regions called enhancer and promoter regions facilitating the recruitment of RNA polymerase (RNA polymerase II for transcription of mRNAs) at an appropriate transcription site [66]. RNA polymerase unwinds DNA strand and the antisense strand of the DNA acts as a template to synthesize complementary pre-mRNA strand. pre-mRNA is elongated until the complete synthesis of strand and is followed by the termination of transcription. pre-mRNA is protected from exonuclease degradation through capping at 5’ end and polyadenylation at 3’ end [66]. Mature mRNA is formed by removing introns from the pre-mRNA through splicing, which then serves as a template for translation in ribosomes.

Only ~1.5% of the human genome is translated into proteins through mRNAs [67]. Although the rest of the genome is actively transcribed to non-coding RNAs, they are not further translated into proteins. Transcriptome usually refers to the total set of all RNAs or gene transcripts expressed in a specific cell or tissue. Transcriptional profiles are time- and tissue-specific owing to the variable expression of genes in different cells and tissues. Transcriptome shows more variation across tissues than individuals [68]. Also, inter-individual variation in gene expression can be mainly due to disease candidate genes associated with sex, ethnicity, and age [68]. Therefore, it is essential to use the appropriate tissue sample to assess the corresponding transcriptome. For instance, in this thesis, Study I used SAT to identify weight-loss associated gene expression changes, as SAT is a highly relevant tissue to study obesity. The Genotype-

Tissue Expression (GTEx) project serves as a comprehensive resource to study tissue-specific expression and regulation [69], currently it has 54 non-diseased tissue sites from more than 1000 individuals.

2.2 Quantifying transcriptome and DNA methylation

DNA methylation and transcriptomic data used in this thesis are generated using microarrays with different chemistries and technology. However, they are very similar in their general workflow. The key steps in the general workflow of microarray chip technology are sample preparation, array processing and scanning followed by data analysis, as outlined in the Figure 3.

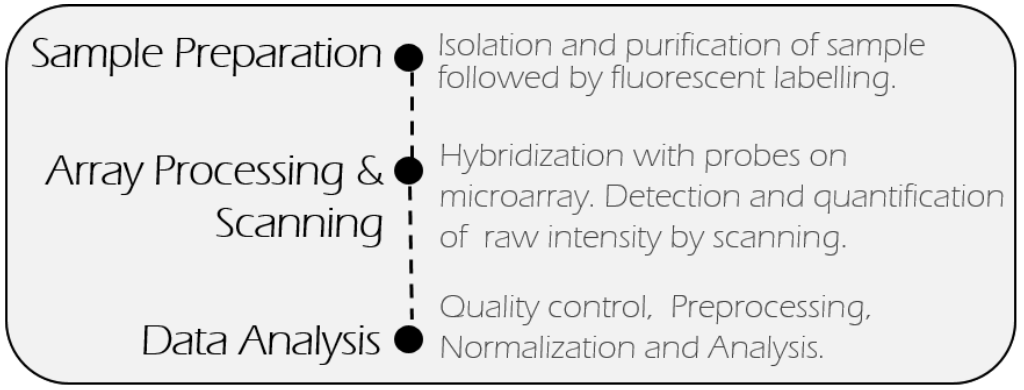

Figure 3: A general workflow of microarray chip technology outlining the key steps involved.

2.2.1 Profiling DNA methylation Variation

DNA methylation has been the most interrogated epigenetic mark because of its stability and ease of accessibility compared to other epigenetic marks. Methods available to measure DNA methylation can be grouped into three major classes: enrichment based-methods, methods using bisulfite treatment and digestion with methylation sensitive restriction enzymes [70]. Here I will focus on bisulfite treatment methods, specifically using microarrays. Bisulfite treatment protects methylated cytosines by converting unmethylated cytosines to uracil residues, which are later converted to thymine during PCR amplification. This step ensures that only methylated cytosines will remain as cytosines and can be interrogated by microarrays or sequencing platforms. Both microarray and sequencing platforms serve as excellent platforms to investigate genome-wide DNA methylation modifications with respect to a biological phenotype at a single base resolution in a hypothesis free manner. Bisulfite sequencing is currently considered as the golden standard to accurately measure genome-wide DNA methylation with a greater coverage [71,72].

Compared to sequencing-based approaches, microarrays provide limited coverage, however, they are affordable enabling to perform studies with larger sample size.

The Illumina Infinium HumanMethylation microarrays are the most widely used microarrays to investigate genome-wide DNA methylation and are currently available in three generations: 27k, 450k and EPIC. To date IlluminaHumanMethylation450 (450k) array is the widely used platform with 485512 probes targeting 99% genes and 96% of CpG island regions [73]. The newest EPIC array contains over 850000 CpGs with more than 90% sites on 450k and an additional 413743 CpGs, of which 333265 CpGs target potential enhancer regions [74]. All the studies in this thesis were performed using 450k, hence the rest of this section focuses only on 450k array.

Probes on the Illumina arrays are attached to silica beads deposited on the surface of Sentrix BeadChip [75]. 27k array is based on Infinium I assay and was biased towards promoter regions [76]. To improve the genomic coverage, 450k array was designed by including additional probes based on Infinium II chemistry to the existing 27k array (Figure 4) [73,77]. Owing to this extension 450k array has probes with two different assays. Infinium I has two bead types for each CpG to measure methylation and unmethylation using the same color channel. While Infinium II uses single bead type with two color channels (red and green) and detects methylation by single base extension (Figure 4) [73]. Because of the dual-channel readout, Infinium II probes show larger variance and are less sensitive to detect extreme methylation values [78]. Comparatively, Infinium assay I is more robust and hence considered as a better estimator of methylation state [78]. Several pre-processing and normalization methods have been developed to account for the two different assays on the 450k array [79–88]. Specific preprocessing and normalization methods used in this thesis are discussed in detail in the Materials and methods section.

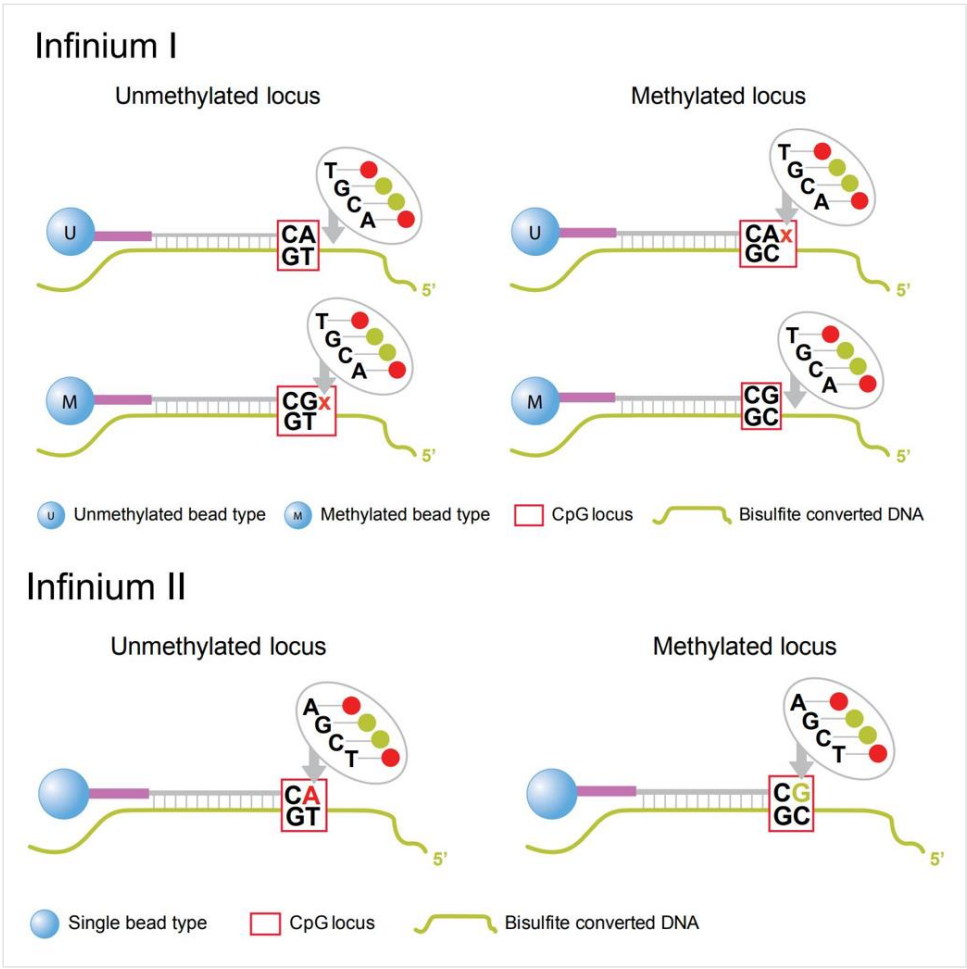

Figure 4: The Illumina Infinium HumanMethylation450 BeadChip (450k) uses probes with two different assays. Inifinium I assay uses two bead types for each CpG locus corresponding to Methylated and Unmethylated state of the CpG site and detected in the same color channel. Infinium II assay employs single bead type for each CpG locus, with two color channels. Methylation state is determined by single base extension. *Reproduced from:* https://www.cancer.gov/about-nci/organization/ccg/research/structural-genomics/tcga/using-tcga/technology/illumina-humanmethylation450-data-sheet

Unlike the human genome, epigenome is tissue-specific and is dynamically changing in response to internal and/or external stimuli. Thus, epigenetic changes can be causal or consequential. Therefore, utmost care should be taken while designing an epigenetic study and the required considerations have been comprehensively reviewed [26,70,89–91]. Most importantly, both phenotype and sample collection must be measured concurrently to appropriately assess the impact of biological phenomenon on the epigenetic mark in the specific tissue of interest. A brief overview of important considerations while analyzing DNA methylation data is presented in the following paragraphs.

Affordability of Illumina arrays coupled with their ability to perform genome-wide interrogation of the DNA methylation lead to explosion of EWASs. However, the computational and statistical analysis methods are still evolving to appropriately analyze methylation data and integrate it with other omics data. As discussed above using specific tissue sample is paramount for understanding DNAm variation in association with a phenotype. In addition to using the appropriate tissue for performing EWAS, adjustment for cell type confounding is essential. That is, the compositions of cells in a tissue could vary with phenotype/disease or tissue sampling. Hence, adjustment for cell type confounding is essential to ensure that measured epigenetic difference is reflecting true DNAm variation and not reflecting differences in cell-type composition of the tissue. Most of the EWASs performed so far used whole blood because of its ease of accessibility and can also serve as proxy for tissues like brain which are difficult to obtain non-invasively. Houseman's reference-based algorithm is the most widely used method to adjust for confounding by blood cell types [92]. Reference-free methods have also been designed allowing for cell-type correction in other tissues [93,94]. Although cell-type correction is an important consideration in the analysis of DNAm data obtained from complex tissues, it should also be noted that the cell-type variation could be a hallmark for certain phenotypes and hence, can in some cases, still be useful as a biomarker.

Because of their dynamic nature, it is difficult to establish causal, consequential or confounding role of epigenetic variation with respect to a disease or phenotype [91]. Furthermore, environmental factors like smoking, and developmental factors like age, impact DNAm and can lead to spurious associations in EWAS. Hence, confounding from these known sources of variation need to be adjusted in EWAS. Additionally, unmeasured confounders can be adjusted by methods such as principal components analysis (PCA), by using principal components correlated with the phenotype of interest as covariates. However, by using informative study designs in EWAS (described below) we can mitigate these problems to some extent and infer the role of DNAm in the phenotype. Finally, to ensure the credibility and reproducibility of the identified associations, EWAS hits need to be replicated, ideally in an independent dataset.

Longitudinal cohorts, following unrelated healthy individuals from birth, by recording phenotypic changes and samples at regular time intervals could serve to differentiate causal and consequential DNAm variation. Monozygotic (MZ) co-twins share the same genotype, age and sex as well as early-life environment, allowing to dissect the genetic and environmental contributions to a disease phenotype [95]. Notably, epigenetic variability within MZ co-twins has been observed with respect to the intrauterine environment and time of splitting of the zygote (see Table 1 for subtypes of MZ twin pairs) [95,96]. Nevertheless, more evidence from larger samples is needed to determine the impact of prenatal development during twinning on the epigenetic similarity of MZ twin pairs. Discordant MZ twin pair design is based on the hypothesis that the observed phenotypic discordance within MZ twin pairs is likely a response to non-genetic (environmental and stochastic) factors. Thus, the underlying phenotypic discordance is likely mediated by epigenetic mechanisms, whether causal or consequential to the respective phenotype. In this

thesis, BMI-discordant MZ twin pairs were used as a validation cohort in Study I. Inter-individual variation in DNAm at specific CpG sites can be attributed to underlying genetic variations (i.e. genetic differences between individuals) [58,97]. Also, genetic and environmental effects on complex trait variation can be estimated by comparing the phenotypic similarity between MZ and DZ twins using twin heritability estimates. By comparing genome-wide epigenetic profiles of twins, regions with high epigenetic heritability estimates can be identified, where DNA methylation could be affected by genetic variation [98]. Loci harboring these genetic variants (usually SNPs) influencing methylation are termed as methylation quantitative trait loci (mQTL). DNAm variation associated with mQTLs can be considered as consequential to the SNP. However, statistical approaches like Mendelian randomization can be used to assess causality and direction of effect of DNAm variants, by testing whether DNAm mediates the effect from genetic variant to phenotype through the same biological pathway [99].

Potential functional consequences of disease-associated DNAm variants can be inferred by integrating DNAm data with transcriptome data. However, to confirm the regulatory role of DNAm in gene transcription, functional studies are required [100]. Integrating DNAm data with other epigenetic marks and other omic layers will probably provide a holistic overview of underlying biological mechanism. However, this would require large datasets with multi omics data and statistical methods for integration and interpretation of data. Thankfully several resources and international consortiums are already striving to achieve this goal. ENCODE [101], NIH Roadmap Epigenomics [102], BLUEPRINT [103], and International Human Epigenome Consortium (IHEC) [104] are some of the excellent available resources facilitating epigenetic research. Additionally, to enable scientific progress datasets are being made publicly available in repositories such as the Gene Expression Omnibus (GEO).

2.2.2 Transcriptome profiling

Transcriptome analysis using microarrays provides a snapshot of transcriptional activity and expression levels of thousands of genes (mRNA transcripts) in a specific cell or tissue. Microarray investigates labelled DNA sequences (targets), using a collection of probes. Probe is a short stretch of DNA representing a specific sequence within a gene. Affymetrix Human Genome U133 Plus 2.0 Array (Affymetrix, Vienna, Austria) was used to assess transcriptome in Study I of this thesis. This is a high-density microarray, with multiple short oligonucleotide probes (25 base pair; bp) per target, synthesized directly on its surface. It has ~ 1300000 unique oligonucleotide probes covering over 47000 transcripts and variants (https://www.affymetrix.com/support/technical/datasheets/human_datasheet.pdf). To ensure accurate quantification and to account for nonspecific hybridization, probes are provided as probesets (~ 54 000 probesets) [105]. Typically each probeset corresponds to a gene with one perfect-match probe and one mismatch probe which differ at the 13th position of the 25 bp probe [105]. Perfect-match probe is designed to exactly match the sequence of interest.

To study transcriptome, mRNA is first converted to complementary DNA (cDNA) and labelled with fluorescent dyes. This labelled target is then hybridized to the microarray with bound probes. The successful hybridization of target and probe results in increased fluorescence intensity compared to background, which is captured by a scanner [75,105]. Expression values are then derived by summarizing probe intensities of each probeset [106]. Unlike microarrays, Ribonucleic acid-sequencing (RNA-seq) allows high-throughput sequencing of cDNA, enabling characterization of the transcriptome with higher coverage and greater resolution [107]. Although RNA-seq is relatively expensive compared to microarrays, it provides higher accuracy and is not limited to the detection of annotated gene transcripts and thus can be used to discover novel transcripts [108]. A general RNA-seq workflow includes sample preparation, library construction, sequencing and data analysis.

Similar to the epigenome, transcriptome is also time- and tissue-specific, and dynamically changes with internal and external stimuli. Also, transcriptome represents a snapshot of gene transcription from a mixture of cells (cellular heterogeneity). As outlined in the section 2.2.1, study design and concurrent collection of phenotype and tissue samples are also crucial in designing transcriptome studies.

2.3 Obesity and Smoking: Complex Interplay of Genetic and Epigenetic factors

2.3.1 Obesity

Obesity is a complex disease associated with several comorbidities and chronic diseases and is also one of the leading risk factors for mortality. Obesity is generally defined as a pathological condition caused by excess accumulation of body fat [109]. It primarily occurs due to the long-term imbalance between energy intake and energy expenditure. However, the underlying causes leading to the development of this imbalance are not fully understood. A rapid increase in the obese population and health risks incurred due to obesity made obesity as a pandemic.

Body mass index (BMI), calculated by dividing weight in kilograms by height in meters squared (kg/m2), is typically used to classify individuals as: underweight (< 18.5), normal (18.5- 24.9), overweight (25–29.9) and obese (>30). More than 1.9 billion adults were estimated to be overweight in 2016, with a global prevalence of obesity nearly tripled since 1975 [110]. With the increase in BMI relative risk for type 2 diabetes (T2D), hypertension cardiovascular diseases and certain cancers also increase [111]. A recent study reported that maintaining a normal BMI could prevent 1 in 7 premature deaths occurring in Europe [112]. Even more alarming is the prevalence of childhood obesity with 41 million children (below age 5) classified as overweight or obese [110]. Childhood obesity is associated with T2D in adolescents [113,114] and premature mortality in adulthood [115]. Moreover, obesity imposes huge clinical and public health burden, in Finland alone the estimated annual costs of obesity are around 300 million euros [116].

Although BMI serves as a crude estimate of overall adiposity, it does not reflect the variation in body fat distribution. Waist circumference provides a measure of abdominal fat distribution, while waist-to-hip ratio (WHR) also assesses different aspects of body composition in addition to fat distribution [117]. Assessment of body composition provides accurate estimation of fat and muscle mass composition, enabling improved clinical evaluation of obesity and weight loss [118]. Bioelectrical impedance analysis (BIA) and dual-energy X-ray absorptiometry (DEXA) can accurately measure body fat and skeletal muscle (comprehensively compared in [118]).

In this thesis, Study I and II use SAT to investigate impact of weight loss and smoking, respectively. The following section provides a comprehensive overview of adipose tissue before reaching a detailed discussion of epigenetic studies in obesity and smoking.

2.3.1.1 Adipose Tissue

Adipose tissue (AT), commonly called as "fat", is the primary energy reservoir in the human body. It stores excess energy in the form of triglycerides, a type of lipids, through lipogenesis. AT is also the largest endocrine tissue secreting various hormones, growth factors and adipokines regulating several physiological and pathological processes. AT is mainly composed of adipocytes, preadipocytes, macrophages, and fibroblasts (Figure 5). Triglycerides are stored as a single large droplet contributing to ~85% weight of an adipocyte [119]. Based on its color, AT can be classified as brown adipose tissue (BAT)

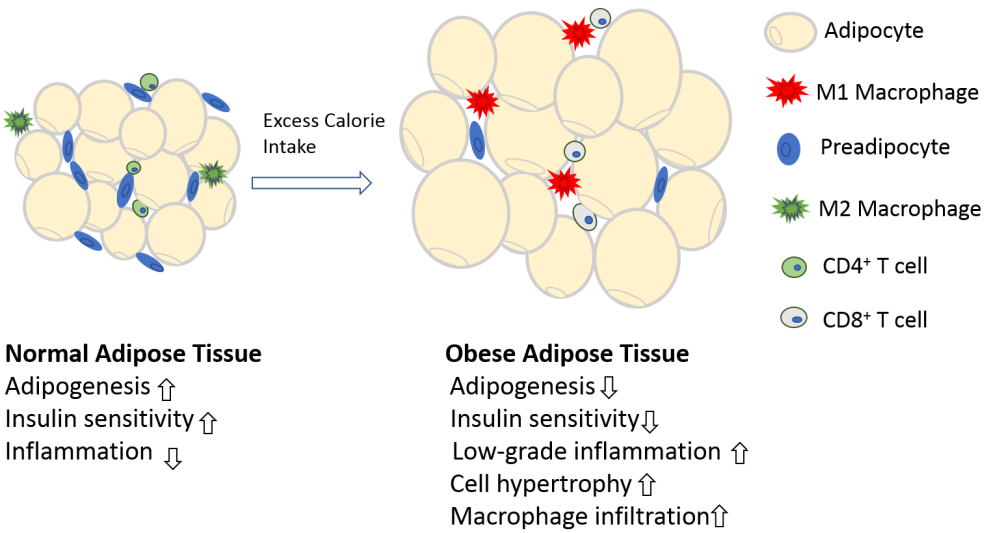

Figure 5: Overview of structural and functional differences in normal and obese adipose tissue.

and white adipose tissue (WAT). BAT predominantly occurs from fetal to adolescence phase and is found in a smaller proportion in the adult body [120]. BAT dissipates energy as heat through thermogenesis via uncoupled protein 1-containing mitochondria [120]. WAT can be further classified based on its location as subcutaneous adipose tissue (SAT, located beneath the skin) and visceral adipose tissue (VAT, associated with internal organs). SAT is the largest body fat reserve accounting for 80% of the total body fat and is distributed across the upper and lower body [121]. SAT and VAT differ in their development, structure, function and are associated with different health risks [122]. Beige or brown-to-white adipocytes are recently identified adipocytes, exhibiting characteristics of both WAT and BAT. They are structurally similar to WAT (formed via browning of WAT) and are capable of thermogenesis like BAT [120]. Beige cells can contribute to heat production when exposed to stimuli such as cold and exercise [120]. Emerging evidence suggests a central role of beige adipocyte thermogenesis in whole-body energy metabolism and thereby obesity [123]. An obesity-associated *FTO* allele (rs1421085 T-to-C single-nucleotide variant) has been shown to repress mitochondrial thermogenesis in adipocyte precursor cells, resulting in a cell-autonomous developmental shift from energy-dissipating beige adipocytes to energy-storing white adipocytes [123].

Leptin, adiponectin and tumour necrosis factor-alpha (TNF-α) are the prominent hormones secreted by AT which perform diverse functions. Leptin is mainly secreted by AT and leptin signalling from adipocytes to hypothalamus is crucial for appetite control and energy balance. Discovery of this specific role of leptin deeply enhanced our understanding of AT as an endocrine organ and its role in obesity [124–127]. Total absence of functional leptin in *ob/ob* mutant mice generates obesity phenotype and injecting leptin has shown to induce weight loss in these mice [128]. Morbidly obese individuals with leptin deficiency showed huge weight loss on leptin therapy [129–131]. Adiponectin, exclusively secreted by adipocytes is known to regulate insulin sensitivity, vascular function and has anti-inflammatory properties [119,126]. TNF-α is a pro-inflammatory adipokine associated with dysregulation of carbohydrate and lipid metabolism through AT dysfunction [132].

To facilitate whole-body energy balance AT undergoes dynamic remodelling based on nutrient supply [133]. In the starvation mode, triglycerides in adipocytes are converted to free fatty acids (FFA) and glycerol through the lipolytic pathway [134]. FFA and glycerol are then distributed throughout the body via blood restoring the energy balance. During excess calorie intake, adipocytes accommodate lipids either by increasing their size (hypertrophy) or number (hyperplasia). Concurrently, hypertrophic adipocytes recruit preadipocytes which are then differentiated into mature adipocytes to store excess energy. However, prolonged periods of AT expansion coupled with chronic excess energy intake leads to AT dysfunction [135]. Adipocytes become overloaded with lipids and can no longer accommodate excess energy after reaching a critical size. This leads to lipid spillover resulting in the storage of lipids in the liver, pancreas, and muscle causing insulin resistance in these organs [134]. Furthermore, hypertrophy of adipocytes

dysregulates secretion of adipokines resulting in a low-grade inflammatory state (Figure 5). Increased adipokine secretion promotes macrophage infiltration into AT and subsequent impairment of preadipocyte recruitment and differentiation. Altogether, increased inflammation, elevated adipokine levels and disrupted lipid metabolism leads to insulin resistance of AT [132]. Insulin resistance is a prominent feature in obesity, metabolic syndrome, and type 2 diabetes (T2D) [136]. Most importantly obesity results in increased AT mass and impaired secretion of adipokines, making AT a direct link to understand pathologies associated with obesity [119,132,135,137].

2.3.1.2 Epigenetics and Transcriptomics of obesity

Genetic predisposition is considered as the primary factor contributing to obesity. Heritability estimates from twin studies estimated that around 45 to 85% variance in BMI could be attributed to genetic variance [138–140]. Fat mass and obesity associated (*FTO*) gene was the first obesity-associated gene identified by GWASs in 2007 [141,142]. A series of GWASs since then identified several hundreds of obesity-associated variants, and explain ~3% variance in BMI [143–146] and ~40% of variance in BMI was explained with whole-genome sequencing [10].

In addition to genetic susceptibility, the dramatic increase in the prevalence of obesity can also be attributed to obesogenic environment with abundant availability of calorie-rich food [147], increased portion size, and reduced physical activity [148]. However, there is a huge variability in the susceptibility of obesity, and not all individuals exposed to obesogenic environment develop obesity [149]. This variability can be attributed to the complex interplay of genetic, behavioral and environmental factors making obesity a multifactorial disorder.

Emerging evidence suggests that epigenetic modifications can be considered as the obvious mechanism that connects the effects of obesogenic environment and genetic susceptibility of obesity [150–155]. Alteration of gene expression by epigenetic mechanisms could partly account for both missing heritability and inter-individual variation of obesity.

DNAm, as one of the epigenetic marks, has been extensively studied to understand its contribution to obesity and associated metabolic complications, like T2D [150]. Especially MZ twin pairs discordant for BMI has served as an ideal design setting to unravel the impact of environment on the epigenome and obesity [58,95,156]. Furthermore, studies performed on the Dutch Hunger Winter showed that adverse intrauterine environment like insufficient maternal diet can cause persistent changes in DNAm along with increased disease risks during later life, including increased risk for obesity and glucose intolerance [157–159]. A recent stepwise genome-wide mediation analysis using the Dutch Hunger Winter data revealed that whole blood DNAm at specific CpGs mediates a significant proportion of the association between prenatal famine exposure and later-life metabolic health i.e. body mass index (BMI), serum triglycerides (TG) [160].

Extensive research has been ongoing to unravel DNAm variants associated with obesity and has been comprehensively reviewed [150,152,154,161–166]. No clear global methylation direction has been established in association with obesity, as studies reported both hyper- and hypomethylation with increase in obesity-related measures [152]. CpG sites located within or near *HIF3A*, *CPT1A*, and *ABCG1* have been consistently reported in association with BMI and/or waist circumference [150]. *HIF3A,* (hypoxia-inducible factor 3 subunit alpha) is involved in hypoxia (low levels of oxygen) regulation and *CPT1A* encodes carnitine palmitoyltransferase 1A enzyme essential for fatty acid oxidation, while *ABCG1* (ATP-binding cassette sub-family G member 1) mediates cholesterol efflux to prevent cellular lipid accumulation. Sayols-Baixeras and colleagues identified 94 CpG sites associated with BMI and 49 CpG sites associated with waist circumference which could explain 26% and 29% of heritability of these traits, respectively [167]. The largest EWAS on BMI till date identified 187 CpGs associated with BMI and most of these identified CpGs were consequential to obesity [168]. This observation was also confirmed by Mendelson and colleagues who further showed that 18% of inter-individual variation in BMI could be explained by methylation of 83 BMI-associated CpGs [169]. Furthermore, they identified differential methylation and expression of *SREBF1* (sterol regulatory element binding transcription factor 1), a key regulator of lipid synthesis, associated with adiposity and cardiometabolic disease.

Results from transcriptome profiling of SAT during obesity showed upregulation of inflammation [170–173], immune response [170], and downregulation of mitochondrial functions [171,174], insulin signalling [172] and lipogenic genes [173,175]. Most of the EWASs so far used whole blood to assess the impact of obesity. Assessing more relevant tissues like SAT, would reveal the role of methylome in pathogenesis of obesity. Rönn and colleagues identified 2825 BMI-associated genes in SAT, showing both differential expression and methylation, including *FTO* and *IRS1* genes [176]. *IRS1* (Insulin receptor substrate 1) initiates stimulation of glucose transport in SAT and muscle tissue. Three *HIF3A* CpG sites identified by an earlier study [177] were also replicated in the female cohort of this study. On overall, obesity is associated with epigenetic dysregulation resulting in DNAm variability and the obesity-associated CpG methylation show modest effect sizes.

2.3.1.3 Epigenetics and Transcriptomics of Weight loss

A modest, sustained weight loss around 5% is estimated to achieve clinically meaningful reductions in blood glucose, triglycerides and the risk of T2D [178]. Despite our greater understanding of obesity-associated changes in SAT functionality, it is still necessary to elucidate distinctive impacts of weight loss on SAT. Presumably, weight loss should reverse the adverse effects of obesity, including pathological expansion of SAT, inflammation and insulin resistance. Therefore, it is crucial to understand how weight loss affects SAT structure, functionality and associated inflammatory profiles.

Table 2 outlines the genome-wide transcriptomic and/or methylome analyses performed in SAT during weight loss by diet and/or exercise (excluding surgical procedures). Findings from these studies show little overlap, likely due to discrepancy in their study designs, duration of the study, sample size, participants considered for the study (overweight to morbidly obese) and sex of participants. Results from the transcriptomic studies indicated that weight loss influences expression levels of genes associated with polyunsaturated fatty acids production [179], improved high-density lipoprotein (HDL)-mediated cholesterol transport [180], insulin secretion from pancreatic beta cells [181], reduced inflammation [180,182] and insulin-like growth factor signalling [183]. In studies with both transcriptome and methylation analyses, weight loss attained through exercise showed differential expression and methylation of genes associated with adipocyte metabolism [60]. Whereas calorie restriction modified expression levels of genes associated with angiogenesis and methylation levels of genes involved in insulin secretion pathways [184]. A recent review on 25 prospective studies comparing DNA methylation in various tissues (including surgical and candidate gene approach studies) concluded that small but widespread changes occur across genome in response to weight loss [185]. This review also suggested that limited reproducibility of results could be partly due to dynamic nature of DNAm, and that inter-individual variation in DNAm at several genomic loci can impact weight loss. In summary, our understanding of SAT transcriptome and methylome and their interplay in response to long-term weight loss still remains limited.

Table 2: Table summarizing the findings from genome-wide weight loss transcriptome and/or methylome studies performed on SAT (in chronological order).

Research Objectives	Study Design	Assay*	Main Findings†	Ref.
Gene Expression Studies: diet and /or exercise interventions				
To investigate the consequence of calorie deficit on the inflammation-related genes in SAT.	Twenty nine obese premenopausal women followed VLCD for 28 days and were compared with 17 non-obese subjects.	Stanford cDNA microarray and RT-PCR	Weight loss improved inflammatory profile of adipose tissue by simultaneously decreasing expression of proinflammatory factors and increasing expression of anti-inflammatory molecules.	[182]
To investigate the impact of two LCDs with same energy content but different compositions of fat and carbohydrate on SAT gene expression.	Ten week intervention of 40 post and pre-menopausal obese women who were randomly assigned to either a low-fat, high-carbohydrate diet (n=20) or a moderate-fat, moderate-carbohydrate diet (n=20).	Affymetrix Human Genome Focus array and RT-PCR	Genes regulating polyunsaturated fatty acids were affected by energy deficit. Although no effect was observed due to varying compositions of carbohydrates and fats.	[179]
1. To identify SAT gene expression profiles differing between weight responders and non-responders to a low-fat diet. 2. To use these	Obese women were grouped into weight responders (n=27) and non-responders (n=26), based on the weight loss following a low-fat diet for 10 weeks. SAT biopsies before the intervention were used to	Agilent 44K whole human genome microarrays	Nine common genes identified from different statistical methods were used to predict weight loss. However, the prediction accuracy was low and couldn't clearly distinguish respondents from non-respondents.	[186]

identified expression profiles to predict whether an individual will lose weight during diet intervention.	identify differential expression profiles.			
To investigate the effects of two LCDs with same energy content but different compositions of fat and carbohydrate on SAT gene expression.	Obese women were randomly assigned to a 10 week low-fat (n=47) or moderate-fat (n=47) diet. Two sets of women combined from both the diets were assessed using a candidate gene approach (n=46) or microarrays (n=48).	Stanford cDNA microarray and RT-PCR	Energy limitation had a predominant impact on the SAT expression profiles compared to the composition of fats and carbohydrates in the diets. Although macronutrient composition may influence SAT function and metabolic response.	[187]
To comprehensively identify gene expression changes occurring in SAT during three stages of a dietary intervention program and to investigate the link with insulin sensitivity.	Twenty two obese women participated in a dietary intervention program with three consecutive phases: a 1-month VLCD, a 2-month LCD and a 3-4-months of a weight maintenance diet. Only 8 biopsies were available for generating microarray data.	Agilent 44K whole human genome microarrays	Distinct molecular mechanisms were observed during VLCD and weight stabilization phase including opposite regulation of genes in adipocytes and macrophages. Also, different genes were responsible for the improvement of insulin sensitivity in both phases.	[188]
To investigate SAT expression profiles of obese women who initially lost weight and then showed different weight trajectories after following diets with varying protein and glycemic index content.	After an initial VLCD of 8 weeks, obese women were randomly assigned to 4 diets with varying protein and glycemic index content for 6 months. SAT expression profiles were compared between women with continuous weight loss (n=22) and women who regained weight (n=22) across the 4 diets.	Agilent 44K whole human genome microarrays	Differences observed in SAT expression profiles of two groups of women were primarily due to weight variations rather than diet compositions. Continuous weight loss was associated with mitochondrial oxidative phosphorylation whereas weight regain was associated with cellular growth and proliferation.	[189]
To investigate if SAT gene expression profiles during a LCD can be used to distinguish subjects with successful weight maintenance from weight regainers.	Forty white women followed an 8 week LCD phase followed by a 6-month weight-maintenance phase. SAT profiles were compared between weight maintainers (WMs, n=20) and weight regainers (WRs, n=20).	Agilent 44K whole human genome microarrays	Although both WMs and WRs lost considerable weight during LCD, their SAT profiles revealed differential regulation of genes associated with fatty acid metabolism, citric acid cycle, oxidative phosphorylation, and apoptosis.	[181]
To identify differentially expressed genes during weight loss and weight maintenance	Nine of twelve obese subjects who followed an initial LCD phase for 3 months and a weight maintenance phase for six months were used to assess SAT expression profiles.	HG-U133 Plus 2.0 array and reverse transcription quantitative PCR	Weight loss and weight maintenance reveal distinct biological mechanisms with reciprocal regulation at several genes. Both CETP and ABCG1, participants of HDL-mediated reverse cholesterol transport, were most upregulated after both processes.	[180]

To investigate the effect of a six-month intervention using calorie restriction, exercise or both on SAT expression profiles.	Forty five obese postmenopausal women were randomly allocated to diet, exercise and diet plus exercise groups. After the six month intervention, all the women including controls were classified based on the extent of weight loss to compare their SAT gene expression profiles.	Illumina Human HT-12 v3 Expression Beadchips	Significant changes in SAT expression profile were identified, particularly in genes associated with sex hormone steroid synthesis, leptin and insulin signaling. Interestingly, no pathways associated with inflammation were implicated in this study.	[183]
Both Transcriptome and Epigenome-wide association studies: diet or exercise interventions				
To determine the contribution of DNAm and gene expression changes to weight loss responsiveness.	Fourteen overweight and obese postmenopausal women followed LCD for six months and were classified as high responders (HR) or low responders (LR) based on their body fat loss percentage. Differential methylation and expression analyses were performed comparing HR and LR before and after LCD.	Affymetrix HG U133 plus 2.0 GeneChip microarray and Human CpG-island 8.1 K array	Significant DNAm changes between HRs and LRs were identified at baseline and after LCD. While differences in gene expression profiles were seen only after LCD. DNAm changes were related to weight control and insulin secretion pathways whereas gene expression changes were associated with angiogenesis and cerebellar long-term depression pathways.	[184]
To examine changes in SAT DNAm and gene expression patterns after a six-month exercise intervention.	SAT DNAm and expression profiles were compared in 23 healthy but sedentary men before and after a six-month intervention.	Affymetrix GeneChip Human Gene 1.0 ST whole transcript based array and Infinium HumanMethylation450 BeadChip assay	Differential methylation patterns were observed at both global and individual CpG site level in response to exercise including candidate genes for obesity and type 2 diabetes. Genes exhibiting both differential methylation and expression in response to exercise were shown to influence adipocyte metabolism.	[60]

DNAm: DNA methylation
RT-PCR: Reverse Transcriptase polymerase chain reaction
SAT: subcutaneous adipose tissue
LCD: low calorie diet
VLCD: very low calorie diet
Assay: Microarray platform and techniques used to assess gene expression or DNAm*
Main Findings†*: Majority of the findings in this table are from early studies in the field, so results have not been adjusted for cell type confounding.*

2.3.2 Smoking

Smoking is a major causal risk factor for several chronic diseases and is a prominent cause of preventable mortality accounting for ~7 million deaths annually [190]. In addition to the well-established negative impact of smoking on lung cancer, chronic obstructive pulmonary disease (COPD) and heart disease, smoking also inflicts comorbidities like tuberculosis, alcohol use and worsens mental illness and HIV infection [191]. The total economic cost of smoking in Finland is around 2589 million euros [191].

Smoking is a complex behavior which progresses through multiple stages, mainly smoking initiation, development of nicotine dependence (among most but not all smokers), nicotine withdrawal when attempting to quit smoking, cessation and relapse [192]. Several factors contribute to smoking initiation such as peer pressure during adolescence [193–195], positive image of smoking, socioeconomic status, parental smoking, sex, ethnicity and other substance use [196–198]. Despite the knowledge of smoking-associated

health risks more than a billion people are still smoking. In Finland, more than 731000 adults (aged above 15 years) use tobacco each day [191]. This highlights the addictive or dependence nature associated with smoking and nicotine intake.

Tobacco contains about 7000 toxic chemicals and 70 carcinogens [191], of which nicotine is the most addictive substance. Nicotine promotes compulsive smoking by creating positive reinforcement in smokers by altering dopamine and adrenaline in the brain. On inhaling smoke from burning tobacco, distilled nicotine enters lungs, where it is rapidly absorbed and then transported to brain via blood stream in less than 20 seconds [199]. Nicotine then binds to nicotine acetylcholine receptors (nAChRs) in the brain tissue releasing adrenaline and dopamine. This rapid spike in the levels of nicotine followed by release of neurotransmitters elicits feeling of pleasure and calmness making smokers nicotine dependent [200], leading to neuroadaptation and a positive feedback leading to greater intake. However, the extent of dependency or addiction varies and smokers who exhibit high nicotine dependence have extreme difficulty in quitting smoking. Furthermore, nicotine withdrawal symptoms such as insomnia, depressed mood, anxiety, restlessness and loss of appetite increases the likelihood of relapse [201–203].

2.3.2.1 Epigenetics of smoking

In addition to behavioral, physiological and environmental factors, genetic factors [204], and perhaps epigenetic factors, also strongly influence smoking behavior. Heritability estimates from twin studies revealed that genetic differences among individuals have a substantial impact on multiple aspects of smoking behavior, including smoking initiation and nicotine dependence [205,206]. Several loci associated with various stages of smoking have been identified by candidate gene approaches and GWASs. The nicotinic receptor genes *CHRNA5–CHRNA3–CHRNB4* at 15q25 [207–213] and the primary nicotine metabolism gene *CYP2A6* at 19q13 [214,215] are the most significant and consistently replicated associations with nicotine dependence, cigarettes per day and smoking cessation.

Smoking is the most widely studied lifestyle factor which substantially influences DNA methylation, with current and never smokers exhibiting different methylation profiles [61,64,216–222]. It has been consistently reported that majority of the smoking-associated CpGs are hypomethylated in current smokers compared to never smokers. It was also shown that methylation levels of former smokers partially reverse upon cessation, towards the levels of never smokers [61,216,219,220,222,223]. However, the extent of reversal is site-specific, determined by the magnitude of smoking-induced methylation alterations at the specific CpG site [216,219]. Interestingly, CpGs with persistent methylation alterations after decades of cessation have been reported, indicating a broader and long-lasting impact of smoking on methylome [216,219,224].

Smoking is a well-established risk factor for several diseases. Differential DNA methylation due to smoking has also been observed in relation to smoking-related diseases (e.g. cancers) [225–227], suggesting a potential role of DNA methylation in the pathway from smoking to disease development.

Furthermore, this also makes DNA methylation as a suitable biomarker to predict both smoking and smoking-associated disease risk.

2.3.2.2 Epigenetic signatures of disease: DNAm-based predictors

Lately, disease-associated genetic and epigenetic signals are being computed into a usable score to predict disease risk. For instance, polygenic risk scores computed using trait-associated genetic loci and their associated weights have been used to predict genetic susceptibility for a trait (e.g. progression of smoking behavior [192]). DNAm serves as an ideal biomarker owing to its dynamic and reversible nature in response to external and internal stimuli. Recently, there has been a growing interest in the development of DNAm-based predictors to predict onset or progression of a disease or phenotype (Table 3).

The following section provides a brief introduction to machine learning concepts to help understand the overview on DNAm-based predictors.

Basic concepts in machine learning

Machine learning (ML) is a branch of artificial intelligence which uses computational algorithms and statistical methods to enable computers to perform a specific task without the need for explicit instructions. ML differs from statistical modelling, as ML primarily focuses on prediction than inferring relationships between variables. The basic premise is that ML learns underlying patterns in the training data which are then used to make predictions on the unseen data. ML involves application of mathematical rules and statistical assumptions. Supervised and unsupervised learning are the main types of ML. Classification is the most commonly used supervised learning algorithm, where the training is performed on a well labelled dataset and learned patterns are then used to map unseen data to labels. Generalization of a model, that is applying a model on unseen data to make reliable predictions needs to avoid both overfitting and underfitting. Overfitting occurs when the model learns the noise in the training data along with underlying structure, making it less generalizable to new data. Underfitting occurs when model is unable to capture the underlying patterns in the data structure and therefore cannot make accurate predictions.

Penalized regression offers a practical alternative to subset the variables in linear regression by applying a penalty constraint which shrinks the coefficients of variables [228]. Ridge, Least Absolute Shrinkage and Selection Operator (LASSO), and elastic net regression are the most widely used penalized regression methods. Ridge regression applies L2 norm (sum of the squared coefficients) and shrinks the coefficients close to zero. LASSO applies L1 norm (sum of absolute values of the coefficients) and shrinks most of the coefficients to exactly zero thereby performing variable selection [229]. Elastic net regression applies a convex combination of ridge and LASSO. Amount of shrinkage can be regulated by a tuning parameter (lambda). Cross-validation can be used to identify an optimal lambda to find the model´s best fit and avoid overfitting. Table 3 below provides a brief overview of different DNA methylation-based predictors

developed using one of the penalized regression methods or using other statistical approaches or a combination of both.

Table 3: An overview of recent studies with focus on development of DNA methylation-based predictors developed for a diverse range of purposes. This is not an exhaustive list and is shown to provide an overview of available DNA methylation-based predictors.

Purpose	Methodology	Ref.
A multi-tissue predictor to estimate the DNAm age trained on DNAm data from 51 healthy tissues and cell types.	Elastic net regression	[16]
To identify heavy smokers from non-smokers (former and never), using smoking score based on 187 smoking-associated CpGs identified in whole blood.	Computed a weighted DNAm score using methylation values of CpGs identified by an earlier EWAS [220] as reference values.	[217]
To distinguish current from never smokers, and former from never smokers, based on methylation score obtained from 4 smoking-associated CpGs in whole blood.	EWAS followed by stepwise logistic regression with forward selection	[221]
To estimate gestational age using DNAm in cord blood.	EWAS followed by elastic net regression	[230]
To estimate gestational age at birth using DNAm in cord blood.	Elastic net regression	[231]
Whole blood-based DNAm score to predict prenatal exposure to maternal smoking.	Computed a weighted DNAm score using methylation values of CpGs identified by an earlier genome-wide consortium meta-analysis [232].	[233]
To predict fetal alcohol spectrum disorder (FASD) using DNAm	Stochastic gradient boosting	[234]
To detect heavy alcohol drinking using alcohol associated CpGs in whole blood.	EWAS followed by LASSO regression	[235]
Three placental clocks estimating gestational age based on placental tissue.	Elastic net regression	[236]

Epigenetic smoking status estimation

The precise knowledge of smoking history facilitates in designing appropriate treatments ranging from preventive interventions for occasional smokers to cessation therapies for heavy current smokers. Further, accurate smoking history can serve as a basis to predict long-term health risks associated with smoking (e.g. lung cancer). Traditionally, smoking exposure is ascertained using self-administered questionnaires. Diagnostic and Statistical Manual of Mental Disorders (DSM) [237] and the Fagerström Test of Nicotine Dependence (FTND) [238] are the most commonly used self-report questionnaires to capture nicotine dependence. However, self-reported smoking status is prone to errors due to under-reporting [239] and poor recall of long-term smoking history. Also, it fails to account for the passive exposure to smoking. Biomarkers like cotinine, can quantify the extent of absorbed nicotine in the body fluids [239]. Nonetheless, its efficacy is limited to measuring recent exposure, as cotinine can be detected only for a few days at most after smoking, given the half-life of 16 hours [240]. Moreover, usage of nicotine replacement therapy, smokeless tobacco and e-cigarettes might also result in high levels of cotinine, resulting in inaccurate evidence of smoking. This clearly demonstrates a requirement for a robust indicator of smoking exposure that overcomes these limitations and can accurately measure current and past smoking.

Numerous independent studies performed on different populations have identified several smoking-associated CpGs [61,64,216–222]. The so-far largest EWAS of ~16000 individuals has identified 18760 significantly differentially methylated CpGs across 7000 genes between current and never smokers [64]. Interestingly, many of these studies consistently reported the same top significant CpGs associated with smoking, demonstrating the robustness of smoking-associated methylation signatures [61,64,216–222]. Methylation status of genes *AHRR* [241,242] and *F2RL3* [222] have been suggested as potential biomarkers to estimate smoking. Notably, two studies attempted to translate EWAS findings to scores that reflect the extent of smoking [217,221]. Although quantifying cumulative methylation exposure into a score is an interesting approach, the key challenges of applicability and interpretation remain. For instance, the smoking score of Elliott *et al* [217] has an ethnic-specific threshold to differentiate smokers from never smokers, limiting its universal applicability and necessitating threshold for each ethnicity. Methylation score of *Zhang et al* [221] can only tackle binary comparisons i.e. current vs never and former vs never smokers. To overcome these existing limitations, Study III in this thesis focused on developing a robust smoking status classifier to estimate smoking status based on DNAm profiles of individuals. A detailed description of the classifier development is provided in the section 4.5.3.

2.3.3 Smoking meets obesity: double jeopardy and a dual challenge

Smoking and obesity are the two leading preventable causes of death associated with a multitude of comorbidities and health risks, with widespread effects across multiple tissues. The Framingham Heart Study estimated that compared to normal-weight non-smokers, obese men and women smokers lost on

average 14 and 13 years of life, respectively [243]. However, their inter-relationship is highly complex and unclear.

Several epidemiological studies concluded that current smokers have lower body weight compared to never smokers and smoking cessation results in weight gain [244–248]. Causal role of smoking on BMI reduction in current smokers has been demonstrated by two Mendelian randomization studies using a SNP in the *CHRNA5-A3-B4* gene cluster as proxy for heavy smoking [249,250]. In contrast to findings from BMI studies, current smokers tend to have more abdominal obesity than never smokers [251]. A recent genome-wide meta-analysis suggested that smoking alters genetic susceptibility to overall adiposity and body fat distribution, showing a preference towards central adiposity with increased cigarette consumption [252]. Conversely, a recent Mendelian randomization study performed on UK Biobank cohort (n=372791) strongly suggested that obesity and higher adiposity may influence smoking behavior and with each standard deviation increase in BMI there is a chance of smoking one additional cigarette per day [253]. This contradictory evidence on causal relationship between obesity and smoking highlights the complexity in the underlying biological mechanisms.

Decreased BMI in current smokers has been associated with increased metabolic rate and reduced appetite caused by nicotine [254]. Increased BMI after smoking cessation could be a result of increased calorie intake and changes in fatty acid catabolism [255]. Regulation of appetite for tobacco and food has been suggested as a possible common biological basis for nicotine addiction and obesity [256]. Furthermore, both nicotine dependence and obesity revealed common neuronal and behavioral circuits triggering regions associated with reward, satiety and self-control within the brain [257,258]. In summary, given the detrimental effects of smoking and obesity, and the associated comorbidities, it is crucial to investigate the impact of their co-occurrence on mortality.

3 Aims

The primary objective of this thesis was to advance our understanding of obesity and smoking by identifying and integrating DNA methylation variants with transcriptomics data by applying statistical methods and bioinformatics tools. This thesis also focused on developing a robust classifier to predict smoking status using DNA methylation profiles.

Rationale and aims specific to each study are listed below:

1. *Little is known about the crosstalk between gene expression and DNA methylation in SAT during weight loss. Moreover, using a study design controlled for genetic variation serves as an ideal setting to unravel weight loss-associated expression and methylation changes independent of genetic influence. Concurrent evaluation of weight-loss associated expression and methylation changes in obesity can provide crucial insights into mechanisms governing both weight loss and weight gain.*

   Study I aimed to identify and integrate gene expression and DNA methylation changes in SAT during a one-year weight loss intervention. We used a validation cohort of BMI-discordant MZ twin pairs to examine the directionality of the identified changes in acquired obesity. We employed a longitudinal and BMI-discordant MZ twin approach to investigate effects of weight loss and obesity independent of genetic background.

2. *Smoking is a well-established risk factor for several cancers including cardiovascular disease and diabetes. Several studies identified smoking-associated methylation signals in blood methylome, however, the broader impact of smoking on other metabolically relevant tissues and obesity remains unclear. SAT is a key metabolic organ with a crucial role in metabolic health and accumulation of adipose tissue has been associated with smoking behavior. Therefore, investigating smoking-associated changes in transcriptome and methylome of SAT provides valuable insights into effects of smoking on metabolic health phenotypes.*

   Study II aimed at comprehensively characterizing the impact of smoking on metabolically relevant SAT by simultaneously performing transcriptome- and methylome-wide association studies. We further aimed to link the identified smoking-associated signals with adiposity phenotypes to understand the impact of smoking on metabolic health.

3. *Methylation-based smoking status prediction has been shown to be more robust than self-reported smoking status and biomarkers like cotinine which can only measure short-term exposure. Existing DNA methylation-based smoking status estimation methods use scores calculated from cumulative methylation levels at smoking-associated CpGs to identify smoking status. However, these approaches have limited applicability as a score threshold value needs to be computed for each dataset and can only perform binary classifications.*

   Study III aimed at overcoming the limitations of existing nicotine biomarker and DNAm score-based approaches by developing a robust smoking status classifier using a machine learning approach to predict the smoking status of individuals based on methylation signatures. To test the prediction performance and global applicability of the classifier three independent whole-blood test datasets and two existing methods were used. Additionally, we aimed to provide our classifier as an R package to facilitate the implementation of the classifier in future studies to predict smoking status.

4 Materials and Methods

This chapter presents the datasets, phenotypes and statistical methods used in the Studies I to III.

4.1 Cohorts/Datasets

This section gives a brief overview of all the datasets used in this thesis. Multiple cohorts originating from the Finnish population were used in the Studies I to III. Also, datasets from public repositories were used to test or replicate the findings. More detailed descriptions of the cohorts can be found in the original publications and references therein. Study-wise sample characteristics of all the datasets used in the thesis are presented in Tables 4 and 5.

4.1.1 The Finnish Twin Cohort (Study I-III)

The Finnish Twin Cohort (FTC), was established in 1974 to investigate genetic and environmental factors contributing to complex diseases and associated behavioral risks (www.twinstudy.helsinki.fi) [259,260]. The three main longitudinal datasets of the FTC are reviewed below:

The Older Finnish Twin Cohort was formed in 1975 by ascertaining same-sex twin pairs (both monozygotic and dizygotic) born before 1958 from the Central Population Registry of Finland [261]. This cohort was further expanded in 1996 by the inclusion of opposite-sex pairs born during 1938-1949. An additional three waves of follow-up data were collected in 1981, 1990 and 2011-2012 through mailed questionnaires [259,260].

***Essential Hypertension Epigenetics* (*EH-Epi*)** is a sub-study of the Older Finnish Twin Cohort launched in 2011 to study hypertension. Twins were recruited based on the responses to the 2011-12 comprehensive questionnaire assessing diagnosed hypertension, history of hypertension and usage of anti-hypertensive medication [262]. Participants in this study went through a comprehensive physical examination, interview and blood sample collection during 2012-2015. A subset of 408 twins with extensive smoking information from this study was used as a test dataset in the Study III.

FinnTwin16 study was initiated in 1991 by recruiting twins born during 1975-1979 [259,263]. The first wave of assessments was performed on twins at the age of 16 along with their parents and siblings. Intensive follow-up assessments were performed on the twins at ages 17, 18.5 and at young adulthood (age 22-25) through mailed questionnaires.

FinnTwin12 study established in 1994 comprises twins born during 1983- 1987 [259,264]. At the baseline, 11 to 12 year old twins were assessed along with their parents and teachers. Twins were then followed up at ages 14, 17.5 and 22.

***TwinFat* (n =109)** [265], a sub-study formed from the FinnTwin16 and FinnTwin12 cohorts to extensively investigate obesity in twins. A rare and deeply phenotyped dataset of 26 BMI-discordant MZ twin pairs (intra-pair difference in BMI 3-10 kg/m2, males n = 9, females n = 17, aged 29.55 ± 4.61 years) from TwinFat was used as a validation cohort in Study I, to assess the expression and methylation of weight responsive genes in acquired obesity. In Study II, 69 individuals (34 full MZ twin pairs, mean age 31.1 ± 4.43 years, mean BMI 27.5 ± 4.72, 44.9% male) from the TwinFat with complete covariate data as per the discovery cohort TwinsUK [266] (e.g. alcohol intake), were used to replicate methylation associations with metabolic health traits.

4.1.2 Weight Loss Study (WLS) (Study I)

Nineteen obese volunteers (mean BMI 34.65 kg/m2) constituting 12 females and 7 males (Table 4) were recruited for a 12-month weight loss program through a newspaper advertisement [118,267]. All participants were healthy non-smoking weight-stable adults without any clinical complications and regular medications. The intervention started with a very-low-energy diet (800–1000 kcal per day) for first 6 weeks, followed by a normal weight loss diet in conjunction with exercise plans. Participants were given customized diet plans at 0, 2 and 5 months.

Table 4: Characteristics of the datasets used in the Studies I and II

Study	Dataset	Age (Mean ± SD)	M/F	BMI (Mean ± SD)	Smokers	Transcriptome Data	Methylation Data
I	WLS	35.21± 7.79	7/12	34.65±2.67[a]	-	19	19
	TwinFat	29.55± 4.61	18/34	*Heavy twins* 31.25±5.18 *Lean twins* 25.28 ±4.52	*only one co-twin smokes*: 6 *both twins smoke*: 4 pairs	26 pairs	24 pairs
II	TwinsUK*	58.40±9.56	0/345	26.82±4.81	54	345	345
	TwinFat	31.05±4.43	31/38	27.47±4.72	21	-	69

[a]At the baseline in weight loss study.
**Methylation and transcriptome dataset from the TwinsUK cohort with only current and never smokers, used in discovery analyses to identify smoking-associated methylation and expression signals.*
SD: Standard deviation

4.1.3 DILGOM (Study III)

FINRISK study [268] comprises of nationwide surveys of the Finnish adult population on risk factors related to chronic diseases performed every five years since 1972. DILGOM (Dietary, Lifestyle and Genetic determinants of Obesity and Metabolic syndrome) (n=5024) [269,270] is a cross-sectional study originated from the FINRISK 2007 study (n=6258), designed to investigate the impact of genetics, environment and

lifestyle factors on obesity and metabolic syndrome. Comprehensive phenotypic data and blood samples were collected from the participants. Genome-wide DNA methylation data and extensive smoking information available from 514 individuals was used in Study III (Tables 5 and 6). We have also used plasma cotinine measurements determined by gas chromatography-mass spectrometry available from 86 current, 31 former and 3 never smokers [271].

4.1.4 Public Datasets (Study III)

In Study III in addition to the FTC dataset (n=408), we have used two publicly available whole-blood datasets [59,61], a buccal tissue [272] and a PBMC dataset [273] quantified on 450k array to test the performance of the classifier (Tables 5 and 6). The first whole-blood dataset is from the EIRA study [59], a population-based rheumatoid arthritis (RA) case-control study conducted in Sweden. We have used methylation data and smoking status information from 687 participants, including 354 RA cases and 333 cases matched for age, sex and smoking status. The second whole-blood dataset consisted of 464 participants from the CARDIOGENICS consortium [61], a European descent case-control study of coronary artery disease, including 238 patients. We have used 80 individuals (after excluding 40 moist-snuff users) with buccal tissue methylation data (n=120) [272] composed of healthy Caucasian and African-American men from North Carolina. The PBMC methylation data [273] was collected from 111 African-American women living in the states of Iowa and Georgia, as a part of the Family and Community Health Study (FACHS).

Table 5: Characteristics of the training and test datasets used to train and evaluate the performance of smoking status classifier (Study III)

Datasets	**N**	**Sex** (M/F)	**Self-reported Smoking Status**			**Age** (Mean, Range, SD)
			Current	Former	Never	
Training Dataset (whole-blood)						
DILGOM	474	215/259	113	118	243	52.2 (25-74,13.6)
Test Datasets (whole-blood)						
EH-Epi study	408	166/242	67	141	200	62.2 (32.3-69.7, 4.3)
EIRA (Epidemiological Investigation of Rheumatoid Arthritis)	687	196/491	266	228	193	51.9 (18-70,11.8)
CARDIOGENICS	464	327/137	22	263	179	55.4 (38-67, 6.7)
Test Datasets						
Buccal	80[a]	80/0	40[b]	-	40[b]	47.2 (35-60, 7.9)
PBMCs	111[c]	0/111	50	-	61	48.4 (NA, 10)

[a]Of these 80 individuals, 58 were Caucasian, 21 were African-American and 1 unknown ethnicity. [b]In buccal tissue data smoking behavior was defined as cigarette smoker and non-tobacco smoker. [c]African-American ancestry. SD: Standard deviation; NA: Not available

4.2 Phenotypes

This section outlines the phenotypes associated with obesity and smoking examined in this thesis to profile methylome and/or transcriptome. Extensive phenotypic information was used in Study I and Study III to assess obesity and smoking-associated changes in adipose and whole-blood tissues, respectively.

4.2.1 Obesity

In WLS (Study I) all the clinical measures were taken at three time points (baseline, 5 and 12 months). To assess the habitual dietary intake WLS participants were requested to maintain a detailed food journal for three consecutive days at 0, 5 and 12 months. Additionally, lifestyle counselling sessions were held twice a month for the first five months and monthly from sixth to twelfth month. At the end of the intervention,

complete data on energy intake and Baecke indices [274] were available from 15 and 16 participants, respectively.

MZ twins from the TwinFat study (Study I validation cohort and Study II) were selected based on the questionnaire data and during a twin's clinical visit, interviews, on-site measurements of body composition and sample collection (adipose tissue biopsy) was performed. All measures were used on continuous scale in statistical analyses unless specified otherwise.

4.2.1.1 Clinical assessments

In the Study I identical protocols were followed in the weight loss- and the validation cohort unless specified otherwise. Weight and height measurements taken after a 12-hour overnight fast were used to calculate BMI and total body composition was assessed by dual energy X-ray absorptiometry (DEXA) (GE Lunar Prodigy Madison, WI, England) [275]. In the weight loss cohort, liver fat was measured by magnetic resonance spectroscopy (MRS) and volumetric subcutaneous adipose tissue (SAT) and visceral adipose tissue (VAT) were measured by magnetic resonance imaging (MRI) [276]. Systolic and diastolic blood pressure was measured in supine position and a mean of three consecutive measurements was considered as the accurate measurement. To calculate homeostatic model assessment (HOMA)-insulin resistance [277] and Matsuda-insulin sensitivity [278], plasma glucose (spectrophotometric hexokinase and glucose-6-phosphate dehydrogenase assay, Roche Diagnostics, Basel, Switzerland) and serum insulin (time-resolved immunofluorometric assay, Perkin Elmer, Waltham, MA, USA) were measured after a 12 hour overnight fast by performing a 75-g oral glucose tolerance test (OGTT) [279] at four time points (0, 30, 60 and 120 min). Fasting plasma total cholesterol, HDL cholesterol, and triglyceride concentrations were determined by enzymatic methods (Roche Diagnostics Hitachi, Hitachi Ltd, Tokyo, Japan) and LDL cholesterol was calculated using Friedewald formula. In Study I fat percentage was considered as a representative measure of adiposity and obesity.

In the Study II total fat mass (TFM) and android-to-gynoid fat ratio (AGR) were determined by DEXA.

4.2.2 Smoking

Smoking status was ascertained through self-reported questionnaire data in all the datasets and was used as a categorical variable in all the analyses. Except for the PBMC dataset, smoking status was defined with respect to the cigarette consumption (Table 6). FTC and EIRA datasets also included additional smoking measures enabling us to comprehensively assess the smoking status of the participants. Table 6 provides a summary of the smoking phenotypes used in this thesis.

In Study III DILGOM data was used as the training dataset to build a smoking status classifier (see Table 6 for detailed smoking status definitions). Hence, to ensure the classification accuracy of the classifier

and to minimize bias, smoking behavior of the participants was thoroughly assessed using a combination of the following three measures:

1. Self-reported smoking status:
    a. Never Smoker
    b. Former Smoker (quit more than a year ago)
    c. Recent quitter (quit 1 month to year ago)
    d. Current occasional smoker
    e. Current daily smoker
2. When did you have your last cigarette? (measured using 7 response alternatives):
    1. Yesterday or today
    2. Two days to one month ago
    3. One month to half a year ago
    4. Half a year to year ago
    5. 1 to 5 years ago
    6. 6 to 10 years ago
    7. More than 10 years ago
3. Cotinine measurements

Self-reported smoking status was validated with cotinine measures where available (86 current, 31 former and 3 never smokers) and using a response measured on a scale of 1-7 about last smoking (Q: when did you have your last cigarette). We considered current occasional smokers with either high cotinine values or who smoked their last cigarette less than six months ago as current smokers. By using a combination of the above three measures I have excluded 28 former, 2 never and 6 occasional smokers with discrepant smoking information from the further analyses.

I used 408 twins from the FTC corresponding to the EH-Epi study as a test dataset in Study III. Comprehensive smoking information available from these participants, including cumulative pack-years, smoking abstinence duration (years since quitting) and passive smoking information was used to perform secondary analyses in Study III. Current smoker category was subdivided into current daily and current occasional smokers in FTC and EIRA datasets based on frequency and extent of smoking.

Table 6: Detailed smoking-status definitions from all the datasets used in Study III

Self-reported smoking status	**DEFINITION**
DILGOM (N=474)	Smoking behavior of the study participants was thoroughly assessed using three measures
Current	(1) Smokes regularly or occasionally, (2) last cigarette was smoked ranging from today to less than six months ago and (3) where available has a cotinine value > 10 (nanogram per milliliter; ng/ml). A sub-class of current occasional smokers was separated from current daily smokers with individuals who had smoked their last cigarette one month to half a year ago.
Former	Has quit smoking at least a year ago, last cigarette was smoked more than 1 year ago and where available has a cotinine value less than 10 ng/ml.
Never	Has never smoked or smoked less than 100 cigarettes during their lifetime.
FTC (n=408)	Smoking was ascertained with response alternatives ranging from 1 to 7 (see numbering below).
Current	Smokes cigarettes less than once a week to 20 or more cigarettes per day (1 - 5). We have further divided them into current daily and current occasional smokers as follows: ➢ Current daily: smokes between > 20 cigarettes per day to < 10 cigarettes per day (1 - 3). ➢ Current occasional: Smokes at least once per week but not every day or smokes less than once a week (4 - 5).
Former	Has quit smoking or is in abstinence (6).
Never	Has never smoked or smoked less than 100 cigarettes during their lifetime (7).
EIRA (n=687)	For patients with RA, smoking status was ascertained based on the smoking habits in the index year (the year in which symptoms of RA onset occurred).
Current	If smoking currently, when did you start smoking and the average number of cigarettes per day.

	For RA cases, if smoked during the index year. Current smokers were further classified into daily and occasional smokers.
Former	Not a current smoker but smoked previously, start year and end year of regular smoking, average number of cigarettes smoked while smoking. In RA cases, patients who quit regular smoking for at least one year before the index year.
Never	Has never smoked before or during the index year.
CARDIOGENICS (n=464)	
Former	Has quit smoking for more than 12 weeks (n=251) or less than 12 weeks (n=12) before the participant recruitment.
Buccal Tissue Dataset (n=80)	
Smokers	Smoked at least 10 cigarettes per day for a minimum of 3 years and had exhaled carbon monoxide (CO) levels between10-100 (parts per million; ppm).
Non-smokers	Abstinent from all nicotine and tobacco containing products for a minimum of 5 years with expired CO levels between 0-5 ppm.
PBMC Dataset (n=111)	
Smokers	Actively smoking
Non-smokers	Denied using any tobacco products

4.3 Sample collection and DNA and RNA extraction

In Studies I and II surgical biopsies of abdominal SAT were obtained from the periumbilical area under local anesthesia and were snap-frozen in liquid nitrogen. In the validation cohort (Study I) [280], SAT biopsies were available from all the BMI-discordant MZ twin pairs (n=26 pairs) for gene expression analyses, whereas only 24 twin pairs had DNA for the methylation analyses. High-molecular weight total RNA was isolated from SAT biopsy using RNeasy Lipid Mini Kit (QIAGEN Nordic, Sollentuna, Sweden) following the manufacturers' instructions and the RNA quality was assessed by 2100 Bioanalyzer using RNA Integrity Number (RIN) algorithm (Agilent Technologies, Espoo, Finland). High-molecular-weight DNA was extracted from whole blood (Study III) and adipose tissue (Study I and II) using QIAamp DNA Mini kit (QIAGEN Nordic, Sollentuna, Sweden) according to the manufacturer's instructions. Quality and concentration of DNA were

assessed using NanoDrop® ND-1000 UV-Vis (ThermoFisher Scientific, Helsinki, Finland) spectrophotometer.

4.4 Omics Data

This section outlines various omics datasets used in the studies summarized in this thesis. Genome-wide transcriptome and methylome data were characterized using microarray technology. Stringent QC and filtering performed in each study to include only high-quality samples and probes for further analyses are described in this section. Figure 6 outlines the general workflow of array-based DNA methylation and transcriptome data analysis.

4.4.1 Expression data

Total RNA isolated from SAT was used to measure gene expression on Affymetrix Human Genome U133 Plus 2.0 Array (Affymetrix, Vienna, Austria) at the Biomedicum Functional Genomics Unit (FuGU), Helsinki, Finland), following a previously validated protocol [281]. All the samples (both WLS and the validation TwinFat cohort) passed QC checks for RNA degradation, hybridization, and amplification performed using R packages: simpleaffy (to read Affymetrix data i.e. CEL files) [282] and affyPLM (to fit probe-level models and quality assessments) [283]. Robust Multi-array Average (RMA) algorithm [284] was applied (R package affy) to perform background correction (correcting for optical noise and non-specific binding), quantile normalization and to summarize expression values on logarithmic scale per each probeset. Probesets were then mapped to the corresponding genes using the Brainarray customized Chip Description File version 18.0 (hgu133plus2hsentrezgcdf) [285]. Expression data from 19598 genes were available for downstream analyses. From the validation cohort of MZ twins, I used only a subset of the expression array data corresponding to the significantly differentially expressed genes identified in the discovery analyses in the WLS to perform validation analyses.

4.4.2 Methylation data

The Illumina Infinium HumanMethylation450 BeadChip (Illumina, San Diego, CA, USA) (450k array) was used to quantify methylation from whole blood (Study III) and adipose tissue (Study I and II) at the Microarray Consortium, Oslo, Norway, at the Technology Centre, FIMM, University of Helsinki, Finland, at The Genomics Facility, University of Chicago, Chicago, IL, USA, and at The SNP&SEQ Technology Platform, University of Uppsala, Sweden. Samples were randomly distributed into 96-well plates to minimize potential batch effects, and discordant co-twins were always placed next to each other on the same plate. Bisulfite conversion of genomic DNA was performed using the EZ-96 DNA Methylation-Gold Kit (Zymo Research,

Irvine, CA, USA) and genome-wide DNA methylation was quantified on the 450k array following the manufacturer's instructions.

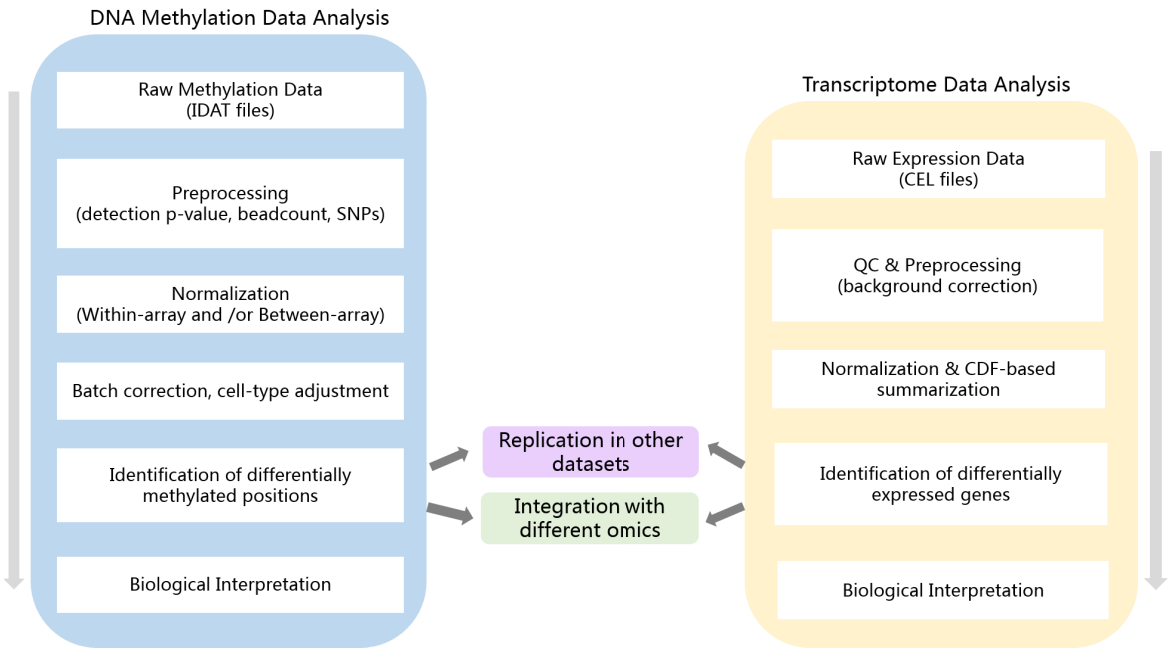

Figure 6: A comprehensive workflow of DNA methylation and transcriptome data analysis

Quality control (QC) and preprocessing steps in Study I-III were performed using R package minfi [86]. Numerous preprocessing and normalization methods are proposed for 450k data, however, there is no clear consensus on the best approach to be followed. This is also reflected in the different preprocessing steps, normalization methods and cut-offs employed in this thesis, to ensure the inclusion of high-quality samples and probes for further analysis. I excluded probes with higher detection P-values to ensure that the measured intensity was not representing background noise. In Study II, I excluded probes with detection P-value > 0.05 as per Illumina recommendations. In Study I, I employed a more stringent cut-off and excluded probes with P-value >0.001. In the Study III, detection P-value threshold was further lowered to $1x10^{-16}$ following more recent recommendations by Lehne *et al,* to improve quantification of methylation and to avoid spurious detection of call rates [87]. Additionally, in Study III probes with more than 2% missing data across samples were also excluded. I removed probes located on X and Y chromosomes and probes specific to SNPs and non-CpG probes (Study I–III). Sample exclusion threshold was set as sample call rate< 95%, based on this criteria four samples were excluded from Study III.

At each CpG site methylation levels (β-values) were calculated as the ratio of methylation signal to the total locus intensity, ranging from 0 to 1, representing 0 to 100% methylation.

$$\boldsymbol{beta\ value} = \frac{\boldsymbol{Methylated}}{(\boldsymbol{Methylated} + \boldsymbol{Unmethylated} + \mathbf{100})}$$

Following the QC and preprocessing steps described above, methylation data was normalized and filtered when needed as per study design. The goal of normalization is to remove technical noise or unwanted variation from the signal (thereby normalized data representing very likely true signal or biological variation) and to make the methylation measures across samples comparable. Different normalization methods were employed in this thesis, reflecting the constant development in methods to efficiently correct for two type of probe chemistries present on the 450k array (Figure 4).

In Study I, quantile normalization (QN) followed by Beta MIxture Quantile (BMIQ) [84] normalization was performed in both WLS and the validation cohort TwinFat. While QN makes all the samples to have the same distribution of probe intensities, BMIQ adjusts the distribution of type II probes with respect to type I probes within each sample. Following normalization, I used ComBat function in the R package SVA [286] to remove unwanted variation introduced by potential batch effects. Finally, unreliable probes (mapping to multiple genomic locations, presence of SNPs in probe body or at the CpG site or deletions, insertions, and repetitive DNA) [287] were removed leaving 292802 probes for further analyses. By filtering low-quality probes multiple testing burden was minimized. In the validation cohort of MZ twins, I have used only a subset of CpG probes needed to verify methylation results from WLS.

In Study II, I first performed within-sample normalization using the BMIQ method and then normalized methylation levels to follow the normal distribution N(0,1) using qqnorm R function. This additional step was performed as most of the probes on the 450k array do not follow the normal distribution which may violate the assumptions of linear regression.

In Study III, I first separated the probe intensity values into six categories based on the color channel, probe-type, and subtype and then performed QN on each probe category using a custom function. In each probe category, I first sorted the actual intensity values within each sample and then calculated average intensity values for each rank across all the samples. I then replaced the actual intensity values with the corresponding average intensity values (quantiles) thereby forcing all samples to have the same distribution. I saved the quantiles obtained from the six probe categories. I then calculated beta values for each CpG probe using the normalized intensity values. I have not rescaled the intensities of Infinium II probes based on Infinium I probes, as it is nonessential for building a classification algorithm. After the normalization, I have removed unreliable probes mapping to multiple genomic positions [288] and weakly varying probes with variance <0.002 across the samples. To assess the performance of our classifier in the three whole-blood test datasets, I have performed quantile normalization using the same six set of quantiles

(corresponding to probe categories) obtained from the training dataset. This approach of fitting test dataset distribution to the training dataset ensures cross-study performance and can be referred to as "frozen" quantile normalization following McCall et al [289]. I performed subset quantile normalization (SQN) [80] and Illumina normalization (ILN) on the datasets to calculate smoking score (SSc) [217] and methylation score (MS) [221], respectively. In SQN, the reference quantiles are first calculated for each probe category of Infinium I signals using CpG annotations (Shore, S shelf, N shore, N shelf and distant), to which the Type II probes are then adjusted. ILN uses internal control probes as a reference to normalize the data. Frozen quantile normalization was not performed on publicly available test datasets from tissues other than blood, as the quantiles used in QN were derived using whole blood training dataset.

I used R package 'IlluminaHumanMethylation450kanno.ilmn12.hg19' for annotating the 450k data in all the studies.

4.5 Statistical Analyses

This section provides a broad overview of statistical analyses employed in the Studies I to III. All statistical analyses used in this thesis were performed in the R statistical environment [290].

4.5.1 Differential expression and methylation analyses (Study I)

We hypothesized that weight loss causes changes in gene expression profiles of SAT. To assess these changes, I performed differential expression analyses for three comparisons: short-term, continuous and long-term weight loss. I used pair-wise moderated t-tests [291] to compare expression levels of individuals with themselves at the current time point (lean) to an earlier time point (obese). Fat percentage was used as a continuous variable and was assessed for normality using Shapiro-Wilk test. I used R package limma [291] to fit gene-wise linear models using the fat percentage as a predictor and normalized gene expression data as a response variable. A design matrix was defined with fat percentage as a continuous variable and a pair-wise comparison (using an individual identification number to pair the samples from two-time points). I then fitted linear models on normalized gene expression data and the design matrix. Empirical Bayes procedure was then performed on the linear models to calculate the moderated t-statistic, to assess differential expression between the lean and obese conditions of individuals. The moderated t-statistic [291] differs from the classic t-statistic as the variance is estimated by borrowing information across all the genes. Hence variability of a gene implies a combination of gene-specific variability and global variability.

In the validation cohort, we hypothesized that weight loss-associated genes identified from WLS will have opposite direction of expression in acquired obesity. I performed paired moderated t-tests to compare BMI-discordant MZ co-twins. A design matrix was defined outlining the condition of the twins (a two-level factor: *Heavy* and *Lean*, using *Heavy* as a reference class) and a pair-wise comparison (using a twin identification number to pair the co-twins). I assessed differential expression between heavy and lean co-

twin to validate significantly differentially expressed genes identified in the WLS comparisons, to test whether the gene expression changes in acquired obesity were in opposite direction to weight loss.

We also investigated changes in SAT DNA methylation profiles during weight loss. I performed differential methylation analyses at three comparisons: short-term, continuous and long-term weight loss, to compare methylation levels of individuals at the current time point to an earlier time point. I have used the same design matrix as outlined above using the fat percentage as a predictor and normalized methylation data as a response variable. R package limma [291] was used to fit probe-wise linear models on normalized methylation data and design matrix. In the validation cohort, I used paired moderated t-tests to investigate differential methylation between the heavier and the leaner co-twins.

In all the analyses above, raw *P*-values were derived from moderated t-statistic. Bonferroni correction was applied to correct for multiple testing and genes or CpG sites with adjusted *P*-values <0.05 were considered as significant.

4.5.2 Integrated DNA methylation and gene expression analyses and Replication analyses (Study II)

The objective of Study II was to identify concurrently occurring smoking-associated changes in methylome and transcriptome of SAT and to test the effects of these identified smoking-associated methylation and expression signals on weight gain and adiposity measures. Discovery analysis was performed using adipose methylome (450k array) and transcriptome (RNA sequencing) from female twins of the TwinsUK cohort (n= 542) [266] by first author, Pei-Chien Tsai. A subset of 345 individuals was used to identify differentially expressed genes and methylated sites between current (n=54) and never smokers (n=291) using linear mixed-effect regression (LMER) model adjusting for appropriate covariates.

A subset of TwinFat participants (n=69) was used to replicate the significant methylation associations with TFM, VFM and AGR. A LMER model with family structure and zygosity as random effect terms and rest of the covariates as fixed effect terms were used to perform replication analyses. Here, fixed effects terms represent the parameters that are invariant across individuals (i.e. the model holds with respect to all individuals in the population of interest) while random effects terms capture the correlation between individuals within twin pairs. For each CpG site, a full model that regressed all of the covariates was compared to a null model that regressed all the covariates except smoking status. ANOVA F statistic was used to compare full and null models.

Full model:

Fixed Effects | Random Effects

$$CpG \sim phenotype + smoking\ status + age + sex + BMI + alcohol + plate + family\ identifier + zygosity$$

Null model:

Fixed Effects | Random Effects

$$CpG \sim phenotype + age + sex + BMI + alcohol + plate + family\ identifier + zygosity$$

4.5.3 Epigenetic Smoking status Estimator (EpiSmokEr) (Study III)

Our objective in Study III was to build a smoking status classifier (EpiSmokEr) using whole-blood methylation data to predict smoking status of an individual from his/her methylation profiles. To build the smoking status classifier I used the DILGOM dataset, which is representative of the general Finnish population with extensive smoking information (including cotinine measurements) and broad age spectrum, as the training dataset. I used multinomial LASSO regression to identify CpG sites predictive of smoking and then tested the performance of our classifier in five independent test datasets. Figure 7 outlines the steps involved in training the classifier and also shows how the output (predicted smoking status) is generated for user data.

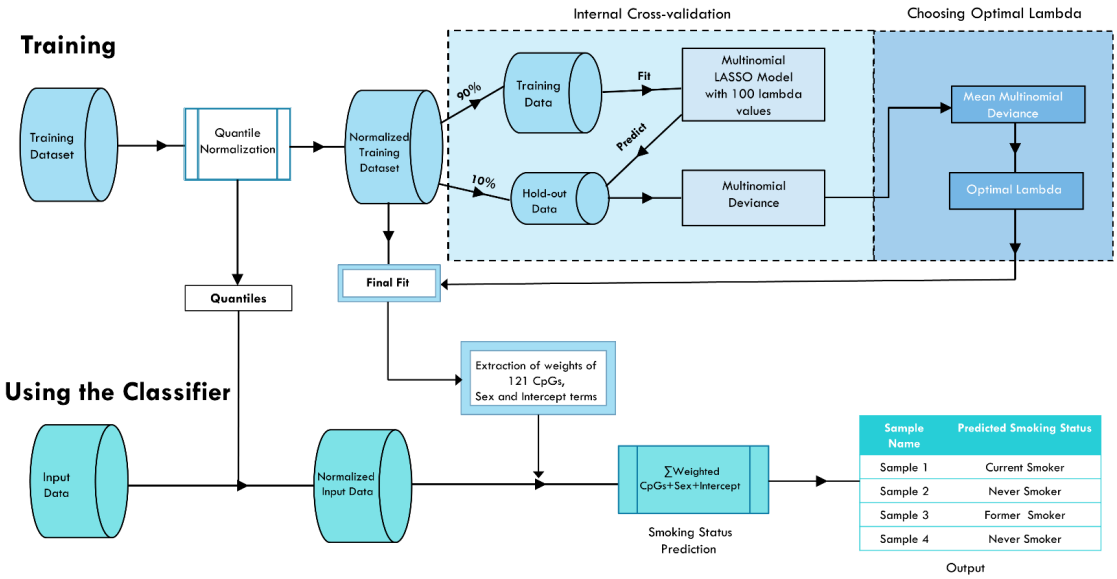

Figure 7: Schematic illustration of the workflow of the smoking status classifier. *This figure is reproduced from* [292] *(Bollepalli et al 2019) with permission of Future Medicine Ltd.*

4.5.3.1 Training the classifier:

Multinomial LASSO regression

I used 52421 high-quality CpG probes available from the DILGOM dataset after stringent quality control and filtering to perform multinomial LASSO regression using the R package glmnet [293]. I fitted a LASSO-penalized generalized linear model of the multinomial family, with three categorical variables (smoking status: current, former and never) and sex as an additional covariate to select CpGs predictive of smoking status. LASSO regression minimizes the residual sum of squares of coefficients by applying L1 norm penalty and forcing several coefficients to become exactly zero.

The following is an outline of the multinomial LASSO regression model used in Study III. This outline provides a mathematical review of our model for obtaining a parsimonious set of smoking-associated CpGs which were then used to build a classifier to predict smoking status (Equations 1 to 4). We represent the index of a CpG probe on the 450k array as i, subject (sample or individual) as j and quantile normalized methylation values on beta scale as x_{ij}. Three levels of smoking status categories are represented as $k' \epsilon K$ = {current, former, never}. In multinomial regression, model fits a linear predictor η_{jk} which is a multinomial equivalent to the log odds of logistic regression, i.e., η_{jk} corresponds to the probability p_{jk} for the subject j for each smoking status k assigned by the classifier via the logistic transformation,

$$Prob(\ subject\ j\ has\ status\ k\ ) = p_{jk} = \frac{e^{\eta_{jk}}}{\sum_{k' \epsilon K} e^{\eta_{jk'}}} \quad (1)$$

Here denominator ensures that the sum of the probabilities from the three smoking statuses are equivalent to 1.

The linear predictor η_{jk} is given as a linear combination of the fitted model coefficients β_{ik},

$$\eta_{jk} = \beta_{0k} + \beta_{Sk} x_{jS} + \sum_i \beta_{ik} x_{ij} \quad (2)$$

Here each CpG probe i has three coefficients β_{ik}, corresponding to each smoking status while the three intercepts β_{0k} acts as thresholds. The sex coefficient β_{Sk} is included as a covariate and is added to the intercept if the subject j is male $(x_{jS} = 1)$ and omitted if the subject j is female $(x_{jS} = 0)$.

These coefficients were obtained by fitting the LASSO regression model, which maximizes the penalized log likelihood as follows:

$$l(\beta) = \sum_j \log \boldsymbol{p}_{\boldsymbol{j}k_j} + \lambda \|\beta\|_{\mathrm{G}} = \frac{1}{N} \sum_{j=1}^{N} (\eta_{ik} - \log \sum_{k' \epsilon \boldsymbol{K}} \boldsymbol{e}^{\boldsymbol{\eta}_{jk'}}) + \lambda \sum_j (\sum_k \beta_{jk}^2)^{\frac{1}{2}} \quad (3)$$

Here $\lambda \|\beta\|_{\mathrm{G}}$, represents the penalty term which prevents overfitting by making the fit to select only those CpG probes i that contribute most to the prediction of smoking status and shrinks the coefficients of rest of the probes to zero. I used the "grouped" shrinkage option where the *glmnet* function links the three coefficients (each coefficient corresponding to a smoking status) for a given probe i such that they are either selected or not selected together.

An optimal value of tuning parameter λ which regulates the amount of shrinkage was chosen through internal cross-validation which is explained below.

Cross-validation

I performed 100 iterations of internal cross-validation on the DILGOM dataset to identify an optimal lambda of 0.55 from a sequence of 100 candidate values. In each iteration, the training dataset, DILGOM, was randomly subdivided into 90% training and 10% hold-out data. A multinomial LASSO regression model was then fitted on the 90% training dataset using the 100 candidate lambda values. For each lambda value, I then tested the fit of the prediction on the 10% hold-out data to obtain estimated probabilities per each class of smoking status.

I calculated multinomial deviance in each iteration for every λ as below:

$$D(\lambda) = -2 \sum_j \log \boldsymbol{p}_{\boldsymbol{j}k_j} \quad (4)$$

Here the sum runs over the 10% of the hold-out data. $\boldsymbol{p}_{\boldsymbol{j}k_j}$ is the probability assigned by the classifier to the held-out subject j using Equation (1), with true smoking status k_j, obtained by using the coefficients from the training with the given penalty parameter λ. I then averaged the deviances for each λ value over the 100 iterations and chose the lambda value with lowest average deviation (between the probability that the classifier has assigned and the subject´s original smoking status) as the optimal λ (here 0.55). I performed a final fit on the full training dataset (DILGOM) to obtain the non-zero coefficients of 121 CpG sites, sex and intercept coefficients. These coefficients were used to build the classifier to predict the smoking statuses in the test datasets.

4.5.3.2 Testing the classifier:

Smoking status prediction

To predict the smoking status of a given test dataset using the classifier, the test dataset is first quantile normalized reusing the quantiles obtained from the training dataset. Then using the Equation (1), for each subject in the test data set, a probability is calculated for each of the three smoking statuses. The smoking status category with the highest probability is reported as the predicted smoking status of the individual.

Evaluating the performance of the classifier

I used three independent and external whole-blood test datasets (FTC, CARDIOGENICS and EIRA) to evaluate the performance of our classifier. As explained above raw methylation data from these test datasets was first quantile normalized using the training dataset quantiles and then smoking statuses were predicted using our classifier.

I also evaluated the performance of our classifier in two additional tissues: buccal tissue and PBMCs, to test the broader impact of smoking on methylation across tissues. No additional normalization was performed in these two datasets owing to the difference in the tissues.

I calculated sensitivity and specificity values to assess the accuracy of the predictions from our classifier. Owing to the multinomial model with three smoking status categories, I calculated these accuracy estimates by comparing one category with the union of the other two categories.

4.5.3.3 Smoking scores (SSc) and methylation scores (MS)

I additionally computed smoking and methylation scores from the two whole-blood test datasets (FTC and EIRA) to compare with the performance of our classifier.

To calculate SSc, test datasets were first normalized using the SQN method and scores were calculated as described by the Elliott *et al* [217], using the methylation values from never smokers of Zeilinger *et al* [220] as reference values.

$$\mathbf{SSc}_j = \sum_{i=1}^{187} \boldsymbol{w}_i (\boldsymbol{x}_{ij} - \boldsymbol{x}_i^{\mathbf{NS}})$$

Here index $\boldsymbol{i}$ runs over the 187 smoking-associated CpGs from the Zeilinger et al. 's Table S2 [220] and $\boldsymbol{x}_{ij}$ denotes the SQN normalized methylation value of an individual for CpG site $\boldsymbol{j}$. The reference methylation value $\boldsymbol{x}_i^{\mathbf{NS}}$ for CpG site $\boldsymbol{i}$ is the median methylation value of never smokers from Zeilinger *et al*, where the methylation values were averaged over discovery and replication cohorts (columns P and S of the Table S2).

The probe weight w_i is obtained as follows:

$$w_i = \frac{x_i^{CS} - x_i^{NS}}{\sum_{i'=1}^{187}(x_{i'}^{CS} - x_{i'}^{NS})}$$

Here x_i^{CS} represents median methylation value of current smokers obtained by averaging methylation values across discovery and replication cohorts (columns Q and T of their Table S2) [220].

To calculate MS, test datasets were normalized using the ILN method and the methylation values of 4 CpG probes (*cg05575921, cg05951221, cg02451831 and cg06126421)* from the test datasets were multiplied with their corresponding weights provided in the Figure 4 of Zhang *et al* [221] and then summed up.

I tested multiple threshold values for SSc and MS to compare with our method because the papers on SSc and MS did not provide a fixed threshold value to use.

4.5.3.4 Secondary analyses

I used the well-annotated FTC dataset (Table 6) to comprehensively scrutinize the misclassifications of our classifier. Here, misclassification refers to the disagreement between self-reported smoking status and predicted smoking status from the classifier. Considering self-reported smoking status as the ground truth can be counter-productive when unreliable self-reports are used. Therefore, I examined the duration of smoking abstinence (years since quitting) and cumulative exposure to smoking (pack-years), the two most informative smoking behavior variables to verify the disagreements. I also examined the effects of passive smoking on the misclassifications. To specifically understand the misclassifications from the current smoking category, I subdivided current smokers into current daily and occasional smokers in the FTC and EIRA datasets.

4.5.3.5 Availability and usage of our classifier

Our smoking status classifier, EpiSmokEr, is available as an R package: https://github.com/sailalithabollepalli/EpiSmokEr

EpiSmokEr expects methylation data from the 450k arrays as an input, either as raw methylation data (IDAT files) or a normalized methylation matrix and a sample sheet with sex information. The *normaliseData* function of our package has a suite of customized internal functions for normalizing and calculating beta values from the IDAT files. I use functionalities from the *minfi* package [86] to perform SQN [80] and ILN normalization, and I use a custom function to perform QN. The output from the classifier is provided as a

label, namely the smoking status category with the highest probability. The output is generated both in HTML and CSV file formats and also includes probability estimates for each of the smoking status categories. It requires only a few minutes for a typical calculation beginning with the IDAT files to the prediction of the smoking status. I also provide the functionality to calculate SSc and MS.

4.5.4 Correlation analysis between gene expression, DNA methylation and clinical measures (Study I)

In Study I, I associated expression and DNA methylation by calculating Pearson correlation coefficients for each comparison. In WLS, correlation coefficients were computed for significantly differentially expressed genes and the CpG sites within the corresponding genes by using the expression and methylation differences within an individual. CpG sites were mapped to corresponding genes using IlluminaHumanMethylation450kanno.ilmn12.hg19 annotation file. To validate these correlations in acquired obesity I have computed correlations in BMI-discordant MZ twins using within pair expression and methylation differences. I also associated gene expression with obesity-related clinical measures by correlating intra-individual gene expression differences with the corresponding intra-individual differences in clinical measures. Pearson correlation coefficients with P-values below 0.05 after adjusting the false discovery rate using the Benjamini-Hochberg procedure were considered as significant.

4.5.5 Pathway Analyses (Study I)

I performed Gene Set Analysis (GSA) [294] on genes from each weight loss comparison in the Study I to gain functional insights. GSA enabled us to assess the significance of pre-defined gene sets representing Reactome pathways [295] rather than individual genes. We expect that closely related genes with similar expression levels belong to a gene set and thereby increase the statistical power by borrowing strength across the genes. I performed a two-class paired comparison with 1000 permutations [296] using 526 of 674 gene sets with a size of 15 to 500 genes. Pathways with FDR adjusted p-values below 0.05 were considered as significant.

4.5.6 Covariates

Various study-specific covariates were included in the statistical models to adjust for confounding. In Study I, no covariates were included in the statistical models as I performed intra-individual or within-pair (in MZ twins) comparisons. In Study II, age, sex, BMI, alcohol, batch effects (plate), family and zygosity structure were used as covariates. In Study III, I performed singular value decomposition (SVD) analysis using R ChAMP [81] package to test whether the top 20 principal components (PCs) of the DILGOM methylation data were associated with the proportions of blood cell subtypes. Only a nominal association was identified between PC-2 and CD8+ (cytotoxic) T cells. I have included sex as a covariate in the LASSO model for building the classifier owing to the higher global prevalence of smoking in men compared to women.

4.6 Ethics permissions and Data availability

All the participants in the Weight Loss Study, FTC and DILGOM/FINRISK have provided written informed consent and the studies were designed and carried out following the principles of the Declaration of Helsinki. Data collection and ethical permissions were approved by the appropriate ethics committees. All the other datasets used in this thesis have obtained permission from their respective ethical boards.

Data used in Study I is available from the Gene Expression Omnibus (GEO) repository under the accession numbers GSE103769, GSE68336, and GSE92405. Data from the DILGOM and FTC cohorts can be obtained through permission from the corresponding data access committees. Four test datasets used in Study III are publicly available from the GEO (EIRA: GSE42861; CARDIOGENICS: GSE50660; Buccal dataset: GSE94876; and PBMC dataset: GSE53045).

5 Results and Discussion

5.1 Gene expression and DNA methylation changes in adipose tissue during weight loss (Study I)

Relentlessly increasing global obesity and its associated co-morbidities are posing a major health-care challenge. Losing weight is the primary recommendation to treat obesity-associated diseases. Despite a plethora of existing weight-loss interventions, only a few obese individuals succeed to attain and maintain long-term weight loss. Consequently, it is crucial to improve our understanding of the underlying genetic and epigenetic mechanisms inducing acquired obesity and weight loss, to design efficient long-term weight loss strategies.

We performed a one-year weight loss intervention program on 19 healthy obese participants to assess longitudinal gene expression and DNA methylation at three time points in the subcutaneous adipose tissue (SAT). Participants consumed a hypocaloric diet for the first six weeks, followed by a normal weight loss diet in conjunction with counselling sessions and exercise plans. We concurrently analyzed SAT expression and methylation to broaden our current knowledge of weight loss mechanism in mildly-obese but clinically healthy individuals.

Based on the biopsy collection our study can be divided into three phases: 0, 5 and 12 months. Several metabolic and clinical parameters were measured at each time point. Total energy consumption reduced by an average of 35.2% over the first 5 months, resulting in a mean weight loss of 11.7 % and a 5 % decrease in the mean fat percentage (Appendix I: Supplementary Table 1). Also, several clinical and metabolic measures considerably altered with weight reduction, suggesting enhanced health status. For instance, all fat depots (SAT, VAT and liver fat), waist circumference and LDL cholesterol decreased while physical activity and insulin sensitivity increased.

After the fifth month of intervention, participants were categorized into two separate groups based on their weight loss trajectory, enabling us to evaluate metabolic parameters, transcriptome and methylome in weight losers (WLs, n=6) and weight regainers (WRs, n=13), separately (Figure 8). While WLs continued to lose weight, WRs either maintained their weight at the fifth month level or began to regain weight. WLs showed a steady decline in BMI, body fatness and waist circumference after the fifth month, as well as an increase in HDL-cholesterol (HDL-C) up to the twelfth month (Appendix I: Supplementary Table 1). By the end of the study WLs achieved a total weight loss of 17% and a 7.4% decrease in the fat percentage. Conversely, at the twelfth month, WRs showed an increase in BMI, body fatness and systolic blood pressure and a decrease in insulin sensitivity (Matsuda index) compared to fifth month. Interestingly, there was no significant difference in the energy intake between WLs and WRs, although WLs had higher physical activity and work index [274] compared to the baseline.

We profiled SAT transcriptome and methylome at the three time points during the intervention (baseline, fifth and twelfth month). With the emergence of two weight loss categories after the fifth month we performed three different analyses: short-term weight loss (baseline to fifth month, all participants), continuous weight loss (fifth to twelfth month, only in WLs) and long-term weight loss (baseline to twelfth month, only in WLs). We identified several differentially expressed genes (DEGs) from these three analyses, however, we did not find any significant changes in methylation levels (differential methylation) with genome-wide significance. We then used a targeted approach to integrate expression and methylation data by correlating significantly differentially expressed genes with their DNA methylation (CpG sites from the respective genes). To gain a broader perspective of the results, we also performed pathway analysis using the significant genes from each comparison. Furthermore, we used a validation cohort of BMI-discordant MZ twins to test the hypothesis whether some of the weight-loss associated genes react in an opposite manner in acquired obesity.

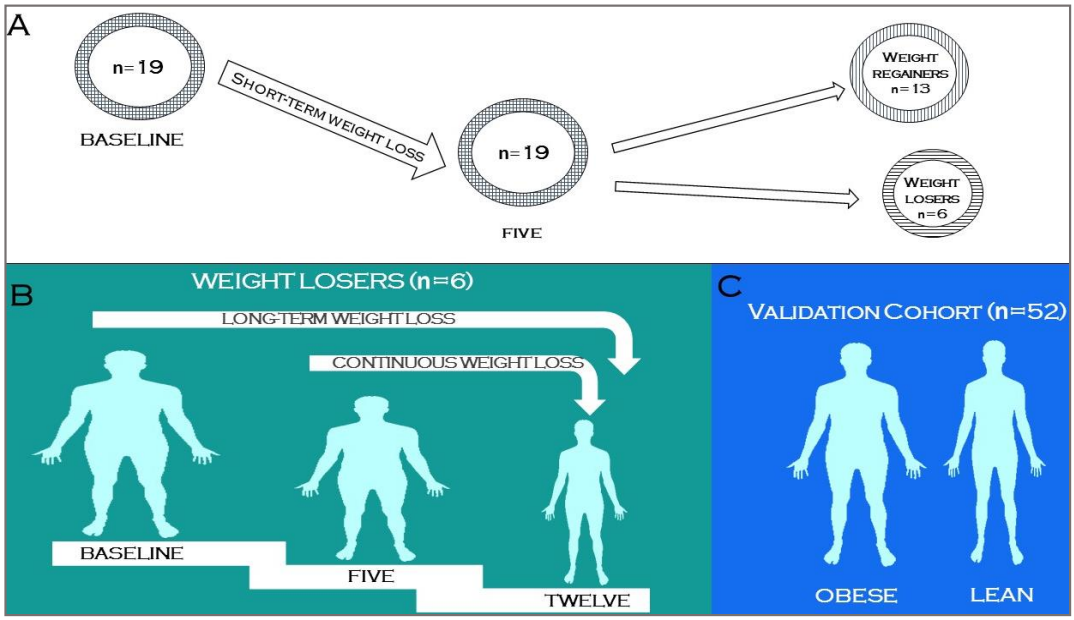

Figure 8: A schematic representation of the weight loss study design. Modified from Figure 1 of [297] (*Bollepalli et al 2018*).

A comprehensive overview of main findings from Study I are illustrated in Figure 9 and are explained in the following paragraphs. We identified 69 significantly differentially expressed genes (Bonferroni corrected *P*-value <0.05) during short-term weight loss (from baseline to fifth month) in the 19 participants using gene-wise linear models. Both the most significantly upregulated gene, *TMEM100,* and the most significantly downregulated gene, *NQO1,* had previously shown the same direction of expression in weight

loss [180,298]. While *TMEM100* is crucial for vascular integrity [299], *NQO1* has been positively associated with adiposity, glucose intolerance and obesity-associated metabolic complications [300]. Altogether, short-term weight loss upregulated genes involved in cholesterol flux (*APOE*) and downregulated genes involved in oxidative stress (*NQO1*, *UCHL1 and CRYAB*), adipogenesis (*CRYAB, AKR1C2* and *ADAM12*) and lipid metabolism (*BHMT2, AKR1C2* and *SEPT11*). Furthermore, most of the genes identified during short-term weight loss have been previously associated with obesity or weight loss [301]. Our findings were further strengthened by the opposite direction of regulation in 60 of these 69 weight-loss associated genes in acquired obesity observed in the within-pair comparisons of the obesity-discordant MZ twins. Pathway analyses revealed enhanced blood HDL-C levels following short-term weight loss, which was evident from the improved blood HDL-C levels in the WLs during fifth to twelfth month weight loss. Typically, increased levels of HDL-C are regarded as a signature of effective cholesterol efflux transporting cholesterol back from peripheral tissues to the liver. Our results are consistent with earlier findings suggesting that weight loss results in increased HDL-C levels [180,301,302]. Integrative analyses revealed that methylation at 21 of 69 genes had significant correlations with gene expression of the corresponding gene indicating the potential regulatory impact of DNA methylation on these genes. Moreover, six CpGs in 5 genes (*CPXM1*, *APOE*, *COL6A3*, *SYNPO and VGLL3)* that showed positive expression-methylation correlations were replicated in the validation cohort of BMI-discordant MZ twins representing acquired obesity.

We next assessed changes in transcriptome during continuous weight loss (fifth to twelfth month) in WLs. A total of 5 genes were identified to be differentially expressed, with three upregulated (*BCL9*, *RPS4XP3* and *TUBGCP5)* and two downregulated (*EGFEM1P* and *SPON1)* genes. Pathway analyses showed elevated signalling by insulin receptor which is in line with earlier studies that demonstrated improved insulin sensitivity following weight loss [181,301]. Also, three of the five genes showed significant expression-methylation correlations.

We identified 35 DEGs (20 downregulated and 15 upregulated) responding to long-term weight loss by comparing the baseline to 12 month in the WL group. *UCHL1* was the most downregulated gene, and previously associated with reducing oxidative stress [301] indicating a positive impact of weight loss. Pathway analyses of long-term weight loss-associated genes showed a wider impact resulting in several pathways related to structural, developmental and metabolic functions of SAT. These included downregulation cell cycle control, metabolism of proteins and gene expression pathways and upregulation of pathways associated with signal transduction. Of the 35 significant genes, gene expression was correlated with methylation at 23 CpG sites corresponding to 16 genes. Both positive and negative expression-methylation correlations were observed for the CpGs located in the promoters of the corresponding genes. However, for the CpGs located in the gene bodies, only positive correlations were observed, except for one CpG site. In the validation cohort of MZ twins, 20 of these 35 genes were associated with acquired obesity and five CpGs residing in four genes (*MAL2*, *FAM129A*, *PPL* and

PDZRN4) were also replicated. Replication in the validation cohort indicates the opposite direction of expression of weight-loss associated genes in acquired obesity. Altogether, 73 of the 99 weight-loss associated genes were also associated with acquired obesity suggesting their high responsiveness to changes in weight.

Although we anticipated to observe overlap between genes from various time points, there was no overlap between all three time points. This suggests that genes may not react linearly and may return to their baseline pre-weight loss function after an initial change in gene expression during weight loss. Notably, in both the short-term and long-term weight loss, seven genes (*UCHL1*, *BAG3*, *TNMD*, *LEP*, *BHMT2*, *EPDR1* and *OSTM1*) were commonly down-regulated. While downregulation of *BAG3*, an anti-apoptotic protein [303] and an indicator of cellular stress [304] may be indicative of reduction in adipocyte size [305]. While downregulation of *TNMD* [306], *LEP* [301,307,308], *BHMT2* [309], *EPDR1* [310] and *OSTM1* [311] have been previously associated with shrinkage of SAT and reduced adipogenesis.

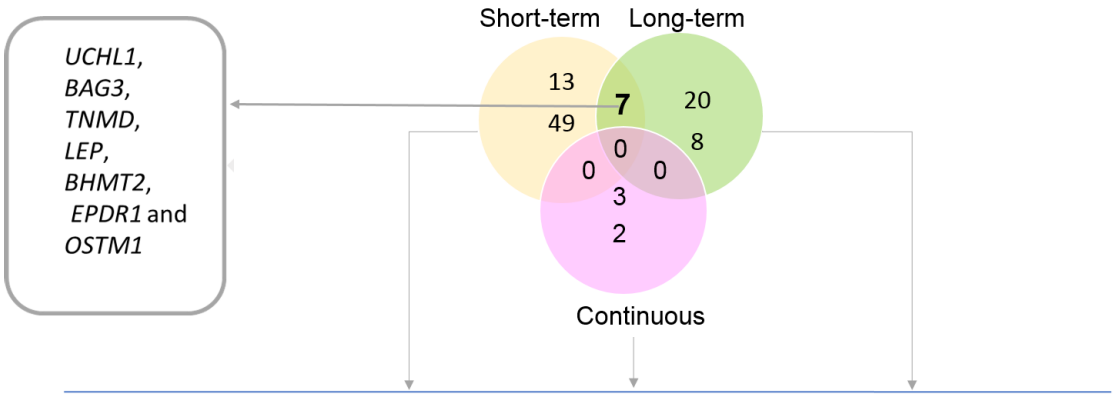

No of DEGs	69	5	35
Most Upregulated Gene	TMEM100	BCL9	MRC2
Most downregulated Gene	NQO1	SPON1	UCHL1
Pathways Grouped by Entities	Lipoprotein Metabolism	Signaling by Insulin receptor, Gene Expression	Signal Transduction, Developmental Biology, Gene Expression, Adaptive immune system, Metabolism, Metabolism of proteins, Cell cycle and DNA repair

Figure 9: A schematic representation of the main findings from Study I.

Alterations in DNA methylation associated with diet [184] and exercise [60] have been reported earlier. We did not observe any genome-wide significant differentially methylated CpG sites during our weight loss intervention. However, we have identified several significant correlations between differentially expressed genes and CpGs in the corresponding genes. We highlight that six CpGs in 5 genes (*CPXM1*, *APOE*, *COL6A3*, *SYNPO* and *VGLL3*) from short-term weight loss and five CpGs in 4 genes (*MAL2*, *FAM129A*, *PPL* and *PDZRN4*) from long-term weight loss which had positive correlation with the expression were also replicated in the validation cohort. These results hint that DNA methylation might potentially regulate the expression of these genes.

The sample size of 19 individuals is a major limitation of our study, especially subgroup analysis of WLs is statistically underpowered to detect modest genome-wide differences in DNA methylation. We also note that due to the cellular heterogeneity of SAT, we may not have captured the same cell-type specific signals at different time points of the study and our findings may partly reflect changes in the composition of SAT during weight loss. In addition to SAT cellular heterogeneity, immune cell infiltration could also impact the overall methylation profile of SAT. Also, expression results from subgroup analysis may have false negatives when there are small or medium effects. However, we validated many of our results by observing opposite direction of gene expression in acquired obesity, and additionally results from our study replicate several previously published results indicating the consistency of observed gene expression changes of these specific genes during weight loss. We were also successful in controlling for several confounding factors by using intra-individual comparisons and a validation cohort of BMI-discordant MZ twin pairs. Moreover, our study was performed for a longer duration compared to other weight loss studies, and our approach of attaining weight loss through diet and exercise was highly similar to the current practice at weight loss clinics. Also, our study fills the gap in the existing literature about the weight loss intervention on healthy obese individuals. Nevertheless, we agree that it is difficult to distinguish between consequences and causes in these analyses with this study design; it is indeed likely that most of the changes that we observe were consequential to weight loss. However, it is possible that some of the gene expression changes are indicators of processes that enable or hinder weight loss or maintenance of weight loss. Validation in the twin sample provided additional verification that the genes indeed were responsive to weight change. We acknowledge that our results are mainly descriptive and needs further functional validation to determine their potential use in clinical setting. However, we believe that the information generated in our study serves to improve our basic understanding of weight loss induced changes in SAT at multiple time points, and the results from our study pave the way forward to the integrative analysis approach by using the information from multiple mechanisms impacting both weight loss and obesity.

5.2 Smoking-associated changes in DNA methylation and gene expression of adipose tissue and their consequences for metabolic health (Study II)

Smoking profoundly impacts DNA methylation levels and numerous independent studies performed on different populations have identified several smoking-associated CpGs in the blood methylome [61,64,216–218,220–222,224]. As outlined in the section 2.3.3, the relationship between smoking and obesity is highly complex, with contradictory findings and limited knowledge about their interaction and co-occurrence. Current smokers have lower BMI and higher adiposity than never smokers, and smoking cessation is associated with weight gain [245–247,249–251,254,255].

Given the global increase of obesity and harmful risks of smoking, it is imperative to investigate and understand the effects of smoking on metabolically relevant tissues. Adipose tissue is not only metabolically relevant but it also serves as an ideal tissue to study the impact of smoking on obesity-related metabolic diseases and adiposity phenotypes. In this study, we investigated concurrently occurring smoking-associated changes in methylome and transcriptome of adipose tissue. We further evaluated the role of the identified adipose tissue methylation and expression signals in metabolic disease risk phenotypes.

Discovery EWAS and transcriptome wide association study (TWAS) were performed in the TwinsUK cohort (n=345) [266] comparing current and never smokers. The EWAS identified 42 significant (at 1% FDR) differentially methylated CpGs which mapped to 29 unique genomic regions (28 genes and 1 intergenic region). And the TWAS across 17399 genes identified 42 significant DEGs (at 1% FDR). Integrating the genome-wide significant results from the above two analyses revealed overlapping signals at five genes (*AHRR*, *CYP1A1*, *CYP1B1*, *CYTL1*, and *F2RL3)* comprising 14 CpG sites (Figure 10). These CpG sites were located at gene body (*CYP1B1*, *AHRR*, and *F2RL3)* and promoter (*CYTL1* and *CYP1A1)*.

Of these 5 genes, *AHRR* and *F2RL3* are the most consistently reported smoking-associated signals and have been suggested as potential biomarkers to estimate smoking habits (smoking cessation for *F2RL3*) from blood methylome [216,222,241,242]. *CYP1A1, a* lung cancer susceptibility gene, is the most differentially expressed gene in this study with differentially methylated signals at the promoter region. Previously promoter methylation of *CYP1A1* has been associated with smoking in lung tumor tissue [312] and placenta [313]. In current smokers, all these five genes were upregulated and a majority of the CpG sites (93%) were hypomethylated compared to never smokers. This clear pattern of negative correlations observed between methylation and expression (at these five genes) implies regulatory effects. This is in line with the well-established gene expression control by promoter- based methylation (promoter hypermethylation) for CpG sites in *CYTL1* and *CYP1A1*. However, the observed negative correlation between methylation and expression for the other three CpG sites located in the gene body is not unusual. Both positive and negative correlations between methylation and expression for CpGs in gene body have been reported earlier [314,315]. CpG sites in the gene body that are negatively associated with expression

levels could be located in alternative promoters that regulate the expression of particular isoforms or in intragenic CpG islands influencing enhancer loci, specifically enriched within large first introns [54].

To characterize the widespread effects of smoking on metabolic health, three metabolic disease risk measures (total fat mass [TFM], android-to-gynoid fat ratio [AGR] and visceral fat mass [VFM]) were assessed with respect to the identified smoking-associated methylation and expression signals. Figure 10 illustrates the discovery and replication analyses performed to associate smoking-associated methylation signals and adiposity measures. Methylation levels at the 42 genome-wide significant CpG sites from the discovery EWAS were tested for association with the three metabolic health traits (adiposity phenotypes) using 288 individuals (42 current and 246 never smokers, mean BMI = 26.70 ± 4.62) adjusting for BMI and smoking. Significant associations were identified for three CpG sites in *CYP1A1* with VFM and AGR. To elaborate, cg23160522 (beta = 1.35×10^{-3}, SE = 3.03×10^{-3}, P = 4.35×10^{-7}) and cg23680900 (beta = − 1.59, SE = 0.44, $P = 6.58 \times 10^{-6}$) were independently and significantly associated with VFM and AGR, respectively. Interestingly, cg10009577 located in the *CYP1A1* promoter, showed an interaction effect with AGR ($P = 5.50 \times 10^{-4}$) exhibiting different patterns of association in current and never smokers. Moreover, a significant inverse association was identified for *NOTCH1* (cg14120703) and AGR (beta = − 1.80, SE = 0.43, $P = 1.07 \times 10^{-7}$). A subset of younger Finnish twins (n=69, 21 current smokers) was used to replicate the methylation associations with metabolic risk factors. The overall inverse association between cg10009577 (*CYP1A1*) and AGR (discovery sample beta = − 0.95, SE = 0.31; replication sample beta = − 0.58, SE = 0.25, $P = 0.02$) and direction of interaction effects remained consistent, however, the replication signal did not reach statistical significance. Expression levels of *F2RL3* showed significant association with all the three risk factors (VFM beta = -1.5×10^{-3}, SE = 3.78×10^{-4}, $P = 7.8 \times 10^{-4}$; AGR beta = 2.3, SE = 0.56, $P = 4.5 \times 10^{-5}$; TFM beta = 1.6×10^{-3}, SE = 3.9×10^{-4}, $P = 5.8 \times 10^{-5}$). *OR51E1* expression was significantly associated with VFM (beta = -1.5×10^{-3}, SE = 3.78×10^{-4}, $P = 7.8 \times 10^{-4}$) and AGR (beta = − 2.85, SE = 0.51, $P = 3.1 \times 10^{-8}$). These significant associations reveal the broader impacts of smoking on metabolic health.

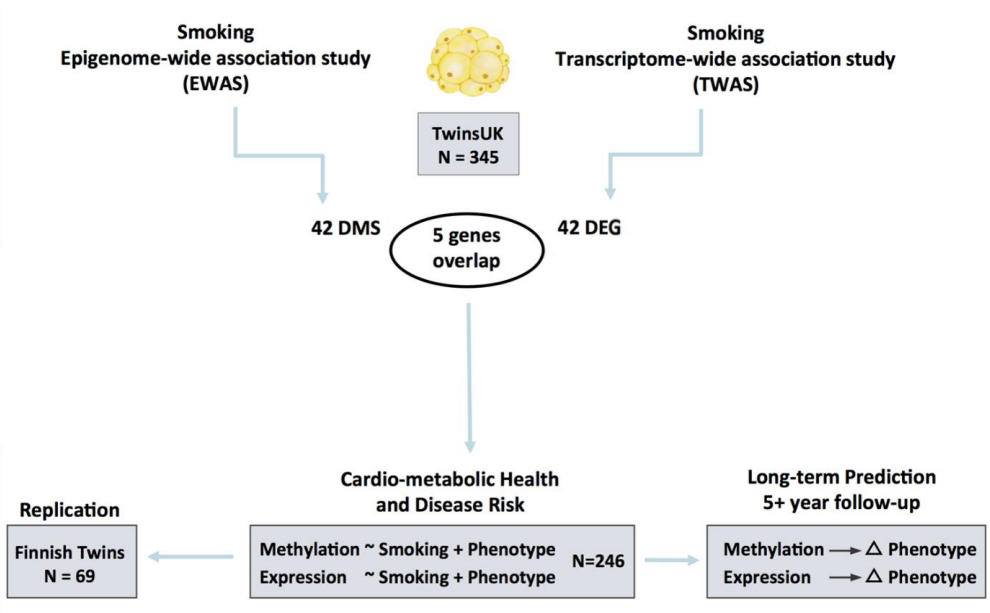

Figure 10: An overview of discovery and replication analyses performed in Study II. DMS: differentially methylated signal; DEG: differentially expressed gene. *Modified from Figure 1 of* [316] *(Tsai P-C et al 2018).*

To test the effects of smoking-associated methylation and expression signals on weight gain and adiposity measures, 248 individuals comprising current, former and never smokers were used. Phenotype differences observed between the two-time points separated by 5-year time interval were correlated with the methylation and expression levels measured at the initial time point. After a 5-year interval, current smokers who quit smoking by time point two and recent quitters (< 4 years) at time point one showed higher levels of adiposity measures. However, this increase seems transient as this effect was not observed in former smokers with higher cessation time (> 5 years) at the initial time point. To explore these associations further smoking-associated methylation and expression signals were used to predict future changes in adiposity, specifically in visceral fat accumulation, upon smoking cessation. Visceral fat is a major risk factor for metabolic diseases and has been strongly associated with type 2 diabetes and cardiovascular disease [122,317]. Two significant signals predictive of future gain in visceral fat were identified for individuals who were current smokers (n=5) or recent quitters (n=13, < 4 years) at time point one, who later quit smoking or continued abstention at time point two. Methylation levels of these current smokers or recent quitters at cg16320419 in *BHLHE40* (by group interaction term $P = 9.3 \times 10^{-4}$) explained 35.5% of the variation in future gain in visceral fat. Similarly, expression levels of *AHRR* (by group interaction term $P = 4.7 \times 10^{-5}$) in these

current smokers or recent quitters explained 44% of the variation in future gain in visceral fat. While these associations indicate a potential impact of environment-mediated molecular mechanisms on metabolic disease risk, replication of these results in a larger sample will enable to make further conclusions. Although correcting for cell composition [93] did not alter the identified associations, usage of adipose tissue data in this study might have identified signals that reflect cell-type specific methylation profiles. Also, infiltration of inflammatory immune cells specifically during obese state could affect the overall methylation profiles of SAT. Technical factors such as the procedure used to retrieve SAT (e.g. surgical biopsy), sample handling and blood cell contamination during SAT acquisition could also influence SAT biopsy composition [318].

This was the first study to comprehensively assess the coordinated changes occurring in the adipose tissue methylome and transcriptome due to smoking and is of great relevance to public health. Several smoking-associated methylation and expression signals were identified indicating a substantial impact of smoking on adipose tissue. Some of these signals were also associated with metabolic health risk factors highlighting the widespread effects of smoking and importance of understanding common basis of smoking and adiposity.

5.3 EpiSmokEr: a robust DNA-methylation based smoking status classifier (Study III)

Epigenetic modifications, especially DNA methylation have been extensively reported to be influenced by environmental exposures. Smoking strongly influences methylation with current and never smokers exhibiting distinct methylation profiles [61,64,216,217,219–222]. Notably, two studies attempted to quantify methylation at smoking-responsive CpGs into a score that reflects smoking behavior [217,221]. However, these score-based approaches are not ideal for predictive purposes as a threshold cut-off value specific to each dataset needs to be determined by the user. For instance, the smoking score (SSc) of Elliott *et al* [217] uses ethnic-specific threshold values to differentiate smokers from never smokers, limiting its universal applicability, while methylation score (MS) of Zhang *et al* [221] can only perform binary comparisons i.e. current vs never and former vs never smokers.

To advance the practical applicability of the smoking-associated methylation signals, we proposed a classifier with an emphasis on smoking status prediction. We have implemented multinomial least absolute shrinkage and selection operator (LASSO) regression on whole blood-derived 450K methylation data from an adult population with a wide age spectrum. We have considered three smoking statuses, current, former and never smokers, to build the classifier. We have demonstrated the accuracy of our classifier in three independent whole blood datasets. We have developed an R package *EpiSmokEr* (*Epi*genetic *Smok*ing status *E*stimato*r*) with functionalities to start from raw intensity files (IDAT), followed by quantile normalization and smoking status prediction. The R package also provides functions to calculate the SSc by Elliott *et al* [217] and MS by Zhang *et al* [221].

Our objective was to build a classifier to predict the smoking status of a person based on their DNA methylation profile. We have used whole blood methylation data from the DILGOM cohort [269,270] to train our classifier. DILGOM is representative of the general Finnish adult population with a wide range of age distribution and well-characterized smoking status information. We considered current smokers (occasional to heavy smokers), former smokers (recent quitters [>1 year] to long-term quitters) and never smokers for training the smoking status classifier (Tables 5 and 6). To ensure the usage of high-quality data to train the classifier and limit misclassification, self-reported smoking status was verified with cotinine measures whenever data was available. Multinomial LASSO regression with nested cross-validation was performed to select a parsimonious set of 121 CpG sites predictive of smoking status (Figure 7).

To assess the performance of our classifier we used three external test datasets: FTC [259], EIRA [59] and CARDIOGENICS [61] from different populations, from which we calculated sensitivity and specificity to quantify the performance of our classifier. These values were calculated for each smoking category by comparing the one versus the union of the other two categories. Results indicated that on average current smokers were identified with a sensitivity of 81% and a specificity of 85% across the three test datasets,

whereas never smokers were identified with 94% sensitivity and 57% specificity. Lower sensitivity values were identified for former smokers averaging to 18% across the test datasets. However, a higher average specificity of 96% was shown by the classifier demonstrating its ability to correctly identify individuals who did not belong to the former smoker category.

Owing to the differences in outputs we could not comprehensively compare our classifier with SSc and MS. However, we calculated sensitivity and specificity from the other two methods to make a fair comparison. We tested multiple threshold values for SSc and MS to compare with our classifier. A threshold value of zero for SSc showed good sensitivity to identify current smokers from other smoking status categories. For MS a threshold value of -7.5 achieved an average sensitivity of 85% and a specificity of 68% to identify current smokers from never smokers. However, we could not determine a single threshold value of MS that could discriminate former from never smokers with reasonable accuracy across all test datasets. We note that this process of determining a threshold value for each test dataset in itself is a serious limitation. We demonstrated this limitation by trying to compute a threshold to calculate sensitivity and specificity for MS and SSc. This also presents a difficulty in interpreting the meaning of the score when dealing with individual samples, as there is no comparable threshold or reference value to determine the sample's smoking status. Additionally, the SSc European ethnic threshold 17.75 was not applicable to any of the test datasets highlighting that this threshold might be dataset-specific, which cannot be generalized to other datasets. We curtail the need of determining the threshold by user as our classifier uses an implicit threshold and determines the smoking status category.

For instance, figures 11A and 11B illustrate that the SSc and MS respectively showed overlapping profiles for different smoking statuses and thus failed to achieve clear classification. Also, the European ethnic smoking score threshold of 17.55 proposed by Elliott *et al* [217] was not applicable, as only two individuals were identified as current smokers based on this threshold. Figure 11C shows the results from our classifier as a confusion matrix with actual self-reported smoking statuses on the X-axis and the predicted smoking statuses on the Y-axis.

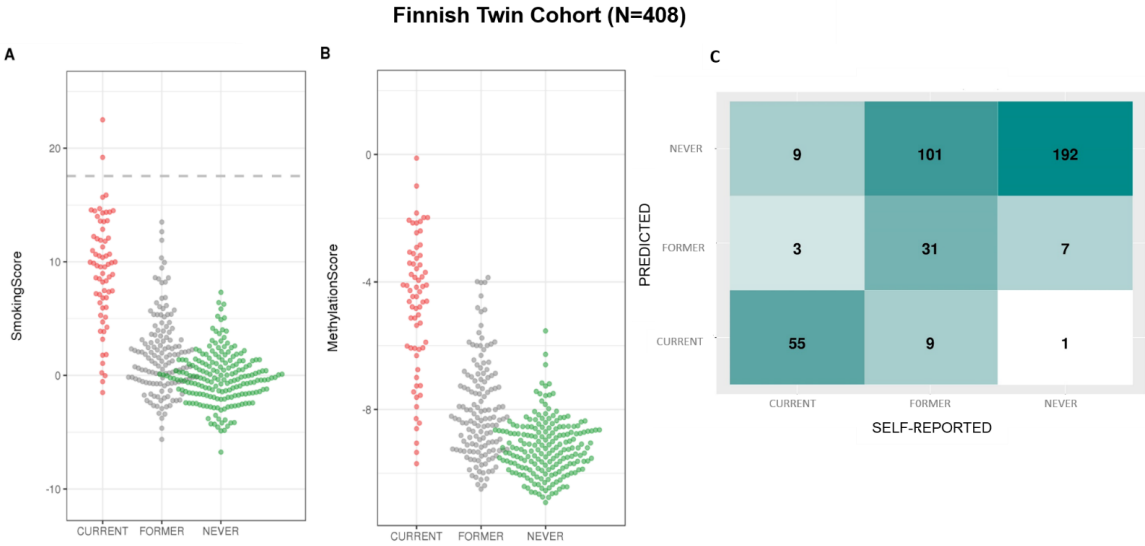

Figure 11: Results from three DNA-methylation based smoking status estimation approaches from the FTC dataset. *Modified from Figure 3 of* [292] *(Bollepalli et al 2019) with permission of Future Medicine Ltd.*

We also observed that in addition to the differences in the approaches to predict smoking status all the three methods also differ in training schemes and normalization methods. The training dataset used by SSc contained only 95 men with 16 heavy smokers while the training data used to develop MS was composed of older age (50-75) individuals. Using only heavy smokers could have resulted in the higher sensitivity and specificity values of SSc in discriminating current smokers from others. We used a cotinine verified training dataset with a broad age spectrum including both men and women and used multinomial LASSO with cross validation to train our classifier by limiting biases and overfitting. In summary, our classifier performed well across all the test datasets in identifying current and never smokers and showed moderate to marginal performance in identifying self-reported former smokers. MS showed good performance for the binary classification of distinguishing current smokers from never smokers.

We next focused on understanding specifically the misclassifications from our classifier using FTC and EIRA datasets. In this context, misclassification refers to disagreement between self-reported smoking status and predicted smoking status from the classifier. We have used self-reported smoking status as the ground truth to evaluate the classifier's performance. However, using less reliable self-reports as a ground truth is counterproductive and results in decreased accuracy estimates of the classifier. Therefore, we used extensive smoking information available from FTC and EIRA to understand the results more thoroughly. First, we wanted to comprehend the misclassifications observed in current smoker category. In both these datasets current smoking category could be further divided into current daily and occasional smokers. When we used occasional smokers as a separate category, we observed that majority of the misclassifications is

because of occasional smokers being identified as either never or former smokers. Of the 66 occasional smokers in the EIRA dataset, 53 were predicted as never smokers and six as former smokers by the classifier. Consequently, the exclusion of occasional smokers has improved the sensitivity values of current smokers in this dataset from 69% to 88%. This highlights the effect of including occasional smokers along with current daily smokers on the ostensible performance of the classifier. This misclassification can be attributed to similarity in methylation profiles of occasional smokers to never and former smokers based on the extent and intensity or frequency of smoking, which also reflects in the results of our classifier.

Next we focused on understanding misclassifications observed in the former smokers category by using the comprehensive smoking behavior information from the FTC dataset. The former smokers class in the FTC had a high misclassification rate where a majority of former smokers (n=101) were predicted as never smokers. We noticed that 85 out of the 101 individuals had quit smoking for more than 10 years prior to blood sampling (Figure 12). This is line with results from earlier studies where the former smokers showed highly similar profiles to never smokers [61,64,216,217,219,220]. Interestingly, nine of the former smokers who were predicted as current smokers had recently quit smoking and had higher mean pack-years than other former smokers. While these results appear to be misclassifications compared to self-reported smoking status, they are biologically meaningful as they indicate the reversal in the methylation patterns of former smokers after cessation of smoking, which after a long period of cessation are indistinguishable from never smokers. Several studies have already shown that the methylation profiles of former smokers may resemble current or never smokers based on the total abstinence time between cessation and sampling [216,219,222–224], and the extent [219] and the duration they have smoked before cessation (pack-year history). Although the magnitude or extent of this reversal varies, a typical abstinence period of more than ten years is likely to reverse the methylation pattern of former smokers making them very similar to never smokers. However, this reversal of methylation levels may also be site-specific, as it has been shown that methylation levels at certain CpG sites remained unchanged even after decades of cessation [61,219,220].

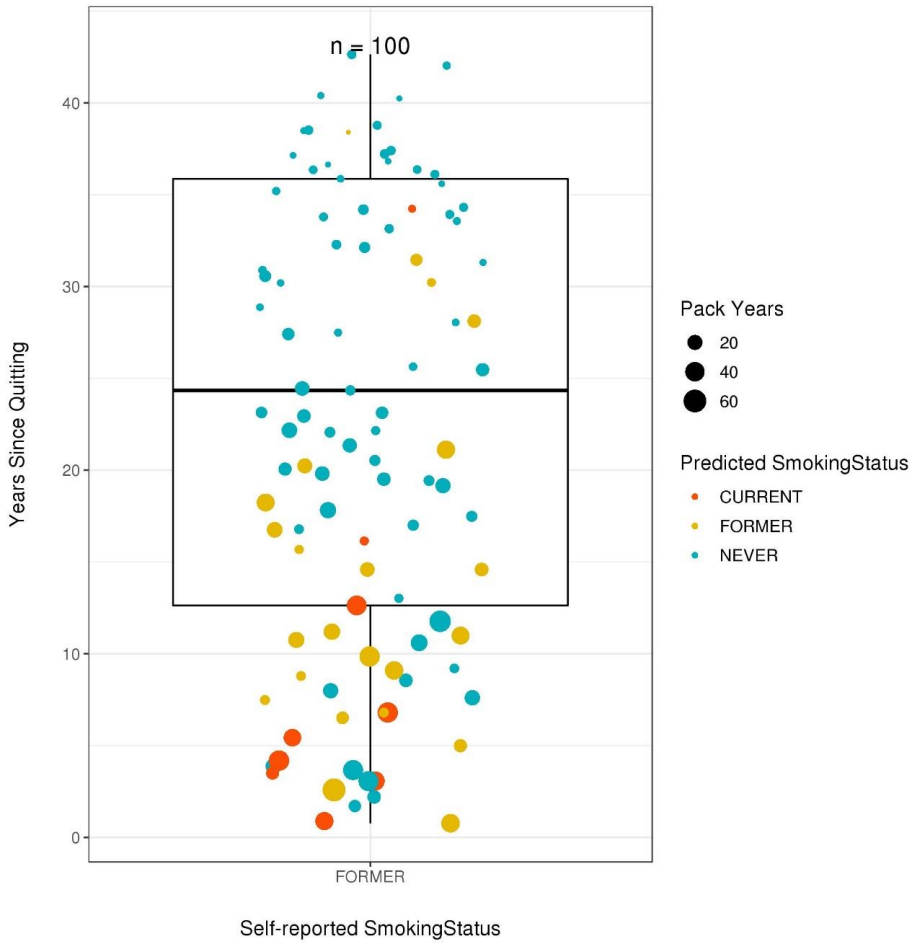

Figure 12: Illustration of results from the classifier with respect to cessation time (years since quitting) and extent of smoking (pack years) of the self-reported former smokers in the FTC dataset. *Modified from Figure 4 of* [292] *(Bollepalli et al 2019) with permission of Future Medicine Ltd.*

Besides active smoking, to some extent every class of smokers in the FTC were also exposed to passive (second-hand) smoking. We also observed that some individuals have been exposed to both active and passive smoking for longer duration. Also, intrauterine exposure to smoking can also impact the methylation levels of never smokers [233]. Although results from our classifier reflect the cumulative exposure to smoking, it is difficult to delineate the extent of passive smoking that resulted in changes in the levels of methylation.

In addition to the transient nature of DNA methylation that resulted in biologically relevant and meaningful discrepancies between self-reported and predicted smoking status, I briefly discuss here other factors that may have led to misclassifications. Typically, accuracy estimates are calculated by comparing the self-reported smoking status with the smoking status predicted by the classifier. However, the self-

reported smoking status is prone to errors due to misreporting and poor recall of long-term smoking history [239]. Accuracy estimates are therefore affected by the reliability of the test dataset's smoking status information. Generally, the classification methods are based on the premise of independence (mutually exclusive) that each smoking status category has a distinctive methylation profile without overlapping with other categories. However, this assumption is not true for smoking-associated methylation profiles (i.e. overlap in methylation profiles between different categories of smoking) and smoking behavior in general. Accuracy of the classifier can also be affected by the presence of SNPs in close proximity to smoking-associated CpG sites [319].

To evaluate our classifier's efficiency in tissues other than blood we used methylation data from buccal tissue [272] and peripheral mononuclear blood cells (PBMCs) [273]. In the buccal tissue dataset current smokers were detected with 95% sensitivity 97% specificity. This dataset had two categories namely "tobacco smoker" and "non-tobacco smoker" based on the self-reported smoking status. However, 15 of the non-tobacco smokers were identified as former smokers by our classifier. This result is consistent with the definition of non-tobacco smoker [272] used in this cohort (Table 6), that is individuals who have been abstinent from tobacco or nicotine-containing products for at least 5 years. The good performance of our whole blood trained classifier on the buccal tissue data was surprising owing to the tissue-specific nature of DNA methylation. However, a similar result was observed when a smoking index developed using blood-derived smoking-associated CpGs showed a good discrimination of smokers from non-smokers in the same dataset [320,321]. We have also observed a good performance in the PBMC dataset and the results are reassuring as PBMCs are extracted from whole blood. These results indicate a broader impact of smoking on methylome spanning across multiple tissues. Additionally, these two datasets allowed us to demonstrate global applicability of our classifier as these datasets comprised individuals of African-American ethnicity. However, to confirm the cross-tissue performance of our classifier further testing in multiple tissues is needed.

Our classifier is publicly available as an R package, *EpiSmokEr* (Epigenetic Smoking Status Estimator) and expects raw (IDAT) or normalized methylation data from the 450K array along with sex information as an input. The package vignette provides extensive documentation with examples and has been already tested on multiple datasets with sample size ranging from 400 to 700. It only takes a few minutes to estimate smoking status starting with the IDAT files. We also provide functionality for SSc and MS approaches offering users with a choice for their analysis. Our classifier offers an objective smoking status measure and is applicable to all datasets, reducing the need for population or ethnic-specific thresholds to be calculated. Predicted smoking status from our classifier is beneficial when self-reported smoking status is unavailable or highly inaccurate and can also reduce misreporting bias by validating self-reported smoking information. Also, the predicted smoking status can be used as a covariate in association analyses like EWAS and GWAS to account for smoking-associated confounding.

Typically, the predictive performance of a classifier can be influenced by the quality of the training dataset used to train the classifier. We have minimized this limitation by using a high-quality dataset with reliable self-reported smoking status data verified by multiple measures. Considering the complex nature of former smoker class it may remain as a challenge for methylation-based prediction algorithms to achieve a higher accuracy in this category. However, results from our classifier reflect the effect of smoking on DNA methylation and potential functional impacts on the genome which are clinically and biologically significant. Although our classifier is trained using the Infinium HumanMethylation450 BeadChip data, our approach can be re-implemented on the EPIC BeadChip array data to build a classifier specific to EPIC derived data.

In this study, we developed a robust smoking status predictor based on DNA methylation which provides an objective measure of smoking status. Our classifier considers three classes of smoking status and can be applied to any dataset. We also performed extensive phenotypic evaluation to examine the reasons for misclassification. By using our R package, *EpiSmokEr*, users can implement our classifier to predict smoking status in their own datasets. In conclusion, methylation-based smoking status predictors are more robust than existing traditional biomarkers with shorter half-lives. Therefore, we recommend using predicted smoking status from our classifier as a covariate to adjust for smoking-associated confounding rather than self-reported smoking status.

6 Implications and Future Directions

We have come a long way in our understanding of the molecular basis of complex diseases in the last two decades. With the rapid progress and advances in technology and increased affordability, we have moved from the candidate gene approach to genome-wide studies. GWASs have identified hundreds of significant associations between genomic regions and diseases, improving our understanding of the genetic architecture of complex diseases. However, a majority of the identified genetic variants exhibit smaller effect sizes, explaining only a smaller proportion of total heritability. Moreover, most of these identified variants reside in non-coding regions of the genome posing a challenge to understand their effects on gene regulation and disease mechanism. Larger sample sizes and better phenotyping as well as using uncommon and rare variants with whole genome and exome approaches can address these challenges.

Epigenetic mechanisms serve as a key nexus between genetic and non-genetic factors that can regulate gene expression profiles and subsequent susceptibility to a complex disease or trait. Akin to GWAS, EWASs have enabled the identification of several disease-associated methylation sites. Both GWAS and EWAS require large sample sizes owing to the multiple testing problem to identify statistically significant associations, specifically to detect associations with smaller effect sizes. Although sample sizes used in Study II and III were modest, we had sufficient power to identify large effects. However, Study I used a smaller sample size, and specifically the subgroup analysis was underpowered to identify modest differences in DNAm. While a larger sample size could potentially identify additional associations, for practical reasons, it is difficult to recruit participants who attend interventions for a longer duration. Comparatively, our study was performed for a longer duration than other weight loss studies that investigated genome-wide methylome and/or transcriptome of SAT. Moreover, we validated results from transcriptomic analysis using a validation cohort representing acquired obesity, showing the opposite direction of gene expression in obesity compared to weight loss. Also, we replicated several previously reported findings indicating the consistency of observed gene expression changes at specific genes during weight loss. Furthermore, identified DNAm differences usually show modest effect sizes, therefore it is necessary to appropriately adjust for potential biological and technical confounding factors to identify these modest associations. Age, BMI and smoking are included as covariates in EWAS owing to their well-established impact on DNA methylation patterns. Also, covariates such as batch, sample plate, microarray slide are usually included in the association studies to account for technical variation. Additionally, techniques like PCA and SVD are also being employed to check and account for the unknown sources of variation.

Performing EWAS and interpretation of its results include additional challenges compared to GWAS. First, the dynamic nature of epigenetic modifications necessitates sample collection at the time of exposure or at a specific time point based on the study hypothesis. Second, the tissue-specific nature of epigenetic

marks requires sampling of relevant tissues. Ideally, tissues that are directly affected by the disease or mediating the disease outcomes need to be studied. However, due to easy availability, whole blood is the most widely used tissue in EWAS. Additionally, buccal cells, saliva, hair follicles, and urine [91] have also been considered as good surrogate tissues for tissues that are challenging to sample (e.g. brain). In addition to inter-individual variation, the dynamic nature of the epigenetic marks results in both spatial and temporal intra-individual variability. That is variation in epigenetic profiles across the tissues and variation in epigenetic profiles of the same tissue with time within an individual. Hence, multiple measurements over time might be needed to test their association with a phenotype. For instance, in Study I to capture the DNAm changes with respect to weight loss trajectory we have collected SAT biopsies at three-time points. Third, using a tissue composed of different mixture of cells might lead to spurious associations, as the DNAm variation captured often reflects the variation in the cellular composition that occurred as a consequence of disease or sample collection. Currently, histological quantification of cell proportions and employing cell-type deconvolution methods are the common practices to correct for the cellular heterogeneity confounding. Preferably, using single-cell types would minimize cellular heterogeneity, although the extent of this minimization depends on the purity of the cell samples. Single-cell RNA sequencing (scRNA-seq) could serve as a useful approach to identify, discriminate and quantify cell subtypes, especially in the tissues where the cell subtypes are not yet well studied [26]. scRNA-seq can be performed on a subset of samples to quantify cell subtypes and their corresponding gene expression profiles in a tissue, which can then be used to estimate the cell-type composition of the remaining set of larger samples with bulk RNA sequencing data [26].

Although DNAm and gene transcription profiles are tissue-specific, some of the trait-associated DNAm changes exhibit tissue-shared effects. For example, several smoking-associated DNAm changes identified in SAT in Study II overlapped with previously reported smoking EWAS hits in whole blood. The smoking status classifier developed in Study III was trained using whole blood data. However, it has shown good predictability in buccal tissue samples. A previous study reported a similar observation of overlap in smoking-associated methylation signals in buccal samples and whole blood [322]. This indicates that complex traits like smoking leaves wide-spread effects on methylation at certain CpGs across tissues, resulting in tissue-shared effects.

In addition to timing and sample collection, study design determines the direction of interpretation of results. It is important to identify disease-associated DNAm variants, however, it is crucial to identify causal DNAm variants to understand disease etiology. Establishing causality is more challenging in EWAS, as the observed DNAm alterations could be causal, consequential or even confounding. Longitudinal cohorts following disease-free individuals from birth are ideal study designs to establish causality of epigenetic marks. However, these cohorts are very difficult to establish and follow-up. For example, Study I used a longitudinal sample of 19 individuals with tissue samples, phenotype, and clinical assessments at three time

points during a one year weight loss intervention. Therefore, it is likely that the observed gene expression and DNAm differences between the time points are due to weight change. However, we cannot definitely determine the causality of the identified changes. From a practical perspective, it is difficult to perform intervention studies for a longer duration, or to follow-up individuals for their lifetime, although they would be the best for understanding the etiology of complex traits and the corresponding role of epigenetic modifications.

MZ twin pairs with divergent phenotypes are also valuable to study epigenetic associations, as within-pair comparisons control for age, sex, genetic and early environment confounding. However, discordant MZ twin pairs are very rare, and it is difficult to establish a large cohort of this nature. MZ twin pairs discordant for BMI were used as a validation cohort in Study I to verify the direction of expression of weight loss-associated genes in obesity. This study design was appropriate as it not only captured weight-loss associated gene expression using intra-individual comparison but also simultaneously verified the findings by within-pair comparison of MZ twins discordant for BMI, as a model for acquired obesity. Nevertheless, it is difficult to distinguish if the observed gene expression or DNA methylation associations are causal or consequential of weight loss and obesity with this study design; it is indeed likely that many of the associations that we observe are due to body fatness or BMI. However, some of the gene expression changes may be indicators of processes that enable or hinder weight loss or maintain it. Furthermore, it is necessary to verify whether the changes observed in gene expression are also translated to corresponding protein levels.

Regarding DNAm and expression changes, efforts are clearly needed to collect large samples followed for a longer duration to determine the direction of effect of DNAm in gene expression and complex diseases like obesity, especially to establish causality. Alternatively, statistical techniques like Mendelian randomization (MR) and causal inference test can be used to assess the directionality of DNAm and to infer causality by combining genetic and epigenetic data. However, care should be taken to model the complex biological data with regard to the underlying assumptions of these statistical models. For instance, a two-step epigenetic Mendelian randomization strategy has been proposed to establish the causal relationships between environmental exposure, epigenetic signature (e.g. DNAm) and outcome [323]. In Step 1, the causal impact of exposure on the epigenetic signature is established using an SNP as a proxy for the exposure. In Step 2, the causal nature of the epigenetic signature on the outcome is interrogated using a genetic proxy for the epigenetic signature. In addition to the requirement of large sample sizes and satisfying the conventional MR assumptions, the epigenetic MR strategy faces the additional challenge of tissue specificity and availability of genetic variants that can be used as a proxy for epigenetic signature (e.g. *cis*-acting SNP can be used as a proxy for DNAm levels). Furthermore, statistically identified causal relationships need to be functionally validated (e.g. with functional laboratory tests on cell lines or animal models) to determine the causal effect of DNAm or gene expression in the corresponding phenotype.

By comprehensively understanding the human genome and the biological layers of information it encodes, we will gain a holistic understanding of biological processes and mechanisms associated with disease phenotypes. In this thesis, only DNAm and transcriptomic data were integrated identifying potential role of DNAm in gene regulation. Combining other informative layers like genotype, proteome, metabolome, and gut microbiome in the analysis would ideally reveal the complex interactions among these layers in relation to disease pathogenesis. Integrating multiple omics data also unravels the reasons for inter-individual epigenetic variation. For instance, recent mQTL studies [2,58,324,325] revealed the influence of genetic variants on methylation at several CpGs, acting both in *cis* and *trans* fashion. In fact, a second-generation EWAS approach was proposed to constitute a necessary panel of multiple complementary genome-wide assays (WGBS, ATAC-seq, RNA-seq, scRNA-seq, and genotyping), enabling multi-perspective interpretation of results [26]. Although DNAm as 5mC is widely studied because of its stability, easy access, and affordable technology to measure it, other forms of cytosine modifications (e.g. 5hmC, 5fC, and 5caC) also need to be investigated to understand their role in disease and development, although their quantification requires additional steps compared to 5mC [326]. Besides, existing array-based technologies mainly measure DNAm in the CpG context. However, it is also crucial to assess and understand the role of DNAm in the non-CpG (CpH; H=A, C, or T) context to enhance our understanding related to development and disease. It is also vital to understand the role of histone modifications and ncRNAs to comprehensively understand the contribution of the epigenome to disease mechanism. However, comprehensive investigation of all the epigenetic measures is expensive as all the measures need to be captured simultaneously. Additionally, efficient computational and statistical methods are crucial to successfully integrate and interpret multiple genetic and epigenetic layers.

In GWAS identifying causal variants is more important than inferred or associated variants, as causal variants help to identify drug targets to treat a disease. Similarly, identifying causal epigenetic variants is of high importance, and epigenetic variants serve as ideal drug targets because of their reversible nature. However, most of the identified DNAm variants so far are shown to be consequential in nature to disease outcomes. Independent of being causal or consequential, dynamic nature of epigenetic marks makes them ideal biomarkers indicating the onset or progress of the disease, or exposure. Currently available and frequently used assays measuring absolute DNAm at single-CpG resolution (e.g. 450k array) are robust to replicate DNAm differences identified in large cohorts, and therefore have the potential to detect DNAm biomarkers [327]. In Study III we built a classifier to predict smoking status based on DNA methylation profiles. We identified smoking-associated CpGs using penalized regression to serve as predictors. Given the cross-sectional nature of the study, we cannot determine the causality, but nevertheless these smoking-associated CpG sites are valuable to identify DNAm patterns to distinguish smoking status categories. Furthermore, we showed that smoking status estimated using DNAm profiles is biologically relevant and more reliable than smoking status based on questionnaires. Our classifier is provided as an R package

enabling identification of smoking status in future studies and can be used in preclinical settings to screen the impact of smoking on methylation profiles of patients. However, the development of a biomarker panel using smoking-associated CpGs would perhaps be more cost-efficient and better suited for clinical purposes.

Although microarray technology (450k and EPIC) allows a cost-effective investigation of genome-wide DNA methylation, they only cover a fraction of the 28 million known genomic CpG sites. Therefore, affordable sequencing technologies are necessary to unravel the complete potential of DNAm in disease mechanisms. Furthermore, developments in statistical methods are needed to enable efficient integration of data across platforms and multiple omics. Machine learning and artificial intelligence are revolutionizing several fields including biomedicine. Deep learning, a subfield of machine learning, is showing exceptional results in image and speech recognition settings. However, larger and well-annotated samples are needed to apply deep learning algorithms to biological settings. In Study III we achieved this by using detailed smoking-behavior specific questions and by validating self-reported smoking status with cotinine to filter the training data. Additionally, independent test datasets are also required to test the performance of predictors. The requirement of large datasets can be partly achieved through publicly sharing data in databases like GEO and by collaborative efforts such as ENCODE and IHEC. However, privacy regulations such as the General Data Protection Regulation (GDPR) limit the extent of this sharing in public domain. For instance, only three whole blood 450k datasets were available from GEO (as of September 2018) with smoking behaviour (e.g. self-reported smoking status) and sex information to test the performance of our classifier in Study III. Fortunately, an increasing number of biobanks with new laws in place (e.g. Finnish biobank act 2013) are making huge datasets available for research.

Studies in this thesis focused mainly on obesity and smoking. Both obesity and smoking are associated with complex interactions among genetic, epigenetic and environmental factors. Despite several campaigns and policies to treat and prevent obesity, there is still a need for more efficient and implementable strategies to combat obesity [328–330]. The prevalence of smoking has reduced in developed countries because of strict policies and taxation, however, increased prevalence is observed in developing and under-developed countries [190,191]. Thus, there is a crucial need to strengthen translational research strategies with the potential to implement promising novel findings directly to clinical practice to treat obesity and smoking. Developing drugs and therapies targeting the reversible epigenetic marks is certainly an avenue to consider and explore.

After a decade of GWAS, we are still in infancy to use causal GWAS hits in a clinical setting, and a similar trajectory is also expected with epigenetic variants. In addition to the biological hypothesis, EWAS should define possible cellular epigenetic models which are thought to mediate the phenotypic changes, which can then be tested by designing appropriate molecular studies [26]. To determine and establish causality of the identified genetic and epigenetic variants, functional laboratory experiments are needed.

Recently, it has been suggested to test the functional value of identified epigenetic associations through epigenetic editing using CRISPR toolbox [331–334]. Epigenetic biomarkers can be considered advantageous over genetic markers as they can capture environmental and lifestyle factors impacting disease. Notably, DNAm-based biomarkers are more stable than RNA-based tests and can be detected in all genomic contexts i.e. not limited to coding regions. However, the cell-type-specific nature of epigenetic marks, and costs associated with screening, still pose limitations. Epidrugs target specific epigenomes with disrupted epigenetic signalling, and reverse the aberrations at the target to restore the signalling. Several epidrugs are already used in clinics, for instance, DNA methyltransferase inhibitor (DNMTi) and histone deacetylase inhibitor (HDACi) drugs are approved for treating hematological malignancies [331]. However, there are certain limitations associated with the epidrugs (e.g. lack of specificity), and further research is needed to overcome the current limitations. Another important aspect of epigenetic findings pertains to sharing the results to participants. As the epigenetic marks reflect the impact of genetic and non-genetic factors, results may have to be shared with participants and other concerned individuals (e.g. sharing the same environment). Also, epigenetic information may not be covered under existing genetic non-discrimination laws, as these laws are specific to “genetic characteristics” and might result in decreased participation of individuals in studies [335]. Therefore, new laws should be enacted specifically covering epigenetic data. In summary, there are certainly several challenges to be met in future research to tailor personalized medicine which can target inter-individual variability in disease, and epigenetic markers will be vital in achieving these goals.

7 Conclusions

Each of us are unique owing to the complex interplay of inherited genetic factors and experienced environmental stimuli. Even MZ twins with identical genotype can exhibit phenotypic divergence with their co-twin as a response to environmental and stochastic factors. By understanding inter-individual variability we can assess an individual's risk for developing a disease and response to treatment. Epigenetic mechanisms, specifically DNA methylation has been shown to contribute to human variation by acting as an additional layer of gene regulation. Integration of multiple layers of omics data is essential to uncover the mechanisms behind complex phenotypes like obesity and smoking, and to design effective and efficient treatments. This thesis focused on integrating transcriptomic and DNA methylation data to understand the regulatory mechanisms in obesity and smoking by employing appropriate study designs and statistical methods.

In Study I, we aimed to understand the temporal changes in expression and methylation profiles of adipose tissue during weight loss. We also integrated gene expression data and methylation profiles, to obtain a holistic view on the impact of methylation on gene expression and thereby weight loss. Both short- and long-term weight loss resulted in several differentially expressed genes, with significant correlations with methylation levels in the respective genes. Furthermore, replication of our results in a validation cohort of BMI-discordant MZ twin pairs indicated that majority of the weight-loss associated genes showed opposite expression in acquired obesity. This study fills the gap in the existing literature regarding SAT transcriptome and methylome changes during weight loss and also adds to our current understanding of the weight loss mechanism in healthy obese individuals from multiple perspectives. This study also highlights the importance of longer duration intervention studies, controlled for genetic and other confounding factors, in identifying biologically relevant findings despite of small sample size.

Obesity and smoking are independently associated with high risk of mortality and are of high public health relevance worldwide. A co-occurrence of these two conditions is even more detrimental to health. Therefore, to understand the impact of smoking on adiposity, we performed transcriptome- and methylome-wide assessment of SAT in Study II. We identified 42 differentially methylated signals and 42 differentially expressed genes associated with smoking with an overlap at five genes, including highly replicated smoking-methylation signals *AHRR* and *F2RL3*. Identified smoking-associated methylation and transcriptome profiles were associated with adiposity phenotypes demonstrating the broader impact of smoking on human metabolic health.

In Study III we extended the practical applicability of smoking-associated methylation sites by building a robust smoking status classifier. We used multinomial LASSO regression in conjunction with internal cross-validation to build the classifier. We have extensively tested the performance of this classifier on several independent test datasets in comparison with two existing approaches. Our classifier showed higher

accuracy compared to other approaches and is globally applicable to all datasets without the need for explicit data-specific threshold. Our classifier is available as an R package, *EpiSmokEr*, to enable smoking status prediction in future studies.

In conclusion, this thesis advances our understanding of obesity and smoking by integrating transcriptome and methylation data. Furthermore, this thesis extends practical applicability of smoking-associated methylation signals and overcomes the limitations of existing score-based approaches by developing a robust smoking status estimator and closes an important gap in the currently available toolbox for methylation studies.

Our findings clearly show that trait associated DNA methylation profiles, independent of causality claims, serve as important biomarkers, and are thus valuable in assessing progression of a disease or trait. Research presented in this thesis provides valuable insights for epidemiological and epigenetic research of obesity and smoking, and paves way forward to application of statistical and machine learning approaches to enhance our understanding of complex diseases and traits. Epigenetic variants hold a great promise and may emerge as vital biomarkers and drug targets, taking us a step closer to understanding inter-individual variability in disease and realizing personalized medicine.

Acknowledgements

The work for this thesis was conducted at the Department of Public Health, University of Helsinki and Institute for Molecular Medicine Finland (FIMM). I wish to acknowledge present and former department heads and directors for providing excellent research facilities and a stimulating research environment. My sincere thanks to the Academy of Finland, Doctoral Programme in Population Health (DocPop), European Commission Marie Skłodowska-Curie Initial Training Network Project EPITRAIN and Sigrid Juselius Foundation for funding the studies in this thesis.

My deepest gratitude goes to my supervisors Professor Jaakko Kaprio and Adjunct Professor Miina Ollikainen for their constructive supervision, expertise and enthusiasm throughout my PhD. Jaakko, you have always amazed me with your enthusiasm towards science, willingness to share your wisdom and for always finding time amidst your busy schedule. I am very grateful for the opportunity to work with you and thank you for being a huge source of inspiration. Miina, I am greatly indebted to you for always being supportive and trusting in my abilities. I immensely appreciate your emotional support and professional guidance over the years. Thank you for your patience, encouragement and understanding throughout.

Assistant Professor Tuuli Lappalainen is warmly thanked for graciously accepting the invitation to act as the official opponent at the public examination of this thesis. My sincere thanks to Dr Christopher Bell and Assistant Professor Juulia Jylhävä for providing constructive feedback on my thesis. Your detailed comments and suggestions were valuable to improve the quality of my thesis. Adjunct Professor Nina Kaminen-Ahola, thank you for accepting the role of faculty representative at the public examination of this thesis. I warmly acknowledge my thesis committee members Professor Sampsa Hautaniemi and Dr Panu Somervuo for their time, continuous support and timely guidance. Special thanks to Sampsa for asking critical and challenging questions.

I warmly acknowledge the contribution and encouragement from Professor Kirsi Pietiläinen, Dr Simon Anders, Adjunct Professor Tellervo Korhonen, Dr Jordana Bell, Dr Pei-Chien Tsai and all the co-authors of the three articles of this thesis. Simon, thank you for pushing my limits and for inspiring me with your technical savvy and effortless ease to spout profound ideas. During this thesis, I had the pleasure to visit and work with wonderful researchers. Thank you very much to Dr Teodora Ribarska, Dr Anthony Mathelier, Dr Aziz Khan and Dr Anders for hosting me and sharing your expertise on different research topics. Teodora, thank you as well for your generosity and friendship. I also wish to thank Assistant Professor Jenny van Dongen, Adjunct Professor Riikka Lund and several national and international collaborators with whom I have had the privilege to work with during this thesis.

I want to express my sincere thanks to the friendly and helpful present and former colleagues in the Kaprio group: Aileen, Aino, Aline, Alyce, Anja, Anna Kankaanpää, Antti, Anu L, Anu R, Beenish, Eero, Eeva,

Elina, Emma, Guiomar, Jade, Jenni, Katerina, Kauko, Khadeeja, Leonie, Linda, Maarit, Mahes, Mia, Milla, Paula, Pauliina, Pia, Richa, Sara Kaartinen, Sara Kuitunen, Sara L, Sari, Shunshuke, Suvi, Teemu, Venla and Yu. You have been the best colleagues, PhD companions, friends I could have hoped for. A very special thanks to Professor Anna Keski-Rahkonen for her compassion, kindness, and instilling inspiration through her courses and writing retreats. I also extend my gratitude to all twins and participants in the studies. I also thank colleagues and friends at FIMM. Thanks to Anja Thiede for your friendship and funny lunch conversations.

I sincerely thank Olle Hansson for accommodating my numerous requests and resolving my computational problems on the FIMM cluster. Thanks to Ulla Tuomainen and Emilia Vanamo for their help in administrative matters.

My deepest gratitude goes to my master's thesis supervisor Dr Martin Trick for trusting in my skills and guiding me to embark on this research journey.

Finally, much gratitude and love to Amma, Nanna and Guru for your unflinching support and unconditional love throughout. Thank you for always believing in me, even when I didn't believe in myself. Sairam, I cannot thank you enough for your love and support throughout this journey. A very special thanks to Coco and Paavo for bringing happiness, peace and joy into my life. Finally, I will be forever grateful to you Baba for your love and blessings.

Appendix I

Supplementary Table 1

Study I: Clinical and Metabolic Characteristics of Healthy Obese Participants at Three Time Points During a One Year Weight Loss Intervention. *This table is modified from the Table 1 of* [297] *(Bollepalli et al 2018).*

	All Participants (n=19)			Weight Losers (n=6)					Weight Regainers (n=13)			
Age range	20 - 48			21 - 48					20 - 45			
Sex (m/f)	7/12			3/3					4/9			
Clinical Parameters	Baseline	5 mo	0 vs 5 mo	Baseline	5 mo	12 mo	5 vs 12 mo	0 vs 12 mo	Baseline	5 mo	12 mo	5 vs 12 mo
Weight (kg)	99.0 (3.2)	87.4 (3.3)	<.0001	101.87 (4.88)	87.13 (5.29)	84.42 (4.68)	0,016	0,071	97.68 (4.19)	87.58 (4.21)	92.72 (4.47)	<.0001
BMI (kg/m2)	34.6 (0.6)	30.6 (0.8)	<.0001	34.64 (0.7)	29.6 (1.2)	28.7 (0.96)	0,014	0,002	34.65 (0.85)	31.06 (1.02)	32.88 (1.07)	<.0001
Body fat (%)	44.6 (1.6)	39.6 (2.0)	<.0001	42.15 (3.21)	37.5 (4.58)	34.7 (4.0)	0,018	0,003	45.76 (1.84)	40.58 (2.09)	43.37 (2.2)	<.0001
Subcutaneous adipose tissue (kg)	13.8 (0.75)	9.8 (0.9)	<.0001	13.22 (0.94)	9.73 (.161)	NA	NA	NA	14.15 (1.04)	10.08(1.25)	NA	NA
Intraabdominal adipose tissue (kg)	3.7 (0.6)	2.3 (0.4)	<.0001	3.19 (0.8)	3.74 (0.81)	NA	NA	NA	4.11(0.79)	2.65(0.6)	NA	NA

Liver fat (%)	6.7 (1.1)	1.8 (0.5)	<.0001	6.7 (2.09)	1.0 (0.45)	NA	NA	NA	6.68(1.28)	2.29 (0.66)	NA	NA
Adipocyte diameter (µm)	102.1 (1.9)	97.7(2.3)	0,150	102.95(3.25)	92.25(4.78)	89.57(4.12)	0,257	0,063	101.66(2.46)	100.13(2.31)	106.77(3.87)	0,046
HOMA index	1.98 (1.5–3.3)	1.88 (1.0–2.5)	0,002	1.32 (0.95-4.5)	1.24 (0.8-4.2)	1.35 (0.6-3.1)	1,000	0,563	2.19 (1.69-3.20)	1.92 (1.22-2.32)	1.64 (1.45-3.34)	0,080
Matsuda index	4.5 (2.7–6.2)	6.6 (4.6–11.0)	0,007	6.62 (1.98-11.34)	10.75 (2.98-14.74)	8.25 (3.74-17.56)	0,844	0,563	4.52(2.56-6.09)	6.27 (4-10.64)	5.78 (2.69 - 7.91)	0,037
Total cholesterol (mmol/L)	4.6 (0.2)	4.2 (0.2)	0,004	4.38 (0.4)	3.8 (0.8)	4.1 (0.34)	0,071	0,690	4.72 (0.15)	4.36 (0.18)	4.53 (0.17)	0,291
LDL cholesterol (mmol/L)	2.9 (0.1)	2.5 (0.1)	0,006	2.8 (0.33)	2.25 (0.23)	2.38 (0.22)	0,328	0,304	2.95(0.16)	2.68 (0.19)	2.69 (0.17)	0,900
HDL cholesterol (mmol/L)	1.4 (0.1)	1.4 (0.1)	0,379	1.33 (0.14)	1.33 (0.1)	1.47 (0.1)	0,027	0,527	1.42 (0.08)	1.49 (0.07)	1.53 (0.09)	0,518
Triglycerides (mmol/L)	0.9 (1.5–3.3)	0.7 (0.5–0.9)	0,001	1 (0.745-1.49)	0.61 (0.5-0.9)	0.62 (0.5-1.2)	0,528	0,031	0.99(0.775-1.615)	0.77 (0.575-0.98)	0.9 (0.76-1.2)	0,124
Systolic BP (mm Hg)	135.1 (3.4)	117.8 (2.2)	<.0001	129 (4.87)	116.7 (2.9)	120.2 (1.4)	0,263	0,115	138.5(4.7)	117.75 (3.13)	127.58 (4.1)	0,013
Diastolic BP (mm Hg)	83.8 (1.9)	81.3 (1.8)	0,269	82.8 (3.18)	80.33 (0.95)	79.5 (2.92)	0,769	<.0001	84.92 (2.51)	81.83 (2.8)	83.42 (3.83)	0,557
Total energy intake (kcal/d)	2457.9 (212.0)	1593.4 (109.9)	0,001	3032.8 (449.6)	1705.824 (216.4)	2281.32	0,184	0.177	2008.71(244.16)	1348.44 (110)	1713.96 (124.37)	0,041

						(378.2 2)						

Data is presented as mean (SE) for variables following the normal distribution and as median (interquartile range) for skewed variables. Paired t-tests were used for computing comparisons between different time points for normally distributed variables. Wilcoxon signed-rank tests were implemented for skewed variables. mo, month; NA, data not available.

References

1 Polderman, T.J.C. *et al.* (2015) Meta-analysis of the heritability of human traits based on fifty years of twin studies. *Nat. Genet.* 47, 702

2 Bonder, M.J. *et al.* (2017) Disease variants alter transcription factor levels and methylation of their binding sites. *Nat. Genet.* 49, 131–138

3 Consortium, I.H.G.S. (2004) Finishing the euchromatic sequence of the human genome. *Nature* 431, 931–945

4 Altshuler, D.M. *et al.* (2010) Integrating common and rare genetic variation in diverse human populations. *Nature* 467, 52–58

5 Visscher, P.M. *et al.* (2017) 10 Years of GWAS Discovery: Biology, Function, and Translation. *Am. J. Hum. Genet.* 101, 5–22

6 MacArthur, J. *et al.* (2017) The new NHGRI-EBI Catalog of published genome-wide association studies (GWAS Catalog). *Nucleic Acids Res.* 45, D896–D901

7 Watanabe, K. *et al.* (2019) A global overview of pleiotropy and genetic architecture in complex traits. *Nat. Genet.* 51, 1339–1348

8 Welter, D. *et al.* (2014) The NHGRI GWAS Catalog, a curated resource of SNP-trait associations. *Nucleic Acids Res.* DOI: 10.1093/nar/gkt1229

9 Yang, J. *et al.* (2015) Genetic variance estimation with imputed variants finds negligible missing heritability for human height and body mass index. *Nat. Genet.* 47, 1114–1120

10 Wainschtein, P. *et al.* (2019) Recovery of trait heritability from whole genome sequence data. *bioRxiv* DOI: 10.1101/588020

11 Trerotola, M. *et al.* (2015) Epigenetic inheritance and the missing heritability. *Hum. Genomics* 9, 17

12 Manolio, T.A. *et al.* Finding the missing heritability of complex diseases. , *Nature*. (2009)

13 Richards, E.J. (2006) Inherited epigenetic variation — revisiting soft inheritance. *Nat. Rev. Genet.* 7, 395–401

14 Waddington and H, C. (1942) The epigenotype. *Endeavour* 1, 18–20

15 Waddington, C.H. (2014) *The strategy of the genes*, Routledge.

16 Horvath, S. (2013) DNA methylation age of human tissues and cell types. *Genome Biol.* 14, R115

17 Gutierrez-Arcelus, M. *et al.* (2015) Tissue-specific effects of genetic and epigenetic variation on gene regulation and splicing. *PLoS Genet.* 11, e1004958

18 Barlow, D.P. and Bartolomei, M.S. (2014) Genomic imprinting in mammals. *Cold Spring Harb. Perspect. Biol.* 6,

19 Sharp, A.J. *et al.* (2011) DNA methylation profiles of human active and inactive X chromosomes. *Genome Res.* 21, 1592–1600

20 Reik, W. (2007) Stability and flexibility of epigenetic gene regulation in mammalian development. *Nature* 447, 425–432

21 Riggs, A.D. (1975) X inactivation, differentiation, and DNA methylation. *Cytogenet. Cell Genet.* 14, 9–25

22 Berger, S.L. *et al.* (2009) An operational definition of epigenetics. *Genes Dev.* 23, 781–783

23 Bird, A. (2007) Perceptions of epigenetics. *Nature* 447, 396–398

24 Dupont, C. *et al.* (2009) Epigenetics: definition, mechanisms and clinical perspective. *Semin. Reprod. Med.* 27, 351–357

25 Feil, R. and Fraga, M.F. (2012) Epigenetics and the environment: emerging patterns and implications. *Nat. Rev. Genet.* 13, 97–109

26 Lappalainen, T. and Greally, J.M. (2017) Associating cellular epigenetic models with human phenotypes. *Nat. Rev. Genet.* 18, 441–451

27 Sharma, S. *et al.* (2010) Epigenetics in cancer. *Carcinogenesis* 31, 27–36

28 Weaver, I.C.G. *et al.* (2004) Epigenetic programming by maternal behavior. *Nat. Neurosci.* 7, 847–854

29 Dias, B.G. and Ressler, K.J. (2014) Parental olfactory experience influences behavior and neural structure in subsequent generations. *Nat. Neurosci.* 17, 89–96

30 Daxinger, L. and Whitelaw, E. (2012) Understanding transgenerational epigenetic inheritance via the gametes in mammals. *Nat. Rev. Genet.* 13, 153–162

31 Guerrero-Bosagna, C. and Skinner, M.K. (2012) Environmentally induced epigenetic transgenerational inheritance of phenotype and disease. *Mol. Cell. Endocrinol.* 354, 3–8

32 Heard, E. and Martienssen, R.A. (2014) Transgenerational epigenetic inheritance: myths and mechanisms. *Cell* 157, 95–109

33 Horsthemke, B. (2018) A critical view on transgenerational epigenetic inheritance in humans. *Nat. Commun.* 9, 2973

34 McGinty, R.K. and Tan, S. (2015) Nucleosome structure and function. *Chem. Rev.* 115, 2255–2273

35 Zhou, K. *et al.* (2019) Nucleosome structure and dynamics are coming of age. *Nat. Struct. Mol. Biol.* 26, 3–13

36 Egger, G. *et al.* (2004) Epigenetics in human disease and prospects for epigenetic therapy. *Nature* 429, 457–463

37 Kouzarides, T. (2007) Chromatin Modifications and Their Function. *Cell* 128, 693–705

38 Trojer, P. and Reinberg, D. (2007) Facultative Heterochromatin: Is There a Distinctive Molecular Signature? *Mol. Cell* 28, 1–13

39 Consortium, R.E. *et al.* (2015) Integrative analysis of 111 reference human epigenomes. *Nature* 518, 317–330

40 Gendrel, A.-V. and Heard, E. (2014) Noncoding RNAs and epigenetic mechanisms during X-chromosome inactivation. *Annu. Rev. Cell Dev. Biol.* 30, 561–580

41 Kaikkonen, M.U. *et al.* (2011) Non-coding RNAs as regulators of gene expression and epigenetics. *Cardiovasc. Res.* 90, 430–440

42 Relton, C.L. and Davey Smith, G. (2010) Epigenetic epidemiology of common complex disease: prospects for prediction, prevention, and treatment. *PLoS Med.* 7, e1000356–e1000356

43 Patil, V. *et al.* (2014) The evidence for functional non-CpG methylation in mammalian cells. *Epigenetics* 9, 823–828

44 Lyko, F. (2018) The DNA methyltransferase family: a versatile toolkit for epigenetic regulation. *Nat. Rev. Genet.* 19, 81–92

45 Okano, M. *et al.* (1999) DNA Methyltransferases Dnmt3a and Dnmt3b Are Essential for De Novo Methylation and Mammalian Development. *Cell* 99, 247–257

46 Okano, M. *et al.* (1998) Cloning and characterization of a family of novel mammalian DNA (cytosine-5) methyltransferases. *Nat. Genet.* 19, 219–220

47 Jeltsch, A. and Jurkowska, R.Z. (2014) New concepts in DNA methylation. *Trends Biochem. Sci.* 39, 310–318

48 Bird, A.P. (1986) CpG-rich islands and the function of DNA methylation. *Nature* 321, 209–213

49 Lister, R. *et al.* (2009) Human DNA methylomes at base resolution show widespread epigenomic differences. *Nature* 462, 315–322

50 Bird, A.P. (1980) DNA methylation and the frequency of CpG in animal DNA. *Nucleic Acids Res.* 8, 1499–1504

51 Suzuki, M.M. and Bird, A. (2008) DNA methylation landscapes: provocative insights from epigenomics. *Nat. Rev. Genet.* 9, 465–476

52 Jones, P.A. (2012) Functions of DNA methylation: islands, start sites, gene bodies and beyond. *Nat. Rev. Genet.* 13, 484–492

53 Blattler, A. *et al.* (2014) Global loss of DNA methylation uncovers intronic enhancers in genes showing expression changes. *Genome Biol.* 15, 469

54 Anastasiadi, D. *et al.* (2018) Consistent inverse correlation between DNA methylation of the first intron and gene expression across tissues and species. *Epigenetics Chromatin* 11, 37

55 Yin, Y. *et al.* (2017) Impact of cytosine methylation on DNA binding specificities of human transcription factors. *Science (80-.).* 356, eaaj2239

56 Greenberg, M.V.C. and Bourc'his, D. (2019) The diverse roles of DNA methylation in mammalian development and disease. *Nat. Rev. Mol. Cell Biol.* DOI: 10.1038/s41580-019-0159-6

57 Wu, X. and Zhang, Y. (2017) TET-mediated active DNA demethylation: mechanism, function and beyond. *Nat. Rev. Genet.* 18, 517–534

58 Hannon, E. *et al.* (2018) Characterizing genetic and environmental influences on variable DNA methylation using monozygotic and dizygotic twins. *PLoS Genet.* 14,

59 Liu, Y. *et al.* (2013) Epigenome-wide association data implicate DNA methylation as an intermediary of genetic risk in rheumatoid arthritis. *Nat. Biotechnol.* 31, 142–147

60 Rönn, T. *et al.* (2013) A six months exercise intervention influences the genome-wide DNA methylation pattern in human adipose tissue. *PLoS Genet.* 9, e1003572

61 Tsaprouni, L.G. *et al.* (2014) Cigarette smoking reduces DNA methylation levels at multiple genomic loci but the effect is partially reversible upon cessation. *Epigenetics* 9, 1382–1396

62 Grundberg, E. *et al.* (2013) Global Analysis of DNA Methylation Variation in Adipose Tissue from Twins Reveals Links to Disease-Associated Variants in Distal Regulatory Elements (vol 93, pg 876, 2013). *Am. J. Hum. Genet.* 93, 1158

63 Wahl, S. *et al.* (2017) Epigenome-wide association study of body mass index, and the adverse outcomes of adiposity. *Nature* DOI: 10.1038/nature20784

64 Joehanes, R. *et al.* (2016) Epigenetic Signatures of Cigarette Smoking. *Circ. Cardiovasc. Genet.* 9, 436–447

65 Marzi, S.J. *et al.* (2018) A histone acetylome-wide association study of Alzheimer's disease identifies disease-associated H3K27ac differences in the entorhinal cortex. *Nat. Neurosci.* 21, 1618–1627

66 Carlberg, C. and Molnár, F. (2016) Overview: What Is Gene Expression? BT - Mechanisms of Gene Regulation. (Carlberg, C. and Molnár, F., eds), pp. 3–16, Springer Netherlands

67 Lander, E.S. (2011) Initial impact of the sequencing of the human genome. *Nature* 470, 187–197

68 Melé, M. *et al.* (2015) Human genomics. The human transcriptome across tissues and individuals. *Science* 348, 660–665

69 Aguet, F. *et al.* (2017) Genetic effects on gene expression across human tissues. *Nature* DOI: 10.1038/nature24277

70 Marabita, F. *et al.* (2015) Introduction to Data Types in Epigenomics BT - Computational and Statistical Epigenomics. (Teschendorff, A. E., ed), pp. 3–34, Springer Netherlands

71 Bock, C. *et al.* (2010) Quantitative comparison of genome-wide DNA methylation mapping technologies. *Nat. Biotechnol.* 28, 1106

72 Li, Y. and Tollefsbol, T.O. (2011) DNA methylation detection: bisulfite genomic sequencing analysis. *Methods Mol. Biol.* 791, 11–21

73 Bibikova, M. *et al.* (2011) High density DNA methylation array with single CpG site resolution. *Genomics* 98, 288–295

74 Moran, S. *et al.* (2015) Validation of a DNA methylation microarray for 850,000 CpG sites of the human genome enriched in enhancer sequences. *Epigenomics* 8, 389–399

75 Miller, M.B. and Tang, Y.-W. (2009) Basic Concepts of Microarrays and Potential Applications in Clinical Microbiology. *Clin. Microbiol. Rev.* 22, 611 LP – 633

76 Bibikova, M. *et al.* (2009) Genome-wide DNA methylation profiling using Infinium® assay. *Epigenomics* 1, 177–200

77 Sandoval, J. *et al.* (2011) Validation of a DNA methylation microarray for 450,000 CpG sites in the human genome. *Epigenetics* 6, 692–702

78 Marabita, F. *et al.* (2013) An evaluation of analysis pipelines for DNA methylation profiling using the Illumina HumanMethylation450 BeadChip platform. *Epigenetics* 8, 333–346

79 Bock, C. (2012) Analysing and interpreting DNA methylation data. *Nat. Rev. Genet.* 13, 705–719

80 Touleimat, N. and Tost, J. (2012) Complete pipeline for Infinium(®) Human Methylation 450K BeadChip data processing using subset quantile normalization for accurate DNA methylation estimation. *Epigenomics* 4, 325–341

81 Morris, T.J. *et al.* (2014) ChAMP: 450k chip analysis methylation pipeline. *Bioinformatics* 30,

82 Pidsley, R. *et al.* (2013) A data-driven approach to preprocessing Illumina 450K methylation array data. *BMC Genomics* 14, 293

83 Laird, P.W. (2010) Principles and challenges of genome-wide DNA methylation analysis. *Nat. Rev. Genet.* 11, 191–203

84 Teschendorff, A.E. *et al.* (2013) A beta-mixture quantile normalization method for correcting probe design bias in Illumina Infinium 450 k DNA methylation data. *Bioinformatics* 29, 189–196

85 Maksimovic, J. *et al.* (2012) SWAN: Subset-quantile Within Array Normalization for Illumina Infinium HumanMethylation450 BeadChips. *Genome Biol.* 13, R44

86 Aryee, M.J. *et al.* (2014) Minfi: a flexible and comprehensive Bioconductor package for the analysis of Infinium DNA methylation microarrays. *Bioinformatics* 30, 1363–1369

87 Lehne, B. *et al.* (2015) A coherent approach for analysis of the Illumina {HumanMethylation450} {BeadChip} improves data quality and performance in epigenome-wide association studies. *Genome Biol.* 16, 37

88 Fortin, J.-P. *et al.* (2014) Functional normalization of 450k methylation array data improves replication in large cancer studies. *Genome Biol.* 15, 503

89 Cazaly, E. *et al.* (2019) Making Sense of the Epigenome Using Data Integration Approaches. *Front. Pharmacol.* 10, 126

90 Ballereau, S. *et al.* (2013) Functional Genomics, Proteomics, Metabolomics and Bioinformatics for Systems Biology BT - Systems Biology: Integrative Biology and Simulation Tools. (Prokop, A. and Csukás, B., eds), pp. 3–41, Springer Netherlands

91 Rakyan, V.K. *et al.* (2011) Epigenome-wide association studies for common human diseases. *Nat. Rev. Genet.* 12, 529–541

92 Houseman, E.A. *et al.* (2012) DNA methylation arrays as surrogate measures of cell mixture distribution. *BMC Bioinformatics* 13, 86

93 Houseman, E.A. *et al.* (2014) Reference-free cell mixture adjustments in analysis of DNA methylation data. *Bioinformatics* 30, 1431–1439

94 Zou, J. *et al.* (2014) Epigenome-wide association studies without the need for cell-type composition. *Nat. Methods* 11, 309

95 van Dongen, J. *et al.* (2012) The continuing value of twin studies in the omics era. *Nat. Rev. Genet.* 13, 640

96 Kaminsky, Z.A. *et al.* (2009) DNA methylation profiles in monozygotic and dizygotic twins. *Nat. Genet.* 41, 240–245

97 van Dongen, J. *et al.* (2016) Genetic and environmental influences interact with age and sex in shaping the human methylome. *Nat. Commun.* 7,

98 Bell, J.T. and Spector, T.D. (2012) DNA methylation studies using twins: what are they telling us? *Genome Biol.* 13, 172

99 Richardson, T.G. *et al.* (2017) Mendelian Randomization Analysis Identifies CpG Sites as Putative Mediators for Genetic Influences on Cardiovascular Disease Risk. *Am. J. Hum. Genet.* 101, 590–602

100 Davegårdh, C. *et al.* (2017) Abnormal epigenetic changes during differentiation of human skeletal muscle stem cells from obese subjects. *BMC Med.* 15, 39

101 Dunham, I. *et al.* (2012) An integrated encyclopedia of DNA elements in the human genome. *Nature* 489, 57–74

102 Bernstein, B.E. *et al.* (2010) The NIH Roadmap Epigenomics Mapping Consortium. *Nat. Biotechnol.* 28, 1045

103 Martens, J.H.A. and Stunnenberg, H.G. (2013) BLUEPRINT: mapping human blood cell epigenomes. *Haematologica* 98, 1487 LP – 1489

104 Bujold, D. *et al.* (2016) The International Human Epigenome Consortium Data Portal. *Cell Syst.* 3, 496-499.e2

105 Lipshutz, R.J. *et al.* (1999) High density synthetic oligonucleotide arrays. *Nat. Genet.* 21, 20–24

106 Irizarry, R.A. *et al.* (2003) Exploration, normalization, and summaries of high density oligonucleotide array probe level data. *Biostatistics* 4, 249–264

107 Stark, R. *et al.* (2019) RNA sequencing: the teenage years. *Nat. Rev. Genet.* 20, 631–656

108 Ozsolak, F. and Milos, P.M. (2011) RNA sequencing: advances, challenges and opportunities. *Nat. Rev. Genet.* 12, 87–98

109 World Health Orgnaization (2000) *Obesity: preventing and managing the global epidemic Report of a WHO Consultation*, World Health Organization.

110 WHO. Obesity and overweight. . [Online]. Available: http://www.who.int/mediacentre/factsheets/fs311/en/. [Accessed: 10-Sep-2019]

111 De Gonzalez, A.B. *et al.* (2010) Body-mass index and mortality among 1.46 million white adults. *N. Engl. J. Med.* DOI: 10.1056/NEJMoa1000367

112 Global BMI Mortality Collaboration *et al.* (2016) Body-mass index and all-cause mortality: individual-participant-data meta-analysis of 239 prospective studies in four continents. *Lancet* 388, 776–786

113 Copeland, K.C. *et al.* (2013) Management of newly diagnosed type 2 diabetes mellitus (T2DM) in children and adolescents. *Pediatrics* DOI: 10.1542/peds.2012-3494

114 Fagot-Campagna, A. (2000) , Emergence of type 2 diabetes mellitus in children: Epidemiological evidence. , in *Journal of Pediatric Endocrinology and Metabolism*

115 Reilly, J.J. and Kelly, J. Long-term impact of overweight and obesity in childhood and adolescence on morbidity and premature mortality in adulthood: Systematic review. , *International Journal of Obesity*. (2011)

116 Finsote (2018) Alueelliset erot aikuisten palvelukokemuksissa ja hyvinvoinnissa –Finsote 2018. *Stat. Rep. 21/2018, June 4, 2018*.

117 van Dijk, S.B. *et al.* (2012) Different anthropometric adiposity measures and their association with cardiovascular disease risk factors: a meta-analysis. *Neth. Heart J.* 20, 208–218

118 Pietiläinen, K.H. *et al.* (2013) Agreement of bioelectrical impedance with dual-energy X-ray absorptiometry and MRI to estimate changes in body fat, skeletal muscle and visceral fat during a 12-month weight loss intervention. *Br. J. Nutr.* 109, 1910–1916

119 Trayhurn, P. (2007) Adipocyte biology. *Obes. Rev.* 8 Suppl 1, 41–44

120 Bartelt, A. and Heeren, J. (2014) Adipose tissue browning and metabolic health. *Nat. Rev. Endocrinol.* 10, 24–36

121 Arner, P. (1997) Regional adipocity in man. *J. Endocrinol.* 155, 191–192

122 Wajchenberg, B.L. (2000) Subcutaneous and visceral adipose tissue: their relation to the metabolic syndrome. *Endocr. Rev.* 21, 697–738

123 Claussnitzer, M. *et al.* (2015) FTO Obesity Variant Circuitry and Adipocyte Browning in Humans. *N. Engl. J. Med.* 373, 895–907

124 Ahima, R.S. and Flier, J.S. (2000) Adipose tissue as an endocrine organ. *Trends Endocrinol. Metab.* 11, 327–332

125 Coelho, M. *et al.* (2013) Biochemistry of adipose tissue: an endocrine organ. *Arch. Med. Sci.* 9, 191–200

126 Scherer, P.E. (2006) Adipose tissue: from lipid storage compartment to endocrine organ. *Diabetes* 55, 1537–1545

127 Friedman, J.M. (2019) Leptin and the endocrine control of energy balance. *Nat. Metab.* 1, 754–764

128 Halaas, J.L. *et al.* (1995) Weight-reducing effects of the plasma protein encoded by the obese gene. *Science (80-.).* 269, 543 LP – 546

129 Farooqi, I.S. *et al.* (1999) Effects of Recombinant Leptin Therapy in a Child with Congenital Leptin Deficiency. *N. Engl. J. Med.* 341, 879–884

130 Montague, C.T. *et al.* (1997) Congenital leptin deficiency is associated with severe early-onset obesity in humans. *Nature* 387, 903–908

131 Licinio, J. *et al.* (2004) Phenotypic effects of leptin replacement on morbid obesity, diabetes mellitus, hypogonadism, and behavior in leptin-deficient adults. *Proc. Natl. Acad. Sci. U. S. A.* 101, 4531 LP – 4536

132 Cawthorn, W.P. and Sethi, J.K. (2008) TNF-α and adipocyte biology. *FEBS Lett.* 582, 117–131

133 Sun, K. *et al.* (2011) Adipose tissue remodeling and obesity. *J. Clin. Invest.* 121, 2094–2101

134 Frayn, K. (2002) Adipose tissue as a buffer for daily lipid flux. *Diabetologia* 45, 1201–1210

135 Longo, M. *et al.* (2019) Adipose Tissue Dysfunction as Determinant of Obesity-Associated Metabolic Complications. *Int. J. Mol. Sci.* 20,

136 Laclaustra, M. *et al.* (2007) Metabolic syndrome pathophysiology: the role of adipose tissue. *Nutr. Metab. Cardiovasc. Dis.* 17, 125–139

137 Lee, M.-J. *et al.* (2010) Adipose tissue remodeling in pathophysiology of obesity. *Curr. Opin. Clin. Nutr. Metab. Care* 13, 371–376

138 Elks, C.E. *et al.* (2012) Variability in the heritability of body mass index: a systematic review and meta-regression. *Front. Endocrinol. (Lausanne).* 3, 29

139 Min, J. *et al.* (2013) Variation in the heritability of body mass index based on diverse twin studies: a systematic review. *Obes. Rev.* 14, 871–882

140 Silventoinen, K. *et al.* (2016) Genetic and environmental effects on body mass index from infancy to the onset of adulthood: an individual-based pooled analysis of 45 twin cohorts participating in the COllaborative project of Development of Anthropometrical measures in Twins (CODATwins). *Am. J. Clin. Nutr.* 104, 371–379

141 Frayling, T.M. *et al.* (2007) A Common Variant in the FTO Gene Is Associated with Body Mass Index and Predisposes to Childhood and Adult Obesity. *Science (80-.).* 316, 889 LP – 894

142 Scuteri, A. *et al.* (2007) Genome-Wide Association Scan Shows Genetic Variants in the FTO Gene Are Associated with Obesity-Related Traits. *PLOS Genet.* 3, e115

143 Locke, A.E. *et al.* (2015) Genetic studies of body mass index yield new insights for obesity biology. *Nature* DOI: 10.1038/nature14177

144 Hoffmann, T.J. *et al.* (2018) A Large Multiethnic Genome-Wide Association Study of Adult Body Mass Index Identifies Novel Loci. *Genetics* 210, 499 LP – 515

145 Speakman, J.R. *et al.* GWAS for BMI: a treasure trove of fundamental insights into the genetic basis of obesity. , *International Journal of Obesity*. (2018)

146 Yengo, L. *et al.* (2018) Meta-analysis of genome-wide association studies for height and body mass index in ∼700000 individuals of European ancestry. *Hum. Mol. Genet.* 27, 3641–3649

147 Walley, A.J. *et al.* (2006) Genetics of obesity and the prediction of risk for health. *Hum. Mol. Genet.* DOI: 10.1093/hmg/ddl215

148 Blundell, J.E. *et al.* Appetite control and energy balance: Impact of exercise. , *Obesity Reviews*. (2015)

149 Van Der Klaauw, A.A. and Farooqi, I.S. The hunger genes: Pathways to obesity. , *Cell*. (2015)

150 Ling, C. and Rönn, T. (2019) Epigenetics in Human Obesity and Type 2 Diabetes. *Cell Metab.* 29, 1028–1044

151 van Dijk, S.J. *et al.* (2015) Recent developments on the role of epigenetics in obesity and metabolic disease. *Clin. Epigenetics* 7, 66

152 van Dijk, S.J. *et al.* (2015) Epigenetics and human obesity. *Int. J. Obes.* 39, 85–97

153 Thaker, V. V (2017) Genetic and epigenetic causes of obesity. *Adolesc. Med. State Art Rev.* 28, 379–405

154 Herrera, B.M. *et al.* Genetics and epigenetics of obesity. , *Maturitas*. (2011)

155 Cordero, P. *et al.* (2015) Epigenetics of obesity: beyond the genome sequence. *Curr. Opin. Clin. Nutr. Metab. Care* 18, 361–366

156 Ollikainen, M. *et al.* (2015) Genome-wide blood DNA methylation alterations at regulatory elements and heterochromatic regions in monozygotic twins discordant for obesity and liver fat. *Clin. Epigenetics* 7, 39

157 Roseboom, T. *et al.* (2006) The Dutch famine and its long-term consequences for adult health. *Early Hum. Dev.* 82, 485–491

158 Heijmans, B.T. *et al.* (2008) Persistent epigenetic differences associated with prenatal exposure to famine in humans. *Proc. Natl. Acad. Sci. U. S. A.* 105, 17046–17049

159 Tobi, E.W. *et al.* (2009) DNA methylation differences after exposure to prenatal famine are common and timing- and sex-specific. *Hum. Mol. Genet.* 18, 4046–4053

160 Tobi, E.W. *et al.* (2018) DNA methylation as a mediator of the association between prenatal adversity and risk factors for metabolic disease in adulthood. *Sci. Adv.* 4, eaao4364

161 Bell, C.G. (2017) The Epigenomic Analysis of Human Obesity. *Obesity* 25, 1471–1481

162 Rohde, K. *et al.* (2019) Genetics and epigenetics in obesity. *Metabolism* 92, 37–50

163 Milagro, F.I. and Martínez, J.A. (2013) Epigenetics of obesity and weight loss. *Endocrinol. Nutr.* 60 Suppl 1, 12–14

164 Martínez, J.A. *et al.* (2014) Epigenetics in adipose tissue, obesity, weight loss, and diabetes. *Adv. Nutr.* 5, 71–81

165 Lopomo, A. *et al.* (2016) Epigenetics of Obesity. *Prog. Mol. Biol. Transl. Sci.* 140, 151–184

166 Nicoletti, C.F. *et al.* (2016) DNA Methylation and Hydroxymethylation Levels in Relation to Two Weight Loss Strategies: Energy-Restricted Diet or Bariatric Surgery. *Obes. Surg.* 26, 603–611

167 Sayols-Baixeras, S. *et al.* (2017) DNA methylation and obesity traits: An epigenome-wide association study. The REGICOR study. *Epigenetics* 12, 909–916

168 Wahl, S. *et al.* (2017) Epigenome-wide association study of body mass index, and the adverse outcomes of adiposity. *Nature* 541, 81–86

169 Mendelson, M.M. *et al.* (2017) Association of Body Mass Index with DNA Methylation and Gene Expression in Blood Cells and Relations to Cardiometabolic Disease: A Mendelian Randomization Approach. *PLOS Med.* 14, e1002215

170 Das, S.K. *et al.* (2015) Adipose tissue gene expression and metabolic health of obese adults. *Int. J. Obes.* 39, 869–873

171 Heinonen, S. *et al.* (2017) Mitochondria-related transcriptional signature is downregulated in adipocytes in obesity: a study of young healthy MZ twins. *Diabetologia* 60, 169–181

172 Walley, A.J. *et al.* (2012) Differential coexpression analysis of obesity-associated networks in human subcutaneous adipose tissue. *Int. J. Obes.* 36, 137–147

173 Pietilainen, K.H. *et al.* (2016) DNA methylation and gene expression patterns in adipose tissue differ significantly within young adult monozygotic BMI-discordant twin pairs. *Int. J. Obes.* 40, 654–661

174 Pietiläinen, K.H. *et al.* (2008) Global Transcript Profiles of Fat in Monozygotic Twins Discordant for BMI: Pathways behind Acquired Obesity. *PLOS Med.* 5, e51

175 Dubois, S.G. *et al.* (2006) Decreased Expression of Adipogenic Genes in Obese Subjects with Type 2 Diabetes. *Obesity* 14, 1543–1552

176 Rönn, T. *et al.* (2015) Impact of age, BMI and HbA1c levels on the genome-wide DNA methylation and mRNA expression patterns in human adipose tissue and identification of epigenetic biomarkers in blood. *Hum. Mol. Genet.* 24, 3792–3813

177 Dick, K.J. *et al.* (2014) DNA methylation and body-mass index: a genome-wide analysis. *Lancet* 383, 1990–1998

178 Jensen, M.D. *et al.* (2014) 2013 AHA/ACC/TOS Guideline for the Management of Overweight and Obesity in Adults: A Report of the American College of Cardiology/American Heart Association Task Force on Practice Guidelines and The Obesity Society. *J. Am. Coll. Cardiol.* 63, 2985–3023

179 Dahlman, I. *et al.* (2005) Changes in adipose tissue gene expression with energy-restricted diets in obese women. *Am. J. Clin. Nutr.* 81, 1275–1285

180 Johansson, L.E. *et al.* (2012) Differential gene expression in adipose tissue from obese human subjects during weight loss and weight maintenance. *Am. J. Clin. Nutr.* 96, 196–207

181 Mutch, D.M. *et al.* (2011) A distinct adipose tissue gene expression response to caloric restriction predicts 6-mo weight maintenance in obese subjects. *Am. J. Clin. Nutr.* 94, 1399–1409

182 Clément, K. *et al.* (2004) Weight loss regulates inflammation-related genes in white adipose tissue of obese subjects. *FASEB J.* 18, 1657–1669

183 Campbell, K.L. *et al.* (2013) Gene expression changes in adipose tissue with diet- and/or exercise-induced weight loss. *Cancer Prev. Res.* 6, 217–231

184 Bouchard, L. *et al.* (2010) Differential epigenomic and transcriptomic responses in subcutaneous adipose tissue between low and high responders to caloric restriction. *Am. J. Clin. Nutr.* 91, 309–320

185 Aronica, L. *et al.* (2017) A systematic review of studies of DNA methylation in the context of a weight loss intervention. *Epigenomics* 9, 769–787

186 Mutch, D.M. *et al.* (2007) Adipose gene expression prior to weight loss can differentiate and weakly predict dietary responders. *PLoS One* 2, e1344

187 Capel, F. *et al.* (2008) Contribution of energy restriction and macronutrient composition to changes in adipose tissue gene expression during dietary weight-loss programs in obese women. *J. Clin. Endocrinol. Metab.* 93, 4315–4322

188 Capel, F. *et al.* (2009) Macrophages and Adipocytes in Human Obesity. *Diabetes* 58, 1558 LP – 1567

189 Márquez-Quiñones, A. *et al.* (2010) Adipose tissue transcriptome reflects variations between subjects with continued weight loss and subjects regaining weight 6 mo after caloric restriction independent of energy intake. *Am. J. Clin. Nutr.* 92, 975–984

190 World Health, O. (2017) WHO report on the global tobacco epidemic 2017: Monitoring tobacco use and prevention policies. at <https://escholarship.org/uc/item/8nw5p0zt>

191 J. Drope, N. Schluger, et al. (2018) The Tobacco Atlas. Atlanta: American Cancer Society and Vital Strategies.

192 Belsky, D.W. *et al.* (2013) Polygenic Risk and the Developmental Progression to Heavy, Persistent Smoking and Nicotine Dependence: Evidence From a 4-Decade Longitudinal Study. *JAMA Psychiatry* 70, 534–542

193 Aloise-Young, P.A. *et al.* (1994) Peer influence on smoking initiation during early adolescence: A comparison of

group members and group outsiders. *Journal of Applied Psychology*, 79, American Psychological Association, 281–287

194 Maxwell, K.A. (2002) Friends: The Role of Peer Influence Across Adolescent Risk Behaviors. *J. Youth Adolesc.* 31, 267–277

195 Simons-Morton, B.G. and Farhat, T. (2010) Recent findings on peer group influences on adolescent smoking. *J. Prim. Prev.* 31, 191—208

196 Mercken, L. *et al.* (2009) Social influence and selection effects in the context of smoking behavior: Changes during early and mid adolescence. , *Health Psychology*, 28. American Psychological Association, 73–82

197 CONRAD, K.M. *et al.* (1992) Why children start smoking cigarettes: predictors of onset. *Br. J. Addict.* 87, 1711–1724

198 Buller, D.B. *et al.* (2003) Understanding factors that influence smoking uptake. *Tob. Control* 12, iv16 LP-iv25

199 Hukkanen, J. *et al.* (2005) Metabolism and Disposition Kinetics of Nicotine. *Pharmacol. Rev.* 57, 79 LP – 115

200 Picciotto, M.R. and Mineur, Y.S. (2014) Molecules and circuits involved in nicotine addiction: The many faces of smoking. *Neuropharmacology* 76 Pt B, 545–553

201 McLaughlin, I. *et al.* (2015) Nicotine withdrawal. *Curr. Top. Behav. Neurosci.* 24, 99–123

202 Allen, S.S. *et al.* (2008) Craving, Withdrawal, and Smoking Urges on Days Immediately Prior to Smoking Relapse. *Nicotine Tob. Res.* 10, 35–45

203 Jackson, K.J. *et al.* (2015) New mechanisms and perspectives in nicotine withdrawal. *Neuropharmacology* 96, 223–234

204 Li, M.D. (2006) The genetics of nicotine dependence. *Curr. Psychiatry Rep.* 8, 158–164

205 Vink, J.M. *et al.* (2005) Heritability of Smoking Initiation and Nicotine Dependence. *Behav. Genet.* 35, 397–406

206 Lessov-Schlaggar, C.N. *et al.* (2008) Genetics of nicotine dependence and pharmacotherapy. *Biochem. Pharmacol.* 75, 178–195

207 Thorgeirsson, T.E. *et al.* (2010) Sequence variants at CHRNB3–CHRNA6 and CYP2A6 affect smoking behavior. *Nat. Genet.* 42, 448–453

208 Chen, L.-S. *et al.* (2012) Interplay of Genetic Risk Factors (CHRNA5-CHRNA3-CHRNB4) and Cessation Treatments in Smoking Cessation Success. *Am. J. Psychiatry* 169, 735–742

209 Saccone, S.F. *et al.* (2006) Cholinergic nicotinic receptor genes implicated in a nicotine dependence association study targeting 348 candidate genes with 3713 SNPs. *Hum. Mol. Genet.* 16, 36–49

210 Freathy, R.M. *et al.* (2009) A common genetic variant in the 15q24 nicotinic acetylcholine receptor gene cluster (CHRNA5–CHRNA3–CHRNB4) is associated with a reduced ability of women to quit smoking in pregnancy. *Hum. Mol. Genet.* 18, 2922–2927

211 Bierut, L.J. *et al.* (2008) Variants in Nicotinic Receptors and Risk for Nicotine Dependence. *Am. J. Psychiatry* 165, 1163–1171

212 Bierut, L.J. *et al.* (2006) Novel genes identified in a high-density genome wide association study for nicotine dependence. *Hum. Mol. Genet.* 16, 24–35

213 Furberg, H. *et al.* (2010) Genome-wide meta-analyses identify multiple loci associated with smoking behavior. *Nat. Genet.* 42, 441–447

214 Benowitz, N.L. *et al.* (2006) CYP2A6 genotype and the metabolism and disposition kinetics of nicotine. *Clin. Pharmacol. Ther.* 80, 457–467

215 Malaiyandi, V. *et al.* (2005) Implications of CYP2A6 Genetic Variation for Smoking Behaviors and Nicotine Dependence. *Clin. Pharmacol. Ther.* 77, 145–158

216 Ambatipudi, S. *et al.* (2016) Tobacco smoking-associated genome-wide DNA methylation changes in the EPIC study. *Epigenomics* 8, 599–618

217 Elliott, H.R. *et al.* (2014) Differences in smoking associated DNA methylation patterns in South Asians and Europeans. *Clin. Epigenetics* 6, 4

218 Gao, X. *et al.* (2015) DNA methylation changes of whole blood cells in response to active smoking exposure in adults: a systematic review of DNA methylation studies. *Clin. Epigenetics* 7, 113

219 Guida, F. *et al.* (2015) Dynamics of smoking-induced genome-wide methylation changes with time since smoking cessation. *Hum. Mol. Genet.* 24, 2349–2359

220 Zeilinger, S. *et al.* (2013) Tobacco smoking leads to extensive genome-wide changes in DNA methylation. *PLoS One* 8,

221 Zhang, Y. *et al.* (2016) Self-reported smoking, serum cotinine, and blood DNA methylation. *Environ. Res.* 146, 395–403

222 Zhang, Y. *et al.* (2014) F2RL3 methylation as a biomarker of current and lifetime smoking exposures. *Environ. Heal. Perspect.* 122, 131–137

223 Wan, E.S. *et al.* (2012) Cigarette smoking behaviors and time since quitting are associated with differential DNA methylation across the human genome. *Hum Mol Genet* 21,

224 Shenker, N.S. *et al.* (2013) DNA methylation as a long-term biomarker of exposure to tobacco smoke. *Epidemiology* 24,

225 Fasanelli, F. *et al.* (2015) Hypomethylation of smoking-related genes is associated with future lung cancer in four prospective cohorts. *Nat. Commun.* 6, 10192

226 Shenker, N.S. *et al.* (2013) Epigenome-wide association study in the European prospective investigation into cancer and nutrition (EPIC-Turin) identifies novel genetic loci associated with smoking. *Hum Mol Genet* 22,

227 Teschendorff, A.E. *et al.* (2015) Correlation of Smoking-Associated DNA Methylation Changes in Buccal Cells With DNA Methylation Changes in Epithelial Cancer. *JAMA Oncol.* 1, 476–85

228 Hastie, T. *et al.* (2009) *The Elements of Statistical Learning: Data Mining, Inference, and Prediction, Second Edition*, Springer Science & Business Media.

229 Hastie, T. *et al.* (2015) Statistical Learning with Sparsity: The Lasso and Generalizations. *Crc* DOI: 10.1201/b18401-1

230 Bohlin, J. *et al.* (2016) Prediction of gestational age based on genome-wide differentially methylated regions. *Genome Biol.* 17, 207

231 Knight, A.K. *et al.* (2016) An epigenetic clock for gestational age at birth based on blood methylation data. *Genome Biol.* 17, 206

232 Joubert, B.R. *et al.* (2016) DNA Methylation in Newborns and Maternal Smoking in Pregnancy: Genome-wide Consortium Meta-analysis. *Am. J. Hum. Genet.* 98, 680–696

233 Richmond, R.C. *et al.* (2018) DNA methylation as a marker for prenatal smoke exposure in adults. *Int. J. Epidemiol.* 47, 1120–1130

234 Lussier, A.A. *et al.* (2018) DNA methylation as a predictor of fetal alcohol spectrum disorder. *Clin. Epigenetics* 10, 5

235 Liu, C. *et al.* (2018) A DNA methylation biomarker of alcohol consumption. *Mol. Psychiatry* 23, 422–433

236 Lee, Y. *et al.* (2019) Placental epigenetic clocks: estimating gestational age using placental DNA methylation levels. *Aging (Albany. NY).* 11, 4238–4253

237 Bell, C.C. (1994) DSM-IV: Diagnostic and Statistical Manual of Mental Disorders. *JAMA* 272, 828–829

238 Heatherton, T.F. *et al.* The Fagerström Test for Nicotine Dependence: A revision of the Fagerström Tolerance Questionnaire. , *British Journal of Addiction*, 86. (1991) , Blackwell Publishing, 1119–1127

239 Benowitz, N.L. *et al.* (2009) Prevalence of Smoking Assessed Biochemically in an Urban Public Hospital: A Rationale for Routine Cotinine Screening. *Am. J. Epidemiol.* 170, 885–891

240 Hsieh, S.J. *et al.* (2011) Biomarkers increase detection of active smoking and secondhand smoke exposure in critically ill patients. *Crit. Care Med.* 39, 40–45

241 Philibert, R. *et al.* (2016) Reversion of AHRR Demethylation Is a Quantitative Biomarker of Smoking Cessation. *Front. Psychiatry* 7, 55

242 Philibert, R. *et al.* (2015) A quantitative epigenetic approach for the assessment of cigarette consumption. *Front. Psychol.* 6, 656

243 Peeters, A. *et al.* (2003) Obesity in Adulthood and Its Consequences for Life Expectancy: A Life-Table Analysis. *Ann. Intern. Med.* 138, 24–32

244 Munafò, M.R. *et al.* (2009) Smoking status and body mass index: A longitudinal study. *Nicotine Tob. Res.* 11, 765–771

245 Kaufman, A. *et al.* (2012) Unraveling the Relationship between Smoking and Weight: The Role of Sedentary Behavior. *J. Obes.* 2012, 11

246 Dare, S. *et al.* (2015) Relationship between smoking and obesity: a cross-sectional study of 499,504 middle-aged adults in the UK general population. *PLoS One* 10, e0123579–e0123579

247 Mackay, D.F. *et al.* (2013) Impact of smoking and smoking cessation on overweight and obesity: Scotland-wide, cross-sectional study on 40,036 participants. *BMC Public Health* 13, 348

248 Piirtola, M. *et al.* (2018) Association of current and former smoking with body mass index: A study of smoking discordant twin pairs from 21 twin cohorts. *PLoS One* 13, e0200140

249 Taylor, A.E. *et al.* (2014) Stratification by smoking status reveals an association of CHRNA5-A3-B4 genotype with body mass index in never smokers. *PLoS Genet.* 10, e1004799–e1004799

250 Winsløw, U.C. *et al.* (2015) High tobacco consumption lowers body weight: a Mendelian randomization study of the Copenhagen General Population Study. *Int. J. Epidemiol.* 44, 540–550

251 Canoy, D. *et al.* (2005) Cigarette Smoking and Fat Distribution in 21, 828 British Men and Women: A Population-based Study. *Obes. Res.* 13, 1466–1475

252 Justice, A.E. *et al.* (2017) Genome-wide meta-analysis of 241,258 adults accounting for smoking behaviour identifies novel loci for obesity traits. *Nat. Commun.* DOI: 10.1038/ncomms14977

253 Carreras-Torres, R. *et al.* (2018) Role of obesity in smoking behaviour: Mendelian randomisation study in UK Biobank. *BMJ* 361, k1767

254 Chiolero, A. *et al.* (2008) Consequences of smoking for body weight, body fat distribution, and insulin resistance. *Am. J. Clin. Nutr.* 87, 801–809

255 Filozof, C. *et al.* (2004) Smoking cessation and weight gain. *Obes. Rev.* 5, 95–103

256 Thorgeirsson, T.E. *et al.* (2013) A common biological basis of obesity and nicotine addiction. *Transl. Psychiatry* 3, e308–e308

257 Criscitelli, K. and Avena, N.M. (2016) The neurobiological and behavioral overlaps of nicotine and food addiction. *Prev. Med. (Baltim).* 92, 82–89

258 Volkow, N.D. *et al.* (2013) Obesity and addiction: neurobiological overlaps. *Obes. Rev.* 14, 2–18

259 Kaprio, J. (2013) The Finnish Twin Cohort Study: an update. *Twin Res. Hum. Genet.* 16, 157–162

260 Kaprio, J. *et al.* (2019) The Older Finnish Twin Cohort - 45 Years of Follow-up. *Twin Res. Hum. Genet.* DOI: 10.1017/thg.2019.54

261 Kaprio, J. *et al.* (1978) The Finnish Twin Registry: formation and compilation, questionnaire study, zygosity determination procedures, and research program. *Prog. Clin. Biol. Res.* 24 Pt B, 179–184

262 Huang, Y. *et al.* (2018) Genetic and Environmental Effects on Gene Expression Signatures of Blood Pressure: A Transcriptome-Wide Twin Study. *Hypertens. (Dallas, Tex. 1979)* 71, 457–464

263 Kaprio, J. (2006) Twin studies in Finland 2006. *Twin Res. Hum. Genet.* 9, 772–777

264 Rose, R.J. *et al.* (2019) FinnTwin12 Cohort: An Updated Review. *Twin Res. Hum. Genet.* DOI: 10.1017/thg.2019.83

265 Naukkarinen, J. *et al.* (2012) Causes and consequences of obesity: the contribution of recent twin studies. *Int. J. Obes.* 36, 1017–1024

266 Moayyeri, A. *et al.* (2013) Cohort Profile: TwinsUK and healthy ageing twin study. *Int. J. Epidemiol.* 42, 76–85

267 Rappou, E. *et al.* (2016) Weight Loss Is Associated With Increased NAD(+)/SIRT1 Expression But Reduced PARP Activity in White Adipose Tissue. *J. Clin. Endocrinol. Metab.* 101, 1263–1273

268 Borodulin, K. *et al.* (2015) Forty-year trends in cardiovascular risk factors in Finland. *Eur. J. Public Health* 25, 539–546

269 Inouye, M. *et al.* (2010) Metabonomic, transcriptomic, and genomic variation of a population cohort. *Mol. Syst. Biol.* 6, 441

270 Inouye, M. *et al.* (2010) An immune response network associated with blood lipid levels. *PLoS Genet.* 6, e1001113

271 Broms, U. *et al.* (2012) Diurnal Evening Type is Associated with Current Smoking, Nicotine Dependence and Nicotine Intake in the Population Based National {FINRISK} 2007 Study. *J. Addict. Res. Ther.* S2,

272 Prasad, G.L. *et al.* (2016) A cross-sectional study of biomarkers of exposure and effect in smokers and moist snuff consumers. *Clin. Chem. Lab. Med.* 54, 633–642

273 Dogan, M. V *et al.* (2014) The effect of smoking on DNA methylation of peripheral blood mononuclear cells from African American women. *BMC Genomics* 15, 151

274 Baecke, J.A. *et al.* (1982) A short questionnaire for the measurement of habitual physical activity in epidemiological studies. *Am. J. Clin. Nutr.* 36, 936–942

275 Pietrobelli, A. *et al.* (1996) Dual-energy X-ray absorptiometry body composition model: review of physical concepts. *Am. J. Physiol.* 271, E941-51

276 Granér, M. *et al.* (2012) Epicardial fat, cardiac dimensions, and low-grade inflammation in young adult monozygotic twins discordant for obesity. *Am. J. Cardiol.* 109, 1295–1302

277 Matthews, D.R. *et al.* (1985) Homeostasis model assessment: insulin resistance and beta-cell function from fasting plasma glucose and insulin concentrations in man. *Diabetologia* 28, 412–419

278 Matsuda, M. and DeFronzo, R.A. (1999) Insulin sensitivity indices obtained from oral glucose tolerance testing: comparison with the euglycemic insulin clamp. *Diabetes Care* 22, 1462–1470

279 Yeckel, C.W. *et al.* (2004) Validation of insulin sensitivity indices from oral glucose tolerance test parameters in obese children and adolescents. *J. Clin. Endocrinol. Metab.* 89, 1096–1101

280 Pietiläinen, K.H. *et al.* (2016) DNA methylation and gene expression patterns in adipose tissue differ significantly within young adult monozygotic BMI-discordant twin pairs. *Int. J. Obes.* 40, 654–661

281 Heinonen, S. *et al.* (2014) Adipocyte morphology and implications for metabolic derangements in acquired obesity. *Int. J. Obes.* 38, 1423–1431

282 Wilson, C.L. and Miller, C.J. (2005) Simpleaffy: a BioConductor package for Affymetrix Quality Control and data analysis. *Bioinformatics* 21, 3683–3685

283 Brettschneider, J. *et al.* (2008) Quality Assessment for Short Oligonucleotide Microarray Data. *Technometrics* 50, 241–264

284 Irizarry, R.A. *et al.* (2003) Summaries of Affymetrix GeneChip probe level data. *Nucleic Acids Res.* 31, e15

285 Dai, M. *et al.* (2005) Evolving gene/transcript definitions significantly alter the interpretation of GeneChip data. *Nucleic Acids Res.* 33, e175

286 Johnson, W.E. *et al.* (2007) Adjusting batch effects in microarray expression data using empirical Bayes methods. *Biostatistics* 8,

287 Naeem, H. *et al.* (2014) Reducing the risk of false discovery enabling identification of biologically significant genome-wide methylation status using the HumanMethylation450 array. *BMC Genomics* 15, 51

288 Chen, Y.-A. *et al.* (2013) Discovery of cross-reactive probes and polymorphic CpGs in the Illumina Infinium HumanMethylation450 microarray. *Epigenetics* 8, 203–209

289 McCall, M.N. *et al.* (2010) Frozen robust multiarray analysis (fRMA). *Biostatistics* 11, 242–253

290 (2012) *R: A language and environment for statistical computing*, R Foundation for Statistical Computing.

291 Smyth Gordon, K. (2004) Linear Models and Empirical Bayes Methods for Assessing Differential Expression in Microarray Experiments. *Stat. Appl. Genet. Mol. Biol.* 3, 1–25

292 Bollepalli, S. *et al.* (2019) EpiSmokEr: a robust classifier to determine smoking status from DNA methylation data. *Epigenomics* 11, 1469–1486

293 Friedman, J. *et al.* (2010) Regularization Paths for Generalized Linear Models via Coordinate Descent. *J. Stat. Softw.* 33, 1–22

294 Efron, B. and Tibshirani, R. (2007) On testing the significance of sets of genes. *Ann. Appl. Stat.* 1, 107–129

295 Fabregat, A. *et al.* (2018) The Reactome Pathway Knowledgebase. *Nucleic Acids Res.* 46, D649–D655

296 Efron, B. and Tibshirani, R. (2010) GSA: Gene set analysis. at <http://cran.r-project.org/package=GSA>

297 Bollepalli, S. *et al.* (2018) Subcutaneous adipose tissue gene expression and DNA methylation respond to both short- and long-term weight loss. *Int. J. Obes.* 42, 412–423

298 Mardinoglu, A. *et al.* (2015) Extensive weight loss reveals distinct gene expression changes in human subcutaneous and visceral adipose tissue. *Sci. Rep.* 5, 14841

299 Somekawa, S. *et al.* (2012) Tmem100, an ALK1 receptor signaling-dependent gene essential for arterial endothelium differentiation and vascular morphogenesis. *Proc. Natl. Acad. Sci. U. S. A.* 109, 12064–12069

300 Palming, J. *et al.* (2007) The expression of NAD(P)H:quinone oxidoreductase 1 is high in human adipose tissue, reduced by weight loss, and correlates with adiposity, insulin sensitivity, and markers of liver dysfunction. *J. Clin. Endocrinol. Metab.* 92, 2346–2352

301 Magkos, F. *et al.* (2016) Effects of Moderate and Subsequent Progressive Weight Loss on Metabolic Function and Adipose Tissue Biology in Humans with Obesity. *Cell Metab.* 23, 591–601

302 Rashid, S. and Genest, J. (2007) Effect of obesity on high-density lipoprotein metabolism. *Obesity* 15, 2875–2888

303 Gandhi, P.U. *et al.* (2015) Analysis of BAG3 plasma concentrations in patients with acutely decompensated heart failure. *Clin. Chim. Acta* 445, 73–78

304 Rosati, A. *et al.* (2011) BAG3: a multifaceted protein that regulates major cell pathways. *Cell Death Dis.* 2, e141

305 Rizkalla, S.W. *et al.* (2012) Differential effects of macronutrient content in 2 energy-restricted diets on cardiovascular risk factors and adipose tissue cell size in moderately obese individuals: a randomized controlled trial. *Am. J. Clin. Nutr.* 95, 49–63

306 Senol-Cosar, O. *et al.* (2016) Tenomodulin promotes human adipocyte differentiation and beneficial visceral adipose tissue expansion. *Nat. Commun.* 7, 10686

307 Arvidsson, E. *et al.* (2004) Effects of different hypocaloric diets on protein secretion from adipose tissue of obese women. *Diabetes* 53, 1966–1971

308 Bastard, J.P. *et al.* (2000) Elevated levels of interleukin 6 are reduced in serum and subcutaneous adipose tissue of obese women after weight loss. *J. Clin. Endocrinol. Metab.* 85, 3338–3342

309 Aguilera, C.M. *et al.* (2015) Genome-wide expression in visceral adipose tissue from obese prepubertal children. *Int. J. Mol. Sci.* 16, 7723–7737

310 Ye, F. *et al.* (2011) Comparative proteome analysis of 3T3-L1 adipocyte differentiation using iTRAQ-coupled 2D LC-MS/MS. *J. Cell. Biochem.* 112, 3002–3014

311 Liu, Y. *et al.* (2013) MicroRNA-140 promotes adipocyte lineage commitment of C3H10T1/2 pluripotent stem cells via targeting osteopetrosis-associated transmembrane protein 1. *J. Biol. Chem.* 288, 8222–8230

312 Tekpli, X. *et al.* (2012) DNA methylation of the CYP1A1 enhancer is associated with smoking-induced genetic alterations in human lung. *Int. J. Cancer* 131, 1509–1516

313 Suter, M. *et al.* (2011) Maternal tobacco use modestly alters correlated epigenome-wide placental DNA methylation and gene expression. *Epigenetics* 6, 1284–1294

314 Gutierrez-Arcelus, M. *et al.* (2013) Passive and active DNA methylation and the interplay with genetic variation in gene regulation. *Elife* 2, e00523–e00523

315 Jjingo, D. *et al.* (2012) On the presence and role of human gene-body DNA methylation. *Oncotarget; Vol 3, No 4 April 2012* at <http://legacy.oncotarget.com/index.php?journal=oncotarget&amp>

316 Tsai, P.-C. *et al.* (2018) Smoking induces coordinated DNA methylation and gene expression changes in adipose tissue with consequences for metabolic health. *Clin. Epigenetics* 10, 126

317 Fontana, L. *et al.* (2007) Visceral fat adipokine secretion is associated with systemic inflammation in obese humans. *Diabetes* 56, 1010–1013

318 Glastonbury, C.A. *et al.* (2019) Cell-Type Heterogeneity in Adipose Tissue Is Associated with Complex Traits and Reveals Disease-Relevant Cell-Specific eQTLs. *Am. J. Hum. Genet.* 104, 1013–1024

319 Gao, X. *et al.* (2017) The impact of methylation quantitative trait loci (mQTLs) on active smoking-related DNA methylation changes. *Clin. Epigenetics* 9, 87

320 Gao, X. *et al.* (2016) Relationship of tobacco smoking and smoking-related DNA methylation with epigenetic age acceleration. *Oncotarget* 7, 46878–46889

321 Nwanaji-Enwerem, J.C. *et al.* (2019) Relationships of Long-Term Smoking and Moist Snuff Consumption With a DNA Methylation Age Relevant Smoking Index: An Analysis in Buccal Cells. *Nicotine Tob. Res.* 21, 1267–1273

322 Teschendorff, A.E. *et al.* (2015) Correlation of Smoking-Associated DNA Methylation Changes in Buccal Cells With DNA Methylation Changes in Epithelial Cancer. *JAMA Oncol* 1, 476–485

323 Relton, C.L. and Davey Smith, G. (2012) Two-step epigenetic Mendelian randomization: a strategy for establishing the causal role of epigenetic processes in pathways to disease. *Int. J. Epidemiol.* 41, 161–176

324 Hannon, E. *et al.* (2015) Methylation QTLs in the developing brain and their enrichment in schizophrenia risk loci. *Nat. Neurosci.* 19, 48–54

325 Gaunt, T.R. *et al.* (2016) Systematic identification of genetic influences on methylation across the human life course. *Genome Biol.* 17,

326 Plongthongkum, N. *et al.* (2014) Advances in the profiling of DNA modifications: cytosine methylation and beyond. *Nat. Rev. Genet.* 15, 647

327 consortium, T.B. *et al.* (2016) Quantitative comparison of DNA methylation assays for biomarker development and clinical applications. *Nat. Biotechnol.* 34, 726

328 Walls, H.L. *et al.* (2011) Public health campaigns and obesity - a critique. *BMC Public Health* 11, 136

329 Frieden, T.R. *et al.* (2010) Reducing childhood obesity through policy change: acting now to prevent obesity. *Heal. Aff.* 29, 357–363

330 Ramos Salas, X. (2015) The ineffectiveness and unintended consequences of the public health war on obesity. *Can. J. Public Heal.* 106, e79-81

331 Berdasco, M. and Esteller, M. (2019) Clinical epigenetics: seizing opportunities for translation. *Nat. Rev. Genet.* 20, 109–127

332 Stricker, S.H. *et al.* (2017) From profiles to function in epigenomics. *Nat. Rev. Genet.* 18, 51–66

333 Bultmann, S. and Stricker, S.H. (2019) Entering the post-epigenomic age: back to epigenetics. *Open Biol.* 8, 180013

334 Brocken, D.J.W. *et al.* (2018) dCas9: A Versatile Tool for Epigenome Editing. *Curr. Issues Mol. Biol.* 26, 15–32

335 Dyke, S.O.M. *et al.* (2019) Points-to-consider on the return of results in epigenetic research. *Genome Med.* 11, 31